



AMERICAN UNIVERSITY OF BEIRUT

A RISK-BASED APPROACH FOR OPTIMIZING PROOF-LOAD  
TEST PROGRAMS FOR DRIVEN PILES

by  
IHAB MAAMOUN HOSSEIKY MALAEB

A thesis  
submitted in partial fulfillment of the requirements  
for the degree of Master of Engineering  
to the Department of Civil and Environmental Engineering  
of the Maroun Semaan Faculty of Engineering and Architecture  
at the American University of Beirut

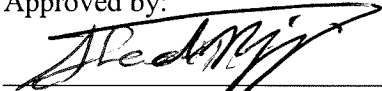
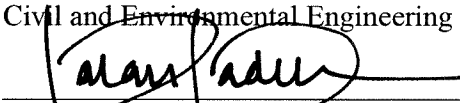

Beirut, Lebanon  
September 2018

AMERICAN UNIVERSITY OF BEIRUT

A RISK-BASED APPROACH FOR OPTIMIZING PROOF-LOAD  
TEST PROGRAMS FOR DRIVEN PILES

by  
IHAB HOSSEIKY MALAEB

Approved by:

 Dr. Shadi Najjar, Associate Professor Civil and Environmental Engineering	Advisor
 Dr. Salah Sadek, Professor Civil and Environmental Engineering	Committee member
 Dr. George Saad, Associate Professor Civil and Environmental Engineering	Committee member

Date of thesis defense: September 28, 2018



## ACKNOWLEDGMENTS

I would like to express my appreciation to my advisors Dr. Shadi Najjar and Dr. George Saad for their valuable and academic assistance. I would also like to thank Dr. Salah Sadek for his tremendous help as a committee member and for reading my thesis.

Finally, I want to thank my family for their full support and commitment to make this journey possible.

# AN ABSTRACT OF THE THESIS OF

Ihab Hosseiky Malaeb for Master of Engineering  
Major: Civil Engineering

Title: A Risk-Based Approach for Optimizing Proof-Load Test Programs for Driven Piles

There is currently an inconsistency in the recommendations that are available in pile design codes and practices regarding the required number of proof-load tests and the level of the proof loads for piles. Najjar et al. (2017) proposed a pre-posterior decision making framework to allow for selecting the optimal pile load test program that would result in the maximum expected benefit to a project while maintaining a target level of reliability in the pile design at the site. The proposed methodology was based on a robust Bayesian approach that allows for updating the capacity distribution of piles at a site given the results of the proof-load test program. In the proposed methodology, Najjar et al. (2017) adopted a simplified statistical model for the pile capacity, whereby the uncertainty in the pile capacity due to spatial variability in a site was assumed to be known and modeled by a fixed coefficient of variation of 0.2. In addition, the application of the proposed decision-making framework was limited to an illustrative design example that targeted driven steel pipelines in sands. The objectives of this thesis are to (1) extend the statistical model that is proposed by Najjar et al. (2017) for the pile capacity by modeling the uncertainty in the pile capacity at the site (coefficient of variation due to spatial variability) as an uncertain variable that is updated with pile load test results, (2) study the sensitivity of the decision making framework to the parameters describing the uncertainty in the capacity and the load, and (3) apply the pre-posterior decision making framework to a number of practical design scenarios that involve driven piles of different characteristics and soils of different nature.

## CONTENTS

ACKNOWLEDGEMENTS .....	v
ABSTRACT.....	vi
LIST OF ILLUSTRATIONS.....	x
LIST OF TABLES .....	xiii

### Chapter

1. INTRODUCTION AND BACKGROUND.....	1
1.1 Background on Proof-Load Testing of Piles .....	2
1.2 Research Objectives and Scope of Work .....	10
1.3 Thesis Outline.....	10
2. REVISED PROBABILISTIC PILE CAPACITY MODEL .....	12
2.1 Modeling Within-Site Variability.....	12
2.2 Probability Distribution of Lower-Bound Capacity .....	15
2.3 Probability Distribution of the Mean Pile Capacity .....	15
2.4 Load Distribution.....	17
3. BAYESIAN UPDATING FRAMEWORK .....	18
3.1 Probabilistic Representation of the Model Parameters.....	18

3.2 Bayesian Updating of the Capacity Distribution.....	20
3.3 Calculation of the probability of failure .....	22
<b>4. UPDATING PILE CAPACITY DISTRIBUTION WITH PROOF LOAD TESTS .....</b>	<b>24</b>
4.1 Prior versus Updated PMFs for $r_{\text{mean}}$ and $r_{\text{COV}}$ .....	24
4.2 Correlation between the COV and the mean distributions .....	29
4.3 Sensitivity of Results to the lower-bound Capacity and Mean Capacity Distributions.....	31
4.4 Sensitivity of the Results to the Pile Prediction Method .....	37
4.4.1 Sensitivity analysis for pile prediction methods for sand.....	38
4.4.2 Sensitivity analysis for pile prediction methods for clay .....	47
<b>5. DECISION MAKING FRAMEWORK .....</b>	<b>50</b>
5.1 Methodology of Decision Framework (Najjar et al. 2017) .....	50
5.2 Model and MATLAB code update .....	53
<b>6. PRACTICAL APPLICATIONS FOR PROPOSED DECISION MAKING FRAMEWORK .....</b>	<b>57</b>



6.1 Site No. 1: The Cimarron River Site (Driven Piles in Loose to Medium Sand).....	58
6.2 Site No. 2: The Pigeon Creek Site (Driven Piles in Dense Sand) .....	65
6.3 Site No. 3: The Port of Khorramshahr, Iran (Short Driven Piles in Clay) ...	68
6.4 Site No. 4: Louisiana Site (Long Pile in Clay) .....	72
6.5 Discussion of Case Histories .....	76
<b>7. SENSITIVITY ANALYSIS ON TEST AND PILE COSTS.</b>	
.....	80
<b>8. CONCLUSIONS</b> .....	87
<b>REFERENCES</b> .....	89
Appendix	
1. Sensitivity Analysis of the Lower-bound.....	93
2. Appendix 2: Mean Sensitivity .....	96

# ILLUSTRATIONS

	Figure	Page
1.	Statistical Model of Pile Capacity by Najjar et al. (2017).....	5
2.	Decision Making Tree for Choosing the Optimum Test Program (from Najjar et al. 2017).....	9
3.	The Capacity Distribution Model that will be adopted in proposed framework (a) Pile Capacity Model, (b) Within-Site variability model, and (c) mean and lower-bound capacity models.....	14
4.	(a) the prior joint PMF between $r_{mean}$ and $r_{COV}$ (b) the updated joint PMF between $r_{mean}$ and $r_{COV}$ after 5 successful proof load tests .....	20
5.	The Prior and Updated Distributions of (a) Within-Site Variability (Truncated Lognormal $r_{cov}$ ), and (b) Mean Pile Capacity ( $r_{mean}$ ).....	26
6.	The Prior and Updated Distributions for (a) Truncated Normal Within-Site Variability, and (b) Uniform Within Site Variability.....	27
7.	Effect of proof load test levels on the reliability index for different $r_{COV}$ distributions (FS =2) .....	29
8.	The effect of the lower bound truncation on the (a) mean capacity with a COV = 0.5 (b) mean capacity with a COV = 0.15 .....	32
9.	The variation of the reliability index as a function of positive proof load tests for different lower-bound to mean ratio applied at a 0.5 COV mean distribution (FS = 2) .....	33
10.	Sample Decision Making Example as Presented in Najjar et al. (2017) .....	53
11.	Characteristics of the Cimarron River Site .....	59
12.	5 Expected benefit of alternative proof load test programs .....	62

13.	The optimal number of proof load test and the percentage of tests as a function of number of piles using the API method in the Cimarron River Site (optimal $r_{proof} = 2 \times DL$ ).....	64
14.	Characteristics of the Pigeon Creek Site.....	65
15.	Characteristics of the Louisiana site .....	73
16.	The optimal number of piles in clay sites (a) test cost 10\$/KN and price 97\$/ft (b) test cost 10\$/KN and the piles' cost of state of Michigan (2003), and (c) test cost 20\$/KN and the piles' cost of state of Michigan (2003). .....	85
17.	The variation of the reliability index as a function of positive proof load tests of 1.5xDL level for different lower-bound to mean ratio applied at a 0.5 COV mean distribution (FS = 2) .....	93
18.	The variation of the reliability index as a function of positive proof load tests of 2.5xDL level for different lower-bound to mean ratio applied at a 0.5 COV mean distribution (FS = 2) .....	94
19.	The variation of the reliability index as a function of positive proof load tests of 1.5xDL level for different lower-bound to mean ratio applied at a 0.15 COV mean distribution (FS = 2) .....	95
20.	The variation of the reliability index as a function of positive proof load tests of 2.5xDL level for different lower-bound to mean ratio applied at a 0.15 COV mean distribution (FS = 2) .....	95
21.	The variation of the reliability index as a function of different proof load tests outcome conducted at 2xDL level for different SPT based method (FS = 2) .....	96
22.	The variation of the reliability index as a function of different proof load tests outcome conducted at 1.5xDL level for different skin-tip combinations for Fugro method (FS = 2) .....	96
23.	The variation of the reliability index as a function of different proof load tests outcome conducted at 2.5xDL level for different skin-tip combinations for Fugro method (FS = 2) .....	97
24.	The variation of the reliability index as a function of different proof load tests outcome conducted at 1.5xDL level for different skin-tip combinations for API-05 method (FS = 2).....	97
25.	The variation of the reliability index as a function of different proof load tests outcome conducted at 2xDL level for different skin-tip combinations for API method (FS = 2) .....	98

26.	The variation of the reliability index as a function of different proof load tests outcome conducted at 2.5xDL level for different skin-tip combinations for API method (FS = 2) .....	98
27.	The variation of the reliability index as a function of different proof load tests outcome conducted at 1.5xDL level for different skin-tip combinations for ICP-05 method (FS = 2).....	99
28.	The variation of the reliability index as a function of different proof load tests outcome conducted at 2xDL level for different skin-tip combinations for ICP-05 method (FS = 2).....	99
29.	The variation of the reliability index as a function of different proof load tests outcome conducted at 2.5xDL level for different skin-tip combinations for ICP-05 method (FS = 2).....	99
30.	The variation of the reliability index as a function of different proof load tests outcome conducted at 2xDL level for different clay methods (FS = 2).....	100

## TABLES

Table	Page
1. Worldwide Recommended Safety Factors for Static and Dynamic Pile Load Test Programs .....	2
2. Candidates for the probability distribution of the COV (within-site variability in pile capacity) that is incorporated in the proposed capacity model .....	13
3. Description of different sand and clay sites .....	58
4. The pile's capacity according to different methods in the Cimarron River Site .....	60
5. pile's capacity according to different methods in the Pigeon Creek Site .....	66
6. pile's capacity according to different methods in the port of Khorramshahr .....	69
7. Soil characteristics in the Louisiana site .....	73
8. pile's capacity according to different methods in the Louisiana site .....	74
9. The pile and test costs for different case histories .....	81

# CHAPTER 1

## INTRODUCTION AND BACKGROUND

Proof-load tests play an important role in verifying the validity of design methods and construction procedures. In current design and construction practices for deep foundations, designers are allowed to utilize reduced factors of safety provided that a pile load testing program is implemented on a number of foundations at the site. Generally, a reduced design factor of safety of 2.0 is considered acceptable provided that the majority of the tested foundations survive proof-load tests up to twice the design load (ASTM D1153 1994). However, many international design codes and practices allow for the use of reduced factors of safety of different magnitudes, with the proposed factors of safety being dependent on the number and type of pile load tests that are conducted.

Some common recommendations from international pile design codes as adapted from Matsumoto et al. (2008) are summarized in Table 1. These recommendations indicate variability in the correlation between the type and number of the specified pile load tests and the recommended reduced design factor of safety. In addition to the variability between the recommendations, a major drawback of any recommendation is that the designer does not have any indication of the inherent reliability/safety that is associated with the resulting design, since the recommendations are generally based on experience and are not associated with any robust reliability/risk analysis that supports their use.

Table 1 Worldwide Recommended Safety Factors for Static and Dynamic Pile Load Test Programs

Country	FS, No Load Tests	FS, with Static Tests	FS, with Dynamic Tests	Comments
USA, ASCE 1996	3	1.6 to 1.9 1.8 to 2.2	1.7 to 2 2 to 2.4	Design capacity is 0.4-1.0 MN Design capacity > 1.0 MN
Europe, EC7 2001	-	1.64	1.95	More than 5 Static, More than 20 Dynamic
Japan	3	2.7	2.7	-
Sweden 2000	-	-	2 1.6	If 25% of piles tested. If 100% of piles tested.
Mexico	3	2	2 to 2.5	Between 1% to 5%. Min is 3 tests.
Singapore	3	2	-	Capacity verified by a number of load tests

### 1.1 Background on Proof-Load Testing of Piles

In the last two decades, several research efforts have targeted analyzing the impact of proof-load tests on the design of foundations in the framework of a reliability analysis. Examples include the work of Zhang and Tang (2002), Zhang (2004), Su (2006), Najjar and Gilbert (2009a), Kwak et al. (2010), Park et al. (2011, 2012), Abdallah et al. (2015a, 2015b), Huang et al. (2016), and Najjar et al. (2017). In these studies, results of proof load tests are used to update the main statistical descriptors of the pile capacity distribution, and the updated distribution is used to calculate an updated estimate of the proof-tested reliability index or probability of failure. Results from previous studies show that different combinations of reduced factor of safety, proof load level, and number of positive proof load tests could be selected to achieve the desired level of reliability. For example, designers have the option of choosing test programs that are based on a few number of load tests that are conducted to a relatively high proof load level, or load tests that include larger number of

proof tests that are conducted to a relatively smaller proof load level. These studies show the need for systematic and rational approaches that would allow for choosing the number of proof-load tests and the magnitude of the proof load that would maximize the value of any pile load test program.

Bayesian techniques can be used to update the probability distribution of the foundation capacity at the site given the result of a pile load test program. This analysis is referred to as a “posterior” analysis. Najjar et al. (2017) proposed a rational decision framework that is aimed at selecting the optimal pile load test program. The decision analysis is based on a “pre-posterior” decision making methodology that allows for selecting the pile load test program (number and level of proof load tests) that would result in the maximum expected benefit while maintaining a target level of reliability in the pile design at the site. The analysis is capable of incorporating all possible test scenarios which could include both failures (capacity of the pile is exceeded at the designated proof load) and successes (pile capacity is higher than the proof load) with their associated likelihoods of occurrence. This methodology is original, practical, and is based on site-specific information that is unique to any given project. The methodology presented is an additional step that is taken to rationalize the process of designing pile load test programs and is expected to help in reducing the current inconsistencies in pile design codes and practices regarding the required number of proof-load tests and the level of the proof loads.

In the methodology, Najjar et al. (2017) adopted a statistical model for the pile capacity that is based on the model proposed by Zhang (2004) which considers that uncertainty in the pile capacity originates from two sources: (1) the uncertainty due to the



model used to predict the capacity, and (2) the uncertainty due to inherent variability in the capacity within the site (within-site variability). The resulting pile capacity model is shown on Figure 1 (Najjar et al. 2017). The methodology assumes that model uncertainty due to bias in the predictions of available empirical models leads to uncertainty in the mean pile capacity at the site. This source of uncertainty is reflected in the probability distribution of the mean pile capacity,  $r_{\text{mean}}$  as indicated in Figure 1 and could be updated using results from pile proof load tests or tests in which the piles are loaded to failure. The mathematical formulation required to update the distribution of the mean pile capacity given results from pile load tests is presented in Zhang (2004).

The main limitation in the model that was proposed by Zhang (2004) and which was adopted by Najjar et al. (2017) is that it assumes that the within-site variability could be represented by a constant coefficient of variation ( $\delta_r = 0.2$ ) that cannot be reduced by conducting pile load tests. The concept of within-site variability of pile capacity originates from the work of Zhang and Tang (2002) who illustrated that piles constructed using the same design method may yield different capacities within one site as a result of spatial variability in the soil properties across the site. By analyzing results from nine different sites where multiple pile load tests that are conducted on identical piles were reported, Zhang and Tang (2002) showed that the COV representing within-site variability in pile capacities varied among sites and ranged from 0.1 to 0.3. Based on this data, an average COV of 0.2 was adopted to model within-site variability in the models presented in Zhang and Tang (2002), Zhang (2005) and Najjar et al (2017). The adoption of a constant COV of 0.2 that is not updated in the Bayesian exercise is a limitation that will be addressed in this study.

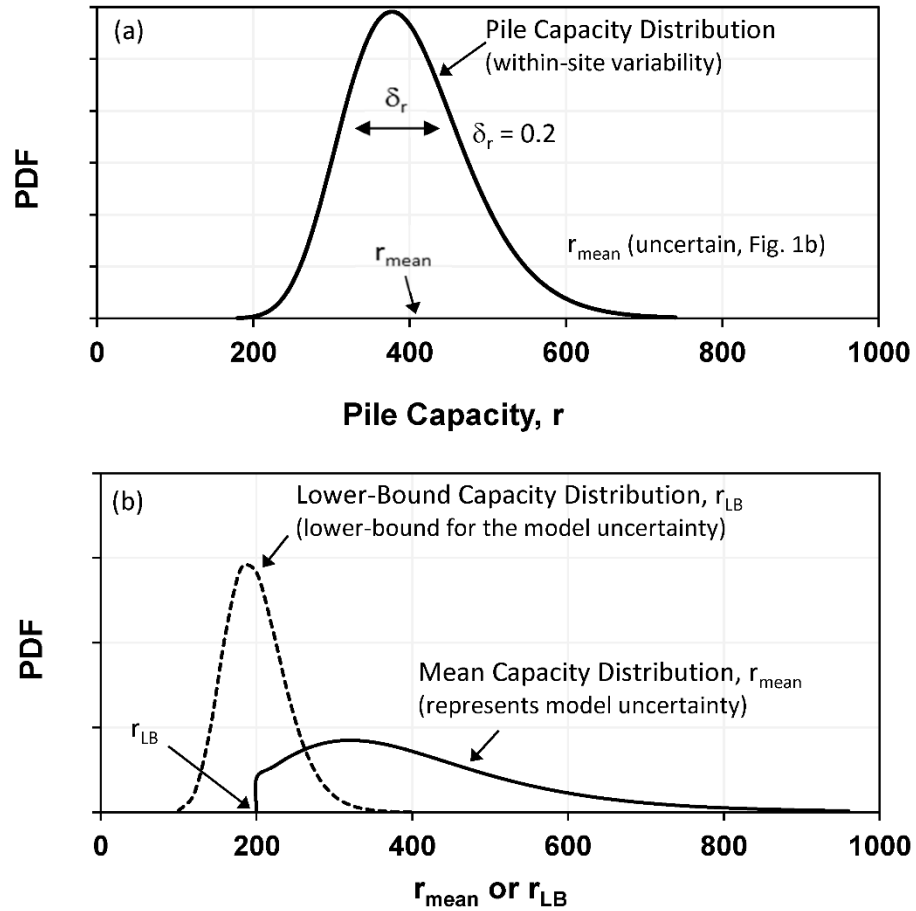


Figure 1 Statistical Model of Pile Capacity by Najjar et al. (2017)

Another feature of the statistical pile capacity model adopted by Najjar et al. (2017) is the incorporation of an uncertain lower-bound capacity in the probability distribution of the mean pile capacity (see Figure 1). Gilbert et al. (2005) and Najjar and Gilbert (2009b) hypothesized that there is a physical limit to the smallest possible capacity for a pile foundation, and that this limit is greater than zero. The basis for this hypothesis is that the strength of soil, even when substantially disturbed, is greater than zero. Gilbert et al. (2005) presented simple models for predicting lower-bound capacities for driven piles in sand and clay. By comparing the measured pile capacities (from load test databases) with the

calculated lower-bound capacities, Gilbert et al. (2005) provided evidence that none of the measured pile capacities fell below the calculated lower bound capacities. For piles in cohesive soils, the ratio of the lower-bound capacity to the predicted capacity ranged from 0.4 to 0.9 and had an average of 0.6. For cohesionless, siliceous soils, the ratio of the lower-bound capacity to the predicted capacity ranged from 0.5 to 0.9 with an average of 0.7. In the Bayesian approach presented in Najjar et al. (2017), the lower-bound capacity was updated using pile load tests. However, results showed that the prior lower-bound distribution was not affected by the updating process, with the focus being on the distribution of the mean capacity.

The main outcome in the study conducted by Najjar et al. (2017) is a rational decision making that would facilitate the choice of a load test program that has the maximum expected benefit to the project. The main decision alternatives were (1) the proof load level  $r_{\text{proof}}$  and (2) the number of proof load tests to be conducted,  $n$ . For each of the potential test outcomes that are associated with a given decision alternative, the updated reliability index could be evaluated using Bayesian techniques. The resulting updated reliability index will depend on the outcome, with relatively high indices expected for cases involving positive tests and relatively low indices for cases involving failures. These reliability indices could be lower or higher than a target reliability index that is set for the piles in the project. As a result, outcomes where the updated reliability index is below the target indicate that the allowable capacity per pile (design load per pile) will have to be reduced in light of the load test results. On the other hand, outcomes where the updated reliability index is above the target allow for an increase in the allowable capacity (design load) per pile in comparison to the base case.

The allowable pile capacity (design load) could be calculated by utilizing the updated capacity distribution for that particular outcome.

From a practical design standpoint, any increase or decrease in the allowable capacity per pile as a result of conducting the proof load tests can be translated to (1) reduction/increase in the total number of piles required to support the superstructure loads without changing the geometry of the piles, or (2) reduction/increase in the geometry of the piles (length and/or diameter) without changing the total number of piles required. For the work presented in Najjar et al. (2017), the consequences associated with the outcomes of any decision alternative are assumed to be reflected in the total number of required piles without resorting to any change in the pile length or diameter. Based on the above, the consequences of any potential test outcome will be reflected in the benefits/costs associated with reducing/increasing the required number of piles to support the superstructure load without changing the geometry of the piles under consideration.

The financial benefit is reflected in the cost savings associated with this reduction in the number of piles. On the other hand, there is a negative financial cost that is associated with the cost of conducting the load test program alternatives and the cost of replacing failed piles when relevant. The net benefit of any test outcome can be calculated by subtracting the benefits due to reducing (or cost due to increasing) the number of piles in the site from the costs associated with conducting the proof load tests including the cost of replacing failed piles. Once the net benefit of all the test alternatives and their associated potential outcomes are calculated, the “expected” benefit of each alternative load test program can be calculated.

The alternative pile testing program that has the highest expected benefit could then be selected as the test alternative that has the highest value.

To illustrate the practicality and value of the proposed decision-making framework, Najjar et al. (2017) presented a practical design example that involves piles that are driven in a site consisting of medium dense sand. The pile design consisted of closed-ended steel pipe piles with an outside diameter of 355 mm and a length of 25 m. The predicted nominal axial capacity of a single driven pile is 1.8 MN and the lower-bound is calculated to be equal to 0.9 MN accounting to about 0.5 of the nominal axial capacity. For the purpose of illustrating the decision-making methodology, hypothetical cases that involve different superstructure loads were adopted, and it was assumed that the superstructure load will be supported by a group of identical steel pipe piles that will share the superstructure load equally.

The example illustrating the use of the decision framework was limited to determining the optimum proof load level and the optimum number of tests to be conducted. The number of pile load tests that were considered as decision alternatives is 1, 2, 3, 5, 7, and 10 proof tests to be conducted at load levels of 1.5, 2, and 2.5 times the design load or 0.75, 1.0, and 1.25 times the predicted capacity. These decision alternatives are presented in the context of a simplified decision tree in Fig. 2 (Najjar et al. 2017) with detailed calculations pertaining to the case of the test alternative that includes a proof load level of 2.0 times the design load presented for illustration. The results indicate that the proof-load test program alternative that is based on conducting 5 proof load tests up to a proof load level of 1.5 times the design load yields the largest expected benefit (\$ 297,965) among all other test alternatives.

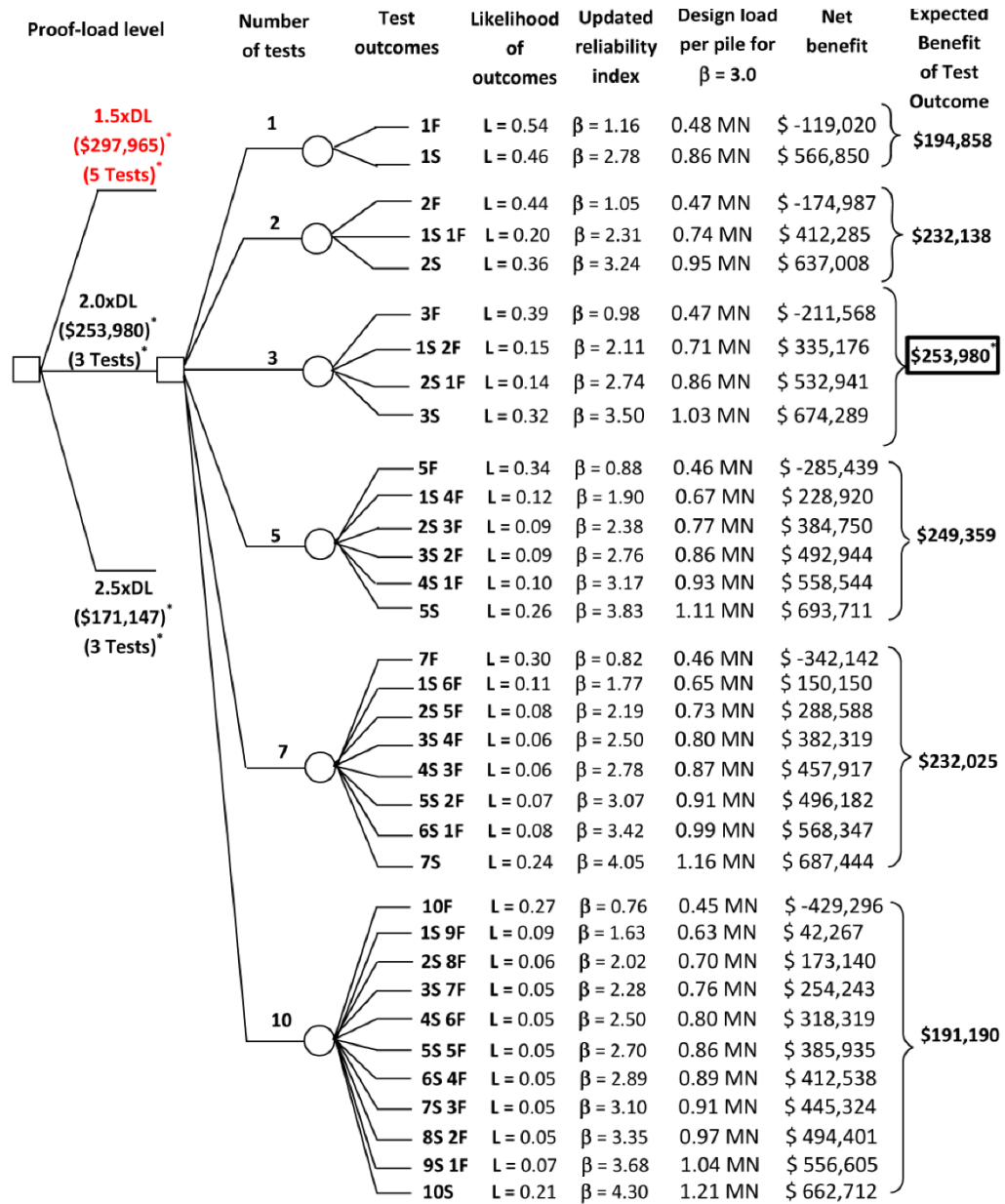


Figure 2 Decision Making Tree for Choosing the Optimum Test Program (from Najjar et al. 2017)

## **1.2 Research Objectives and Scope of Work**

The main objective of this thesis is to extend the decision making framework proposed by Najjar et al. (2017) to achieve the following three main goals: (1) upgrade the statistical model that is proposed by Najjar et al. (2017) for the pile capacity by modeling the uncertainty in the pile capacity at the site (coefficient of variation due to spatial variability) as an uncertain variable that is updated with pile load test results, (2) study the sensitivity of the decision making framework to the parameters describing the uncertainty in the capacity and the load, and (3) apply the pre-posterior decision making framework to a number of practical design scenarios that involve driven piles of different characteristics and soils of different nature. The ultimate goal is to formulate a general set of recommendations regarding the design of proof load tests for driven piles that are designed using different empirical design procedures in soil profiles that range from cohesive to cohesionless soils.

## **1.3 Thesis Outline**

The thesis is divided into eleven chapters. Chapter 1 is an introduction on the topic with a brief background, and a summary of the research objectives and methodology. Chapter 2 presents a revise on the statistical model used. Chapter 3 details the Bayesian updating framework used throughout the thesis. Chapter 4 studies the different uncertain within site variability. Chapters 5 discusses a sensitivity analysis on the lower-bound and the mean distribution which reflects the method's uncertainty, Chapter 6 presents a brief background

on the pre-posterior analysis, Chapter 7 details the different sites used in the pre-posterior analysis. Chapter 8 and 9 studies the pre-posterior analysis of different methods in different sites with and the cost sensitivity respectively. Chapter 10 explains the designed interface on MATLAB, and Chapter 11 concludes the research and gives recommendations.



## CHAPTER 2

### REVISED PROBABILISTIC PILE CAPACITY MODEL

#### 2.1 Modeling Within-Site Variability

Zhang and Tang (2002) showed based on limited field data that the variability in the capacity of identical piles within a site varies and could be represented by coefficients of variation ranging between 0.1 to 0.3. In the previous work of Zhang and Tang (2002) and Najjar et al. (2017), the spatial variability was modeled with a deterministic COV of 0.2. In this work, an effort will be made to model the COV representing within site variability as an uncertain parameter that follows a number of potential probability distributions. The effect of the choice of the probability distribution of the within-site variability on the updating process will be studied in the following chapters.

Three potential probability distributions for modeling the COV representing within-site variability were studied. The distributions are listed in Table 2 and include a uniform distribution, a truncated normal distribution, and a truncated lognormal distribution. The statistics of these distributions were selected based on the limited data presented in Zhang and Tang (2002). For the uniform distribution, lower and upper bounds of 0.1 and 0.3 were selected based on the data available. For the truncated normal and lognormal distributions, a mean of 0.2 and a COV of 0.3 were calculated from the field data and selected to define the distributions which were also truncated between 0.1 and 0.3 for practical considerations.

Table 2 Candidates for the probability distribution of the COV (within-site variability in pile capacity) that is incorporated in the proposed capacity model

Distribution of COV	Distribution coefficients
Uniform distribution	Lower bound = 0.1; upper bound = 0.3
Truncated normal distribution	Mean = 0.2; COV = 0.3; lower = 0.1; upper = 0.3
Truncated Log-normal distribution	Mean = 0.2; COV = 0.3; lower = 0.1; upper = 0.3

A graphical representation of the revised probability capacity model is presented in Figure 3. As indicated in the figure, the pile capacity distribution (Fig. 3a) will be modeled by a lognormal distribution that is described by a mean and a coefficient of variation. The coefficient of variation which reflects within site variability is assumed to be uncertain as indicated in Figure 3b. The mean capacity is also assumed to be uncertain and is reflective of the model uncertainty in the empirical models used to predict the capacity of the pile. The uncertainty in the mean capacity is presented in Fig. 3c and reflects the presence of an uncertain lower-bound capacity that will be used to truncate the tale of the mean capacity distribution. A major change in the proposed model compared to the Najjar et al. (2017) model is that the probability distribution of the lower bound pile capacity in the proposed model will not be updated given the results of proof load test. This decision is based on the results presented in Najjar et al. (2017) and which showed that the lower-bound capacity is not affected by the updating process.

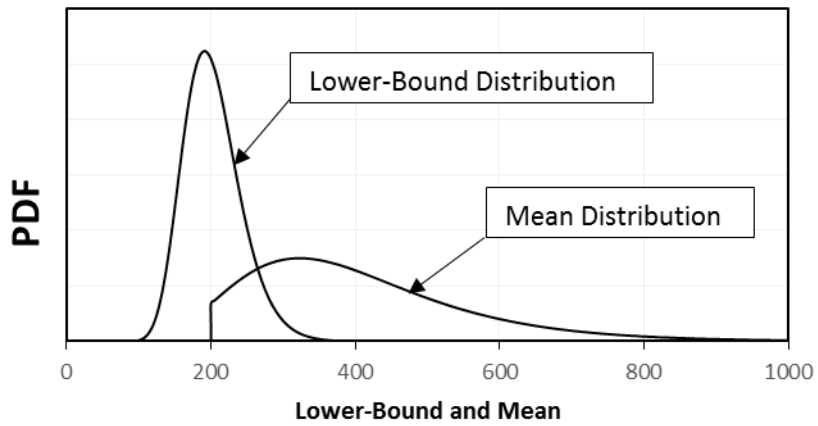
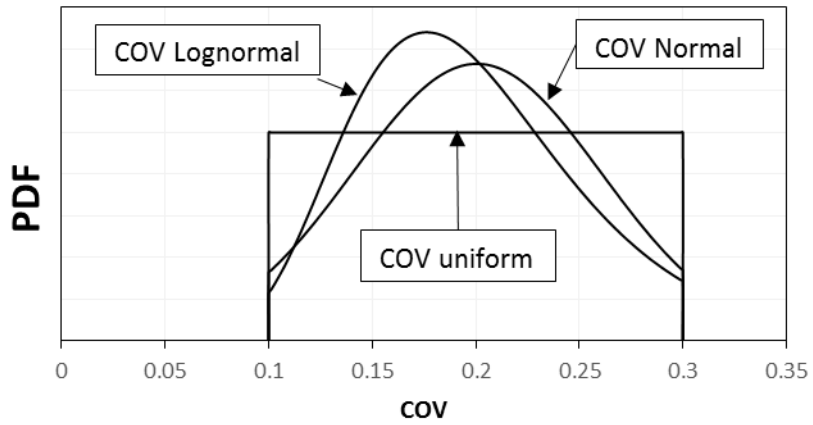
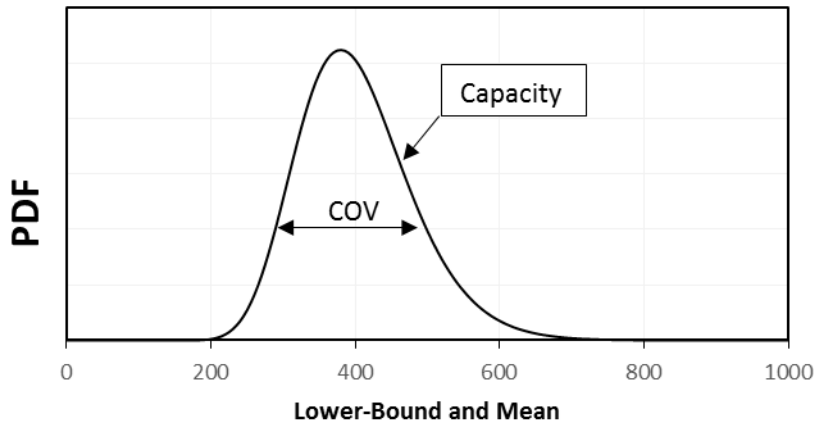


Figure 3 The Capacity Distribution Model that will be adopted in proposed framework (a) Pile Capacity Model, (b) Within-Site variability model, and (c) mean and lower-bound capacity models.

## **2.2 Probability Distribution of Lower-Bound Capacity**

Gilbert et al. (2005) presented evidence of the existence of a lower-bound capacity for driven piles in sand and clays. This capacity is a physical quantity that should be predicted using methods/models that takes into consideration the pile dimensions and the soil properties. In the study conducted by Najjar et al. (2017), the mean of the lower-bound capacity was assumed to be 0.5 of the mean of the mean capacity distribution. Gilbert et al. (2005) showed, based on analysis of the databases for driven piles in clays and sands, that the ratio of the lower-bound to the mean capacity of driven piles could range between 0.4 to 0.9. In this study, a sensitivity analysis will be conducted on the mean value of the lower bound capacity by varying the mean lower bound from 0 (no lower-bound), to 0.4, 0.5, and 0.6 of the mean capacity. The coefficient of variation of the lower-bound is assumed to be equal to 0.2 and the distribution of the lower-bound capacity is assumed to be lognormal based on Najjar and Gilbert (2009b).

## **2.3 Probability Distribution of the Mean Pile Capacity**

The mean of the mean capacity represented in Fig. 3 is typically estimated from databases of pile load tests as the product of the bias factor of the capacity prediction model and the nominal predicted capacity. The bias factor is defined as the average of the ratio of measured to predicted capacities based on available databases. On the other hand, the COV of the  $r_{\text{mean}}$  is generally calculated as the coefficient of variation of the ratio of measured to predicted capacities for the cases analyzed in the database. Therefore, the values of the bias

factor and the COV are linked to the method used to calculate the pile capacities. In this work, the statistics representing model uncertainty will be obtained from previous work done by Gilbert et al. (2005), Zhang (2004), Lacasse et al. (2013), and Lehane et al. (2017).

The latest study that reported statistics for the model uncertainty of available pile capacity prediction models is that of Lehane et al. (2017). The analyzed capacity models that were considered in Lehane et al. (2017) were tailored to predicting the capacity of offshore piles in sand and clays. The selection criteria for the database limited the cases studied to: (1) driven piles only, (2) steel and concrete piles, and (3) piles with a minimum diameter of 20 cm. The statistics of the model factors for driven piles in sands and clays as predicted using two commonly used design approaches (American Petroleum Institute and ICP methods) are summarized in Table 3.

The revised probabilistic capacity model that is presented in Figure 3 could be updated given results from proof load test programs. The updating is conducted within a Bayesian framework whereby the distributions of the mean capacity and the COV representing within-site variability can be updated.

Table 3 The Statistics of current-API and ICP Methods Used for Piles in Sand and clay

Methods	Bias factor	COV	References
Current-API (Sand)	1.66	0.56	Lehane et al. (2017)
Current-API (Clay)	1.54	0.33	Lehane et al. (2017)
ICP method (Sand)	1.04	0.27	Lehane et al. (2017)
ICP method (Clay)	0.98	0.31	Lehane et al. (2017)

## **2.4 Load Distribution**

Most of the reliability analyses in the literature treat the applied load as an uncertain parameter that follows a lognormal distribution. In this work, the load distribution is considered similar to Najjar et al. (2016) as a lognormal distribution with a COV of 0.15. This choice of the coefficient of variation is illustrated by the coefficient of variation specified by AASHTO (2004) (0.13 for the dead load and 0.18 for the live load).

## CHAPTER 3

### BAYESIAN UPDATING FRAMEWORK

#### **3.1 Probabilistic Representation of the Model Parameters**

The revised probabilistic model that describes the pile capacity consists of 3 random variables: the mean capacity which represent the model uncertainty, the lower bound capacity, and the coefficient of variation that represent the within site variability. The model parameters to be updated based on proof-load test results are the mean and the coefficient of variation, whereas the lower-bound will not be updated. The probabilistic representation and the updating process of the model parameters will be similar to the approach presented in Najjar et al. (2017). Since updating the probability density function of the mean capacity and the coefficient of variation involves mathematical complexities, a decision was made to transform the probability density functions of the mean, lower-bound, and coefficient of variation into representative probability mass functions (PMFs) while ensuring a realistic representation of the PDF.

Since the distributions are lognormal, the minimum value in the PMF range was determined as the mean value minus 4 standard deviation while the maximum value is the taken as the mean plus 12 standard deviation. After identifying the minimum and maximum value of each distribution, the range is then divided into intervals that result in values that form the PMF.

After constructing the three PMFs, the joint probability mass function between  $r_{\text{mean}}$  and  $r_{\text{LB}}$   $p_{R_{\text{mean}}, R_{\text{LB}}}(r_{\text{mean}}, r_{\text{LB}})$  is established as:

$$p_{R_{\text{mean}}, R_{\text{LB}}}(r_{\text{mean}}, r_{\text{LB}}) = p_{R_{\text{mean}}|R_{\text{LB}}}(r_{\text{mean}}|r_{\text{LB}}) \times p_{R_{\text{LB}}}(r_{\text{LB}}) \quad (1)$$

Such that  $p_{R_{\text{mean}}|R_{\text{LB}}}(r_{\text{mean}}|r_{\text{LB}})$  is the conditional probability mass function of  $r_{\text{mean}}$  given the lower bound capacity  $r_{\text{LB}}$  and  $p_{R_{\text{LB}}}(r_{\text{LB}})$  is the marginal probability mass function of  $r_{\text{LB}}$ . This conditional probability  $p_{R_{\text{mean}}|R_{\text{LB}}}(r_{\text{mean}}|r_{\text{LB}})$  is defined by a PMF that represents a truncated lognormal distribution where:

$$p_{R_{\text{mean}}|R_{\text{LB}}}(r_{\text{mean}}|r_{\text{LB}}) = \begin{cases} 0, & \text{if } r_{\text{mean}} < r_{\text{LB}} \\ \frac{p_{R_{\text{mean}}, NT}(r_{\text{mean}})}{1 - F_{R_{\text{mean}}, NT}(r_{\text{LB}})}, & \text{if } r_{\text{mean}} > r_{\text{LB}} \end{cases} \quad (2)$$

Where  $p_{R_{\text{mean}}, NT}(r_{\text{mean}})$  is the probability of a given  $r_{\text{mean}}$  as obtained from the PMF of the non-truncated distribution of  $r_{\text{mean}}$  and  $F_{R_{\text{mean}}, NT}(r_{\text{LB}})$  is the cumulative distribution function of  $r_{\text{mean}}$  evaluated at the lower-bound capacity  $r_{\text{LB}}$  with the CDF being calculated from the non-truncated distribution of  $r_{\text{mean}}$ .

As discussed, the lower-bound distribution is not updated whereas the mean distribution is to be updated based on proof load-test results. Therefore, a new PMF of the mean distribution is constructed due to the effect of truncation of the lower-bound distribution. The values of the new PMF of the mean are calculated such that:

$$p_{R_{\text{mean}}, T}(r_{\text{mean}}) = \sum_{i=1}^{n2} p_{R_{\text{mean}}, R_{\text{LB}}}(r_{\text{mean}}, r_{\text{LB}, i}) \quad (3)$$



Where  $p_{R_{mean,T}}(r_{mean})$  is the updated marginal probability mass function due to the truncation of the lower-bound distribution. After constructing the new PMF of the mean distribution, the joint probability mass function between  $r_{mean}$  and  $r_{COV}$   $p_{R_{mean,T},R_{COV}}(r_{mean}, r_{COV})$  is established as:

$$p_{R_{mean,T},R_{COV}}(r_{mean}, r_{COV}) = p_{R_{mean,T}}(r_{mean}) \times p_{R_{COV}}(r_{COV}) \quad (4)$$

Where  $p_{R_{mean,T}}(r_{mean})$  and  $p_{R_{COV}}(r_{COV})$  are the marginal probability mass functions of the truncated  $r_{mean}$  and the marginal probability mass function of  $r_{COV}$  respectively. An example prior and updated joint PMF between  $r_{mean}$  and  $r_{COV}$  is presented in Figure 4.

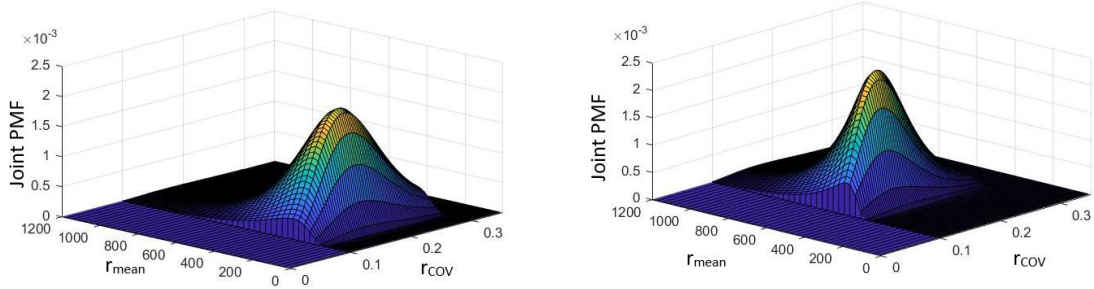


Figure 4 (a) the prior joint PMF between  $r_{mean}$  and  $r_{COV}$  (b) the updated joint PMF between  $r_{mean}$  and  $r_{COV}$  after 5 successful proof load tests conducted at 2xDL

### 3.2 Bayesian Updating of the Capacity Distribution.

In any particular site, a limited number of proof load tests are conducted on piles. Therefore, to update the probability distribution of the model parameters, Bayes' Theorem (equation 5) should be used such that:

$$f_{\Phi|\varepsilon}(\Phi|\varepsilon) = \frac{L(\varepsilon|\Phi)f_{\Phi}(\Phi)}{\int_{-\infty}^{+\infty} \dots \int_{-\infty}^{+\infty} L(\varepsilon|\Phi)f_{\Phi}(\Phi)d\Phi_1 \dots d\Phi_n} \quad (5)$$

Where  $f_{\Phi|\varepsilon}(\Phi|\varepsilon)$  and  $f_{\Phi}(\Phi)$  are the updated and prior joint distributions of the model parameters,  $\Phi$ ,  $L(\varepsilon|\Phi)$  is the likelihood function, and  $\int_{-\infty}^{+\infty} \dots \int_{-\infty}^{+\infty} L(\varepsilon|\Phi)f_{\Phi}(\Phi)d\Phi_1 \dots d\Phi_n$  is a normalizing constant.

The mean capacity and the coefficient of variation of the pile are modeled as probability mass functions instead of probability density function in order to facilitate the calculation of equation 5. To update the capacity's distribution, we assume that “n” proof-load tests are conducted at a level  $r_{proof}$  and “k” tests out of these “n” tests survive (positive load tests). Therefore, “n-k” tests will not survive (negative proof load tests) and the likelihood of observing the result of the pile load test program giving a combination of  $r_{mean,i}$  and  $r_{cov,j}$  is given in equation (6) such that:

$$P(\varepsilon|r_{mean,i}, r_{cov,j}) = [P(r > r_{proof}|r_{mean,i}, r_{cov,j})]^k [P(r \leq r_{proof}|r_{mean,i}, r_{cov,j})]^{n-k} \quad (6)$$

For the case under consideration where the capacity follows a lognormal distribution that has an uncertain mean and an uncertain coefficient of variation  $r_{cov}$ , the likelihood function can be expressed in equation 7 such that:

$$P(\varepsilon|r_{mean,i}, r_{cov,j}) = \left[1 - \Phi\left(\frac{\ln r_{proof} - \lambda_i}{\xi_j}\right)\right]^k \left[\Phi\left(\frac{\ln r_{proof} - \lambda_i}{\xi_j}\right)\right]^{n-k} \quad (7)$$

Where  $\lambda$  and  $\xi$  are the parameters of the lognormal capacity distribution and are calculated according to equations 8 and 9.

$$\lambda_i = \ln(r_{mean,i}) - \frac{\xi_j^2}{2} \quad (8)$$

$$\xi_j = \sqrt{\ln(1 + r_{cov,j}^2)} \quad (9)$$

The likelihood function is used to update the joint prior probability mass function such that:

$$p'_{R_{mean,T,R_{COV}}}(r_{mean,i}, r_{COV,j} | \epsilon) = \frac{P(\epsilon | r_{mean,i}, r_{COV,j}) \cdot p_{R_{mean,T,R_{COV}}}(r_{mean,i}, r_{COV,j})}{\sum_{i=1}^{m1} \sum_{j=1}^{m2} P(\epsilon | r_{mean,i}, r_{COV,j}) \cdot p_{R_{mean,T,R_{COV}}}(r_{mean,i}, r_{COV,j})} \quad (10)$$

$p'_{R_{mean,T,R_{COV}}}(r_{mean,i}, r_{COV,j} | \epsilon)$  and  $p_{R_{mean,T,R_{COV}}}(r_{mean,i}, r_{COV,j} | \epsilon)$  are the updated

and the prior joint probabilities of the combination  $r_{mean,i}$  and  $r_{COV,j}$ , respectively, and n1 and n2 are the number of bins in the PMFs of the truncated mean and COV distributions, respectively.

It is important to note that the results of the proof load tests are assumed to be statistically independent. Therefore, the tests should be conducted at well separated distances between the piles to minimize any bias in the results due to the correlation in the soil properties and to represent the full range of spatial variability across the site.

### 3.3 Calculation of the probability of failure

A MATLAB code was developed to model the parameters, update the joint prior PMF of  $r_{mean}$  and  $r_{cov}$ , and calculate the prior and updated probability of failure due to proof load tests. In all the case studies represented in this thesis, the load distribution is modeled as a lognormal distribution with a fixed mean and COV, and the capacity distribution is modeled as a lognormal distribution with a variable mean and COV. Therefore, an exact solution for the probability of failure exists such that:

$$p_f = \Phi \left( -\frac{(\lambda_R - \lambda_S)}{\sqrt{(\xi_R)^2 + (\xi_S)^2}} \right) = \Phi(-\beta) \quad (11)$$

Where  $\beta$  is the reliability index, and  $\Phi()$  is the standard normal cumulative distribution functions. In addition,  $\lambda_R$  and  $\xi_R$  are the parameters of the lognormal distribution of the capacity calculated from  $r_{\text{mean}}$  and  $r_{\text{COV}}$ , and  $\lambda_S$  and  $\xi_S$  are the parameters of the lognormal distribution of the load calculated from  $s_{\text{mean}}$  and  $\delta_S$ . It is important to note that equation 11 is used in case the mean and the COV of both the capacity and the load are constants. In our work, the mean of the capacity and the COV are random variables. Therefore, the theorem of total probability is required to incorporate all possible values of  $r_{\text{mean}}$  and  $r_{\text{COV}}$  with their corresponding likelihood. The prior probability of failure in such a case can be obtained from equation 12, whereas the updated probability of failure, due to the proof load tests results, can be calculated according to equation 13 such that:

$$\mathbf{p}_f = \sum_{i=1}^{n1} \sum_{j=1}^{n2} \Phi \left( -\frac{(\lambda_{R,i} - \lambda_S)}{\sqrt{(\xi_{R,j})^2 + (\xi_S)^2}} \right) \mathbf{p}_{R_{\text{mean},T}, R_{\text{COV}}}(\mathbf{r}_{\text{mean},i}, \mathbf{r}_{\text{COV},j}) = \Phi(-\beta) \quad (12)$$

$$\mathbf{p}_f = \sum_{i=1}^{n1} \sum_{j=1}^{n2} \Phi \left( -\frac{(\lambda_{R,i} - \lambda_S)}{\sqrt{(\xi_{R,j})^2 + (\xi_S)^2}} \right) \mathbf{p}'_{R_{\text{mean},T}, R_{\text{COV}}}(\mathbf{r}_{\text{mean},i}, \mathbf{r}_{\text{COV},j}) = \Phi(-\beta) \quad (13)$$

These two equations are coded as a double loop operation on MATLAB to account for the contribution of all possible values of the mean and the coefficient of variation of the capacity.

## CHAPTER 4

### UPDATING PILE CAPACITY DISTRIBUTION WITH PROOF LOAD TESTS

In this chapter, the probabilistic pile capacity model will be updated using results of proof load tests and the effect of the updating process on the probability of failure will be studied. The sensitivity of the updating process to the choice of the lower-bound capacity, mean pile capacity, and the proof load test program will be investigated.

#### 4.1 Prior versus Updated PMFs for $r_{\text{mean}}$ and $r_{\text{COV}}$

The effect of the updating process on the marginal PMFs of  $r_{\text{mean}}$  and  $r_{\text{COV}}$  is illustrated in Fig. 5. The analysis pertains to the case where 5 successful proof load tests are conducted on piles designed with factor of safety of 2.0 and tested at a proof load level of 2 times the design load. Results are presented for the case where a truncated lognormal distribution is used to model the uncertainty in within site variability ( $r_{\text{COV}}$ ). The corresponding results for the other two candidate distributions (uniform and truncated normal) for  $r_{\text{COV}}$  are presented in Fig. 6 to investigate the effect of the choice of the probability distribution on the results. For all the cases analyzed, results on Figs. 5 and 6 indicate that the effect of conducting proof load tests is concentrated on the distribution of the mean pile capacity  $r_{\text{mean}}$  compared to the distribution of  $r_{\text{COV}}$ . The distribution of  $r_{\text{mean}}$  is shifted significantly to the right as a result of the successful proof load test results. With regards to

the effect of the updating process on  $r_{COV}$ , results show that the probability of smaller values of  $r_{COV}$  increased after updating whereas the probability masses for the higher values of  $r_{COV}$  were reduced. This observation was valid, irrespective of the type of distribution used to model  $r_{COV}$ . This is expected to have a positive impact on the updated reliability index for the proof-loaded design.

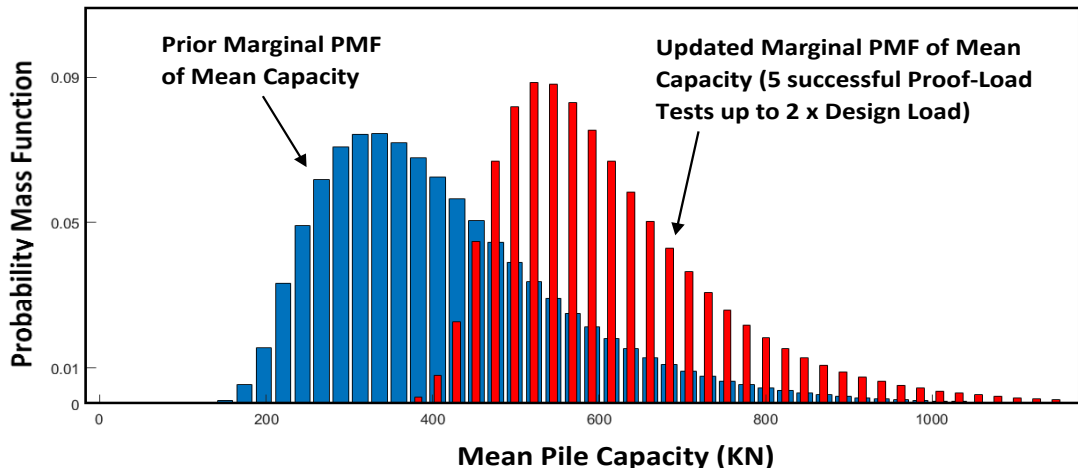
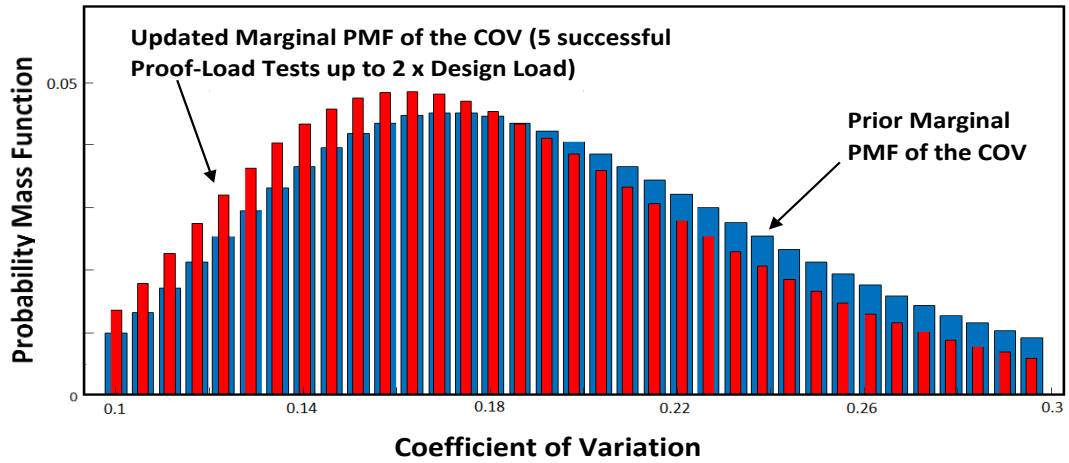


Figure 5 The Prior and Updated Distributions of (a) Within-Site Variability (Truncated Lognormal  $\rho_{cov}$ ), and (b) Mean Pile Capacity ( $r_{mean}$ )

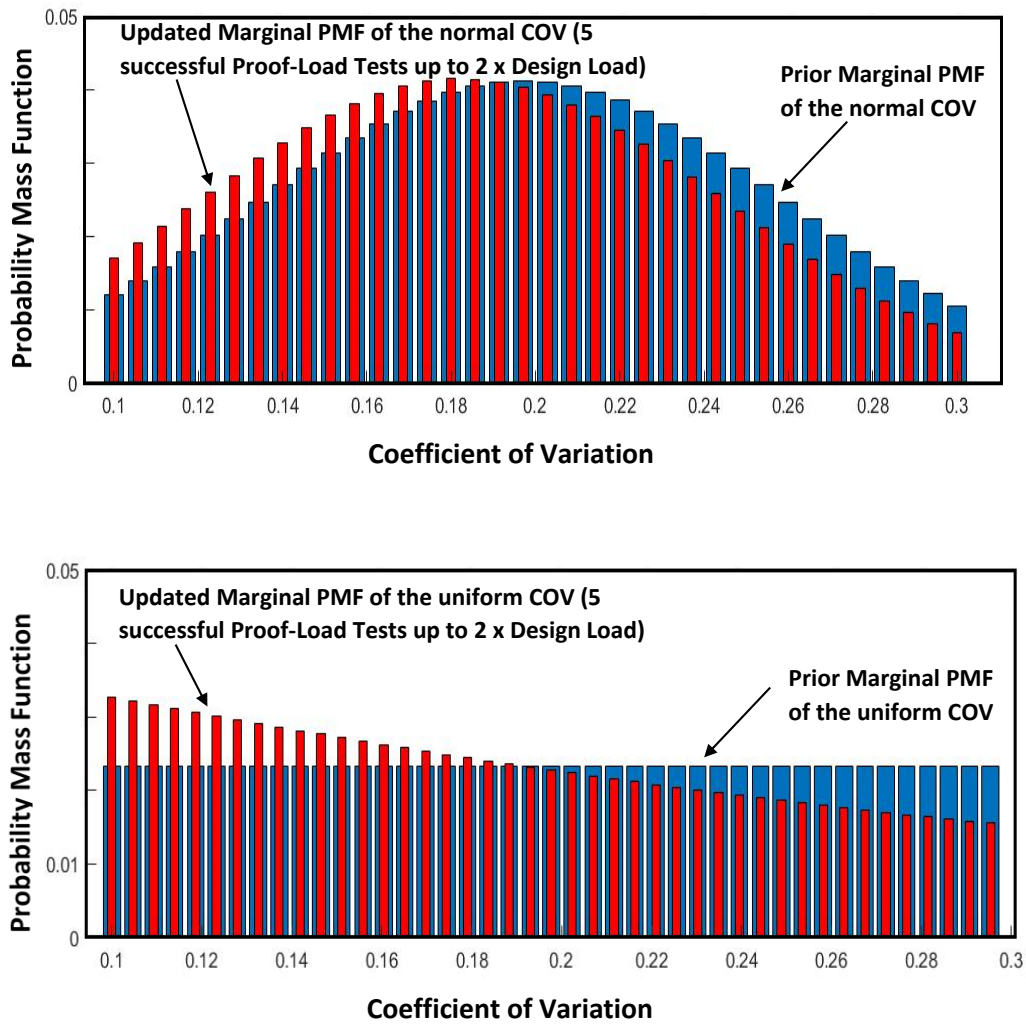


Figure 6 The Prior and Updated Distributions for (a) Truncated Normal Within-Site Variability, and (b) Uniform Within Site Variability.

The effect of the updating process on the reliability index of the design is studied in Figure 7 which shows the variation of the reliability index with the number of positive load tests. Results are shown for different proof load levels (1.5 to 3 times the design load) and for the three candidate probability distributions of  $r_{COV}$ . Also shown on Fig. 7 are results pertaining to the case where  $r_{COV}$  is assumed to be a deterministic value that is equal to the mean of  $r_{COV}$  for the other three distributions.



Results on Figure 7 indicate that the effect of the choice of the probability distribution on the reliability index is relatively small and can be considered negligible. The assumption of a uniform distribution for  $r_{COV}$  seems to produce reliability indices that are slightly smaller than those obtained for the truncated normal and lognormal distributions for all proof load levels. Since the updated reliability indices were found to be insensitive to the choice of the probability distribution describing  $r_{COV}$ , it could be concluded that the prior capacity distribution which represents within-site variability of identical piles could be represented by a coefficient of variation  $r_{COV}$  that follows a truncated log-normal distribution bounded between 0.1 and 0.3, with a mean of 0.2 and a COV of 0.31.

Although the updated reliability indices were insensitive to the distribution of  $r_{COV}$ , results on Fig. 7 show that the assumption of a deterministic  $r_{COV}$  that is not updated in the Bayesian exercise results in reliability indices that are larger than the cases involving an uncertain  $r_{COV}$ . This indicates that the assumption of a deterministic  $r_{COV}$  which was adopted by Najjar et al. (2017) may lead to conservative results which incorrectly magnify the impact of proof-load tests on the updated reliability index. This is particularly true for cases involving larger levels of proof load and number of positive proof load tests varying between 1 to 10. It is thus recommended that  $r_{COV}$  be considered an uncertain parameter that is updated in the Bayesian updating exercise. This recommendation is adopted in this thesis.

Analysis of the data on Figure 7 also indicates that, irrespective of the assigned  $r_{COV}$  distribution, the updated reliability index appears to be very sensitive to the initial 5 proof load tests. The sensitivity of the reliability index to the number of tests seems to decrease as the number of successful proof load tests increase further.

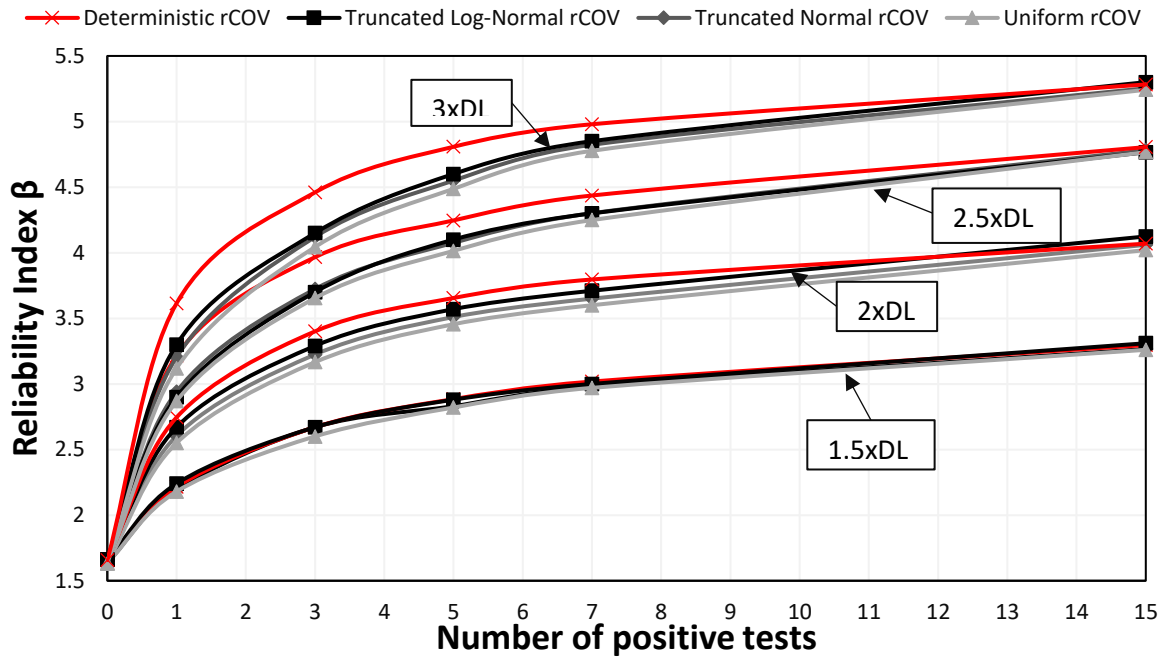


Figure 7 Effect of proof load test levels on the reliability index for different rCOV distributions (FS =2)

#### 4.2 Correlation between the COV and the mean distributions

In the prior pile capacity model that is adopted in this paper, the prior distributions of the mean capacity and the COV are considered to be uncorrelated (statistically independent). This assumption is based on the lack of any physical reason that would imply positive or negative correlation between the two parameter (mean and COV). Since both parameters are updated during the Bayesian exercise, the updated joint PMF could be used to back-calculate any correlation that exists after the updating. The correlation coefficient ( $\rho$ ) between  $r_{\text{mean}}$  and  $r_{\text{COV}}$  could be calculated from the covariance ( $cov$ ) between  $r_{\text{mean}}$  and  $r_{\text{COV}}$  in the updated joint PMF such that:

$$\rho_{mean,COV} = \frac{cov(mean,COV)}{\sigma_{mean} \times \sigma_{COV}} \quad (14)$$

$$cov(mean, COV) = \sum_i \sum_j p'_{R_{mean}, R_{COV}}(r_{mean}, r_{COV} | \varepsilon) \times R_{mean} \times R_{COV} - E(mean) \times E(COV) \quad (15)$$

$$\sigma_{mean} = \sqrt{E(mean^2) - E(mean)^2} \quad (16)$$

$$\sigma_{COV} = \sqrt{E(COV^2) - E(COV)^2} \quad (17)$$

Where  $cov(mean, COV)$  is the covariance between  $r_{mean}$  and the  $r_{COV}$  and  $\sigma_{mean}$ ,  $\sigma_{COV}$

are the standard deviation of  $r_{mean}$  and  $r_{COV}$ , respectively.  $E(mean)$  and  $E(COV)$  are the expected values of  $r_{mean}$  and  $r_{COV}$ , respectively and  $p'_{R_{mean}, R_{COV}}$  is the updated joint probability mass function of the combination of  $r_{mean i}$  and  $r_{COV j}$ .

The resulting correlation coefficients for cases where the number of successful proof load tests and the proof load level are varied are presented in Table 4 for the case where  $r_{COV}$  is assumed to follow a truncated lognormal distribution. For the case where no tests are conducted, the correlation coefficient between  $r_{mean}$  and  $r_{COV}$  is zero as expected. For the cases involving proof load tests of different numbers and levels, results on Table 4 indicate that small positive or negative correlations exist between the mean distribution and the COV ranging between -0.127 for 1 positive proof load test at 3xDL level and 0.28 for 15 positive load tests conducted at a high level (3xDL). These correlations could be considered to be small and are not expected to play a significant role in determining the reliability of the proof load tested design.

Table 4 correlation between  $r_{\text{mean}}$  and  $r_{\text{COV}}$  after updating (FS=2)

		Proof load test level				
		1xDL	1.5xDL	2xDL	2.5xDL	3xDL
Number of successful proof load tests	0	0	0	0	0	0
	1	0.013	0.008	-0.029	-0.070	-0.127
	3	0.035	0.060	0.062	0.047	0.026
	5	0.050	0.090	0.115	0.118	0.112
	15	0.090	0.178	0.229	0.260	0.280

### 4.3 Sensitivity of Results to the lower-bound Capacity and Mean Capacity Distributions

In this section, the sensitivity of the updating process to the assumptions of the lower-bound capacity distribution and the pile capacity prediction method will be studied as part of a comprehensive parametric analysis. The sensitivity of the problem to the assumption of the distribution of the lower-bound capacity will be tested for different scenarios which involve different pile capacity prediction methods using different ratios of lower-bound to mean capacity. The values of this ratio will vary from 0 (no lower bound), to 0.4, 0.5, and 0.6 of the mean pile capacity. Since the lower-bound distribution truncates the tail of the mean capacity distribution, it is important to study the effect of the COV of the mean capacity (representing model uncertainty in pile capacity predictions) on the results.

The sensitivity of the updating process to the lower-bound capacity will be studied on two types of  $r_{\text{mean}}$  distributions: (1) a mean capacity distribution with a relatively high COV of 0.5 (indicative of pile capacity predictions in sands) and (2) a mean capacity with a relatively low COV value of 0.15 (indicative of pile capacity predictions for clay). The two distributions are presented in Figure 8. In Figure 8(a), the lower-bound has a mean of 200

KN and a COV of 0.2 while  $r_{\text{mean}}$  has a mean of 400 KN and a high COV of (0.5). Figure 8(b) shows the same distributions but with a low COV of 0.15 for  $r_{\text{mean}}$ . The figure reflects the expected important role that a lower-bound capacity could play in defining the capacity model for the case with a higher COV of 0.5 compared to the negligible effect for the case with a COV of 0.15. For the case with higher COV for  $r_{\text{mean}}$ , the lower-bound capacity truncates the tail of the distribution of  $r_{\text{mean}}$  and eliminates lower capacity values.

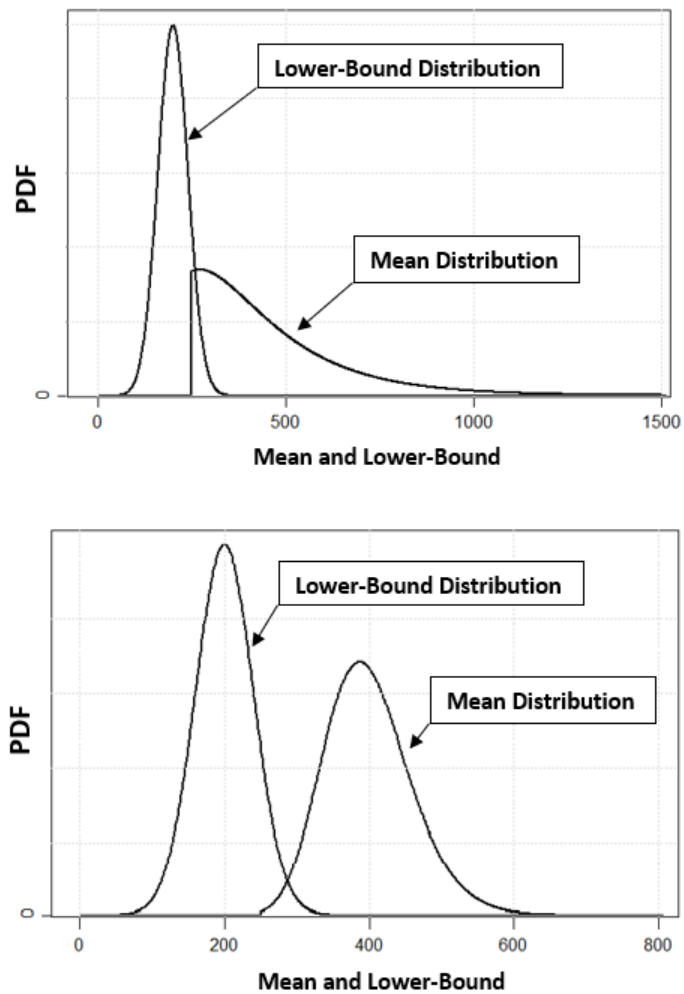


Figure 8 The effect of the lower bound truncation on the (a) mean capacity with a COV = 0.5 (b) mean capacity with a COV = 0.15

Figure 9 shows the variation of reliability index as a function of positive proof load tests for a high COV mean distribution. Results are shown for three levels of proof load tests (1.5xDL, 2.0xDL, and 2.5xDL) and four values of the mean lower-bound capacity (0, 0.4, 0.5, and 0.6 times the mean capacity).

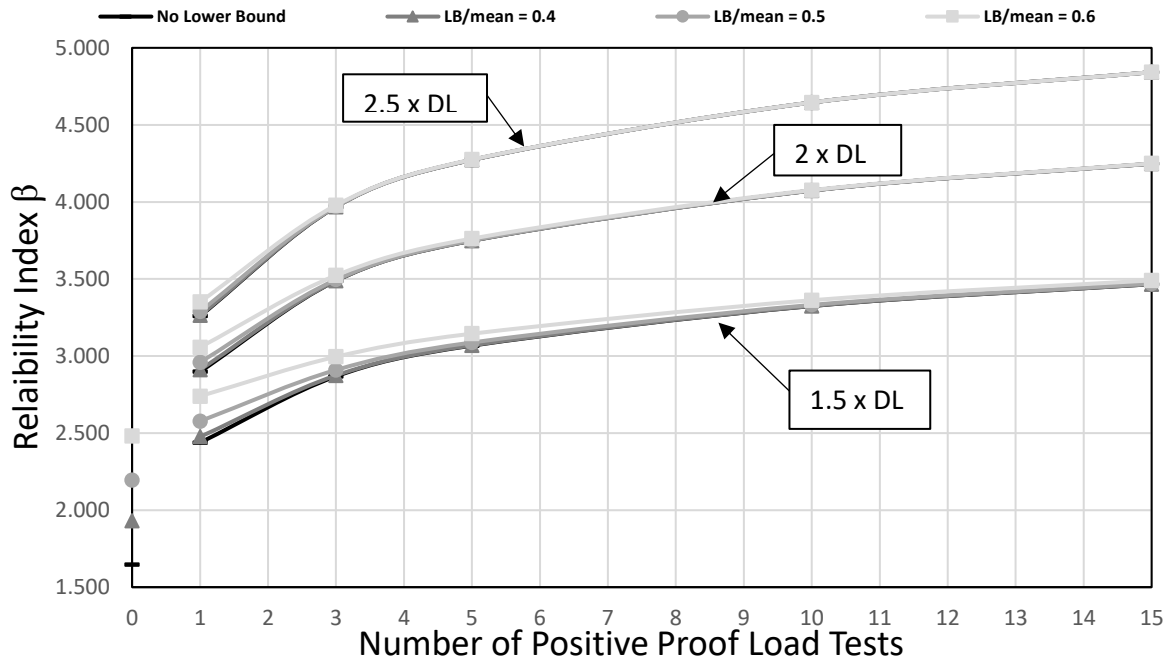


Figure 9 The variation of the reliability index as a function of positive proof load tests for different lower-bound to mean ratio applied at a 0.5 COV mean distribution (FS = 2)

Results on Fig. 9 show that for the case where no proof load tests are conducted (prior case), the value of the lower-bound capacity has a significant impact on the reliability index which is shown to vary from 1.6 (for the case with no lower-bound capacity) to about 2.5 (for the case with a lower-bound capacity equal to 0.6 times the mean capacity). The effect of the lower-bound capacity tends to decrease as the number of positive load tests increase, but this effect varies for different levels of proof load tests. For a smaller proof load level (1.5 x DL), the reliability index for different prior lower-bound capacities starts to converge

from the fifth positive test. For higher proof load levels (2xDL and 2.5xDL) the reliability index of different lower bounds converges from the second and first positive proof load test, respectively. These results are expected due to the fact that the updated mean capacity distribution is shifted to the right due to the positive load tests and therefore away from the lower bound distribution which leads to a decrease in the effect of truncation of the lower bound distribution on the reliability index.

Results on Fig. 9 pertain to the case where all the proof load tests are assumed to be positive. The effect of failures on the reliability index for different mean ratios of lower-bound capacity to mean capacity is studied on Fig. 10a for the same cases analyzed in Fig. 9 (COV of  $r_{\text{mean}} = 0.5$ ). The analysis entails four scenarios as follows: (1) all the tests are positive, (2) one test is negative, (3) three tests are negative, and (4) five tests are negative.

The variation of the reliability index as a function of the proof load test (2xDL) outcome of these four scenarios are represented in Figure 10a. Whereas the results of the same scenarios conducted at different proof load levels are presented in Appendix 1. Results on Figure 10 indicate that the assumption of different lower-bound capacities has a significant impact only on cases where all the tested piles fail in carrying the proof load. In these cases, a difference of about 1.0 exists in the updated reliability index for the case involving no lower bound and the case involving a mean lower-bound capacity that is taken as 0.6 times the mean capacity. Interestingly, results also show that successive negative proof load tests followed by one positive proof load test is sufficient for the convergence of the reliability index for the four assumed values of the mean lower-bound capacity. As an example, if 6 proof load tests are conducted where 5 tests are negative and the sixth test is positive, the

results show that the reliability index of the 4 lower-bound ratios varies between 1.8, when there is no lower-bound, and 2 when the ratio of the lower-bound to that of the mean is 0.6.

This detailed study reveals that the effect of the ratio of the lower bound to that of the mean on the updated reliability index is negligible (for the case with a COV of 0.5 for  $r_{\text{mean}}$ ) for at least one positive proof load test, whereas this effect is significant for the prior results (no tests are applied) or for the case where all the proof load tests are negative.

The results on Figures 9 and 10a pertain to the case where the COV of the mean capacity is relatively high (COV = 0.5, ex. case of piles in sands). To illustrate the effect of the lower-bound for cases involving a smaller level of uncertainty in the mean capacity (COV = 0.15, ex. case of piles in clay) the same procedure is applied and the results are presented in Fig. 10b). Figure 10b shows the effect of positive and negative proof load tests conducted at 2xDL level, on the 0.15 COV mean distribution for different lower-bound ratios. The effect of other proof load tests levels for the same mean distribution is found in Appendix 1.

The results show that the prior reliability index (no tests are conducted) varies between 2.45 when there is no lower bound and 2.5 when the ratio of the lower bound to that of the mean is 0.6. This reveals that the lower bound has no effect on the prior reliability index. This result is expected given the low COV of the mean capacity distribution, rendering the lower bound ineffective when truncating the left hand tail of the mean capacity distribution. More importantly, results on Fig. 10b indicate that the reliability index is insensitive to the assumption of the ratio of the mean lower-bound capacity to the mean capacity for both positive and negative proof load test results.



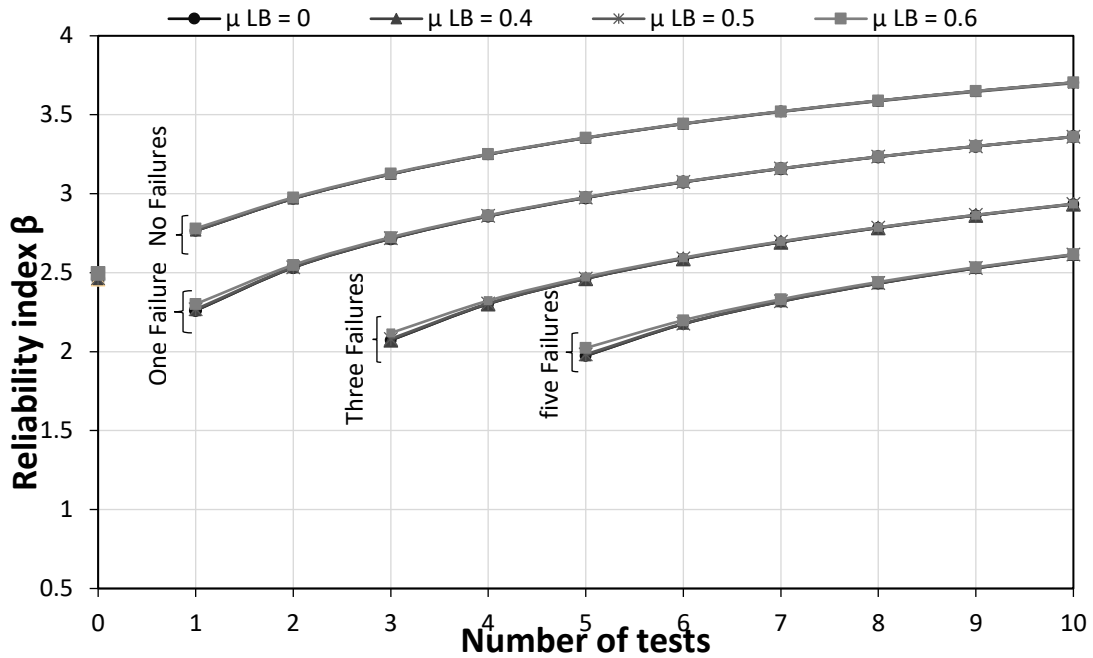
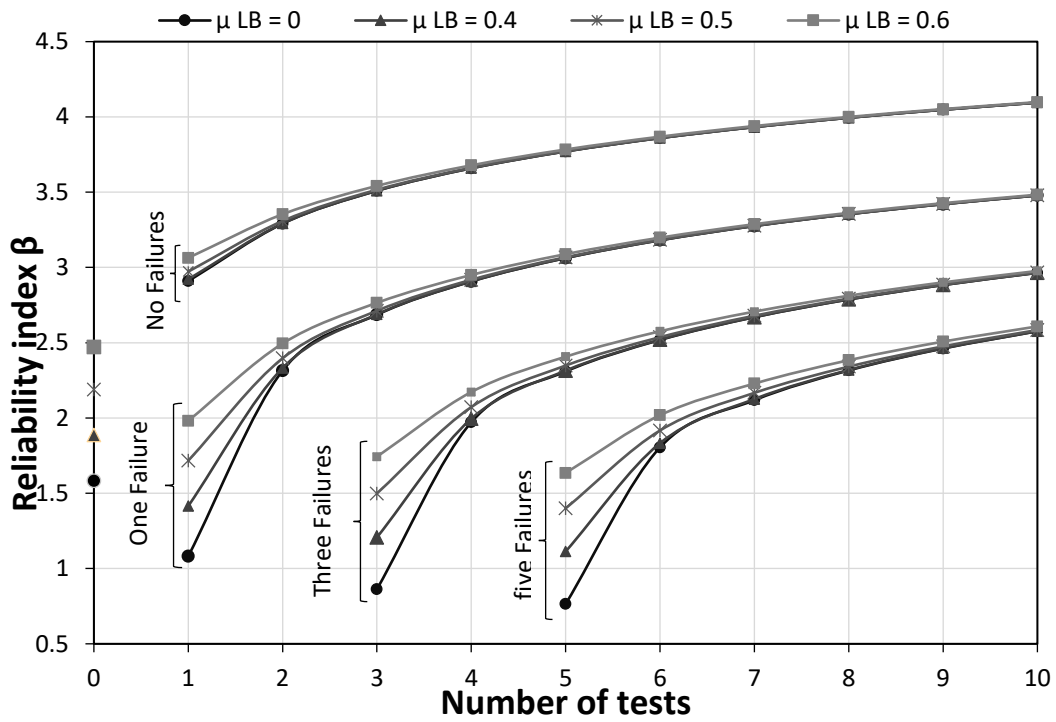


Figure 10 Effect of the mean lower-bound capacity on the reliability index for cases involving proof load levels of 2xDL and (a) COV of  $r_{mean} = 0.5$  and (b) COV of  $r_{mean} = 0.15$  (FS = 2).

For the rest of this study, the mean of the lower-bound capacity is chosen to be half that of the mean capacity. However, in the decision making exercises that will be presented in chapter 7, the mean lower-bound capacity will be calculated for each case history analyzed based on the lower-bound prediction models proposed by Gilbert et al. (2005).

#### **4.4 Sensitivity of the Results to the Pile Prediction Method**

Pile prediction methods suffer from model uncertainty that could be quantified using databases of pile loads tests. The study by Lehane et al. (2017) showed that different pile prediction methods exhibited different levels of model uncertainty. The statistics describing the bias in the model predictions show significant differences between methods (SPT-based or CPT-based) and soil types (sands versus clays). These model uncertainties are reflected in the probability distribution of the mean pile capacity in the pile capacity model adopted in this thesis (Figure 3c). It is thus expected that the results of the Bayesian updating exercise in the presence of proof load tests will be affected by the choice of the method used to predict the pile capacity.

The pile prediction methods differ for every soil type and can be classified into methods that target driven piles in sand and others that target driven piles in clay. For pile prediction methods in sands, these methods can be further classified as Standard Penetration Test (SPT) – based methods and Cone Penetration Test (CPT)-based methods. A summary of the statistics describing model uncertainty for SPT-based methods and CPT-based methods for driven piles in sands and clays are presented in Tables 5 and 6, respectively.

Table 5 The Statistics of Methods Used for Piles in Sand

Methods (Sands)	Skin friction		End bearing		References
	Bias	COV	Bias factor	COV	
API (SPT)	1.58	0.61	1.60	0.57	Lacasse et al. (2013)
NGI-05 (CPT)	1.09	0.23	1.02	0.21	Lacasse et al. (2013)
ICP-05 (CPT)	1.09	0.23	1.16	0.21	Lacasse et al. (2013)
Fugro-96 (CPT)	1.25	0.30	0.90	0.24	Lacasse et al. (2013)
UWA-05 (CPT)	1.05	0.35	1.10	0.25	Lacasse et al. (2013)

Table 6 The Statistics of Different Methods Used to Design Piles in Clays

Methods (clays)	Bias factor	COV	References
API	1.11	0.27	Lacasse et al. (2013)
NGI-05	1.06	0.16	Lacasse et al. (2013)
ICP-05	0.99	0.23	Lacasse et al. (2013)
Fugro-96	1.01	0.18	Lacasse et al. (2013)

The two main parameters that will affect the result of the prior and updated reliability index are the bias factor and the COV. The bias factor is the mean of the ratio of the measured capacity to that predicted capacity as obtained from pile load test databases. The bias factor governs the position of the mean capacity distribution. The second factor is the COV, which is calculated as the COV of the ratio of the measured to predicted pile capacities as obtained from the databases. The COV will govern the uncertainty/spread in the distribution of the mean pile capacity.

#### 4.4.1 Sensitivity analysis for pile prediction methods for sand

Table 5 presents the bias factor and the COV of different SPT and CPT based methods for sand. These parameters were suggested by Lacasse et al. (2013) based on a comprehensive state-of-the-knowledge database of full-scale pile load tests. These statistical parameters are divided into statistics related to the skin friction and statistics related to the

tip resistance. As expected, the statistics of the model uncertainty factors differ between the tip resistance and the skin friction in any given prediction method. Therefore, the prior and updated reliability indices of the piles could differ from site to site depending on the percentage of the load that is carried by tip resistance relative to the percentage that is carried by skin friction even using the same prediction model.

To analyzed representative cases with different relative percentages of tip versus skin resistances in the reliability analysis, three combinations of skin friction and tip resistance are analyzed: (1) 80% of the total resistance is governed by skin friction and 20% by tip resistance. (2) 50% for skin friction and 50% for tip resistance, and (3) 20% for skin friction and 80% for tip resistance. Since the MATLAB code that was developed for this thesis adopts as input only one value for the bias factor and COV for the mean capacity distribution, a first order approximation was used to combine the contributions of the bias factor from skin friction and tip resistance into one bias factor and COV for each of the three cases analyzed such that:

$$\lambda = \%_{skin} \times \lambda_{skin} + \%_{tip} \times \lambda_{tip} \quad (18)$$

$$COV = \frac{\sqrt{(\%_{skin})^2 \times (COV_{skin})^2 \times (\lambda_{skin})^2 + (\%_{tip})^2 \times (COV_{tip})^2 \times (\lambda_{tip})^2}}{\%_{skin} \times \lambda_{skin} + \%_{tip} \times \lambda_{tip}} \quad (19)$$

Where  $\lambda$  and COV are the combined bias factor and COV of the mean capacity distribution, respectively. The results of the first order approximation are presented in Table 7 for the methods involving driven piles in sand. Results indicate that the SPT-based API method has the highest combined bias factor (~1.6) and highest COV (between 0.42 and 0.50). The NGI and the ICP methods exhibit relatively similar model factor statistics with bias factors in the order of 1.04 to 1.08 for NGI and 1.10 to 1.15 for ICP with COVs ranging

from 0.17 to 0.19 for both methods. The COVs for FUGRO and UWA methods are relatively larger and range from 0.20 to 0.28 with associated bias factors ranging from 0.97 (80% skin friction vs 20% end bearing) to 1.18 (20% skin friction vs 80% end bearing) for FUGROs method and 1.06 to 1.09 for the UWA method. It should be noted that for almost all the methods analyzed the lower values of COV tend to be for cases involving 80% end bearing and 20% skin friction, which is reflective of the larger COVs that are associated with skin friction predictions in Table 5.

Table 7 The bias factor and COV results for different skin friction and tip resistance combinations for CPT based methods

Methods	Percentage skin friction	Percentage tip resistance	Calculated bias factor	Calculated COV
Current API	80	20	1.584	0.500
	50	50	1.59	0.417
	20	80	1.596	0.473
NGI-05	80	20	1.076	0.191
	50	50	1.055	0.156
	20	80	1.034	0.173
ICP-05	80	20	1.104	0.187
	50	50	1.125	0.155
	20	80	1.146	0.176
Fugro-96	80	20	1.180	0.257
	50	50	1.075	0.203
	20	80	0.970	0.201
UWA-05	80	20	1.060	0.282
	50	50	1.075	0.213
	20	80	1.090	0.213

To illustrate the effects of the method used to predict the pile capacity and the percentages of the skin and tip resistances to the total capacity on the reliability index, cases

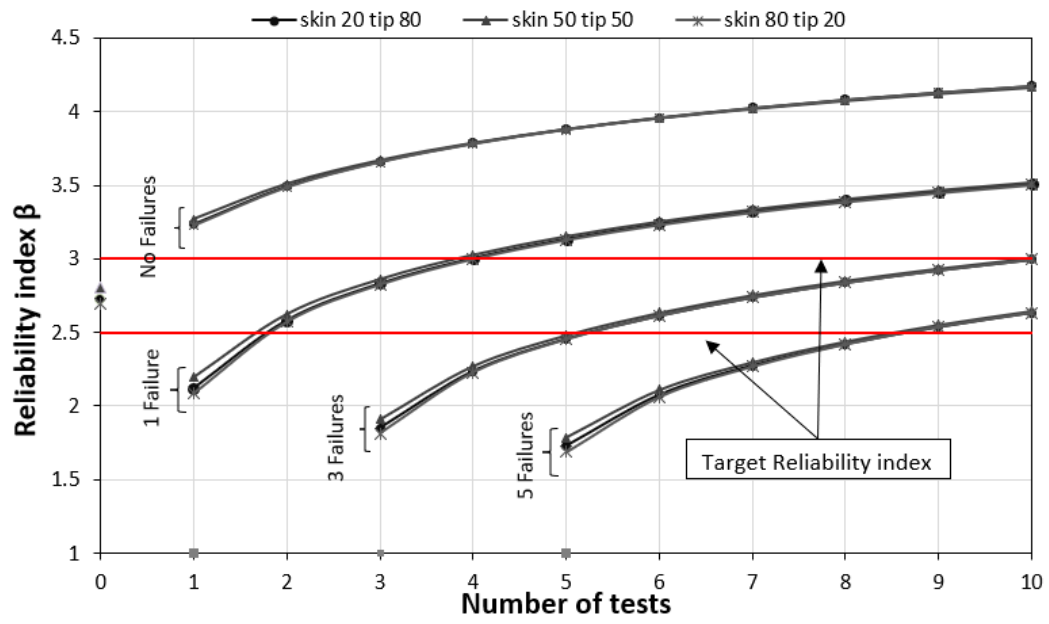
involving piles that are designed with a factor of safety of 2.0 and subjected to proof load tests with a proof load level of 2xDL are considered. In all the cases analyzed, a lower-bound capacity with a mean that is equal to 0.5 times the mean pile capacity is considered. Figures 11a to 11d show the prior and updated reliability indices for the 3 proportions of skin friction and tip resistance for the API, Fugro-96, ICP, and UWA method, respectively as a function of the number of proof load tests including possible failures.

For the API method, results on Fig. 11a indicate that the prior and updated reliability indices were not sensitive to the different proportions of skin friction and tip resistance. The prior reliability indices were about 2.7 and increased to values exceeding 3.0 for proof load test programs with no failures. For cases involving failures, results for the API method indicate that at least 50% of the tests have to be positive in order for the updated reliability index to exceed 2.5 and that at least 75% of the tests have to be positive so that a target reliability index that exceeds 3.0 is achieved, with the minimum number of four proof load tests.

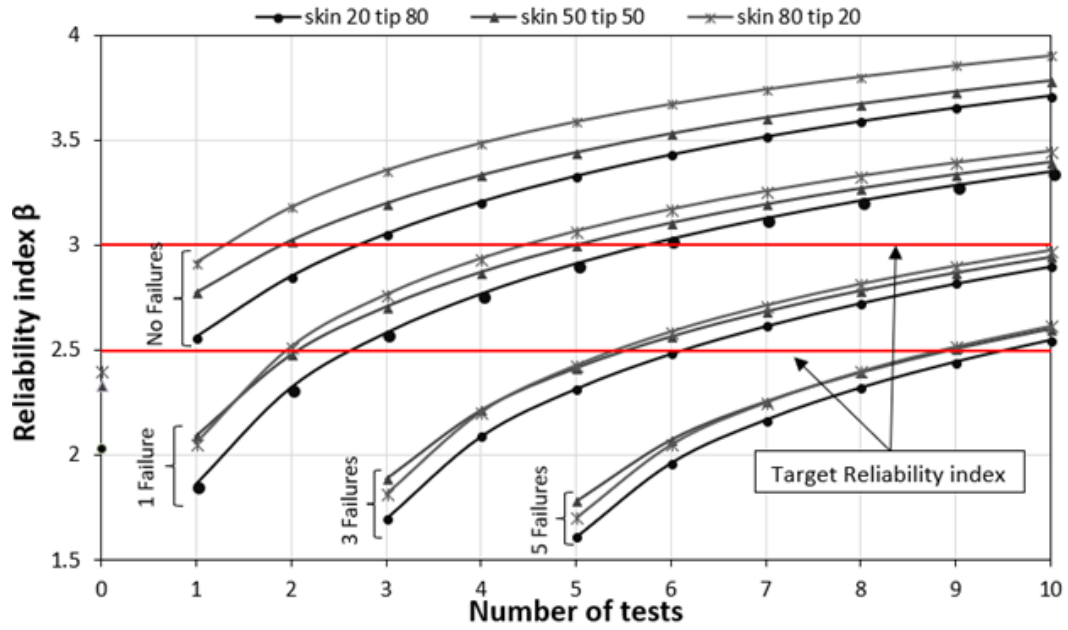
Results for the FUGRO method (Fig. 11b) show that the prior and updated reliability indices are sensitive to the 3 combinations of skin friction and end bearing. For the prior cases, a higher reliability index of 2.41 is achieved when the pile resistance is governed by the skin resistance (80% skin and 20% tip resistance) compared to a reliability index of 2.04 when the pile's tip is 80% of the total resistance. This result is expected since the combination of (80% skin and 20% tip resistance) has the higher bias factor, even though it has the highest COV but the difference in the bias factor in this method dominates the COV variation.

To bring the reliability index to values that are greater than 2.5 and 3.0, proof load test programs that consist of one positive test and three positive tests are needed, respectively. For test programs that may involve failures, results for the FUGRO method show that at least 50% of the tests should be positive for the cases involving 80% and 50% skin friction, and at least 67% of the tests should be positive for the cases involving 20% skin friction. If a higher target reliability index of 3.0 is required, results indicate that a minimum number of 6 proof load tests should be conducted, with a percentage of successful piles of at least 85% for all skin friction and end bearing combinations. These numbers are higher than those witnessed for the API method indicating the need for additional proof load tests and a larger percentage of successful piles in the FUGRO method to achieve target levels of reliability in the proof-tested designs.

Results for the ICP method (Fig. 11c) show that for the prior cases, a higher reliability index of 2.65 is achieved when the pile resistance entails 20%-80% and 50%-50% combinations of skin friction to tip resistance. The prior reliability index is reduced to 2.50 for the case where the skin resistance governs (80%-20%). Upon implementing proof-load test programs, an updated target reliability index of 3.0 can be achieved with a minimum of 2 positive tests, irrespective of the skin friction to tip resistance proportions. For the cases involving possible failures, results indicate that test program with at least 50% positive tests are required to achieve a target reliability index of 2.5. To achieve the higher reliability index of 3, at least 5 tests have to be conducted with a minimum of 80% of the tests being positive.

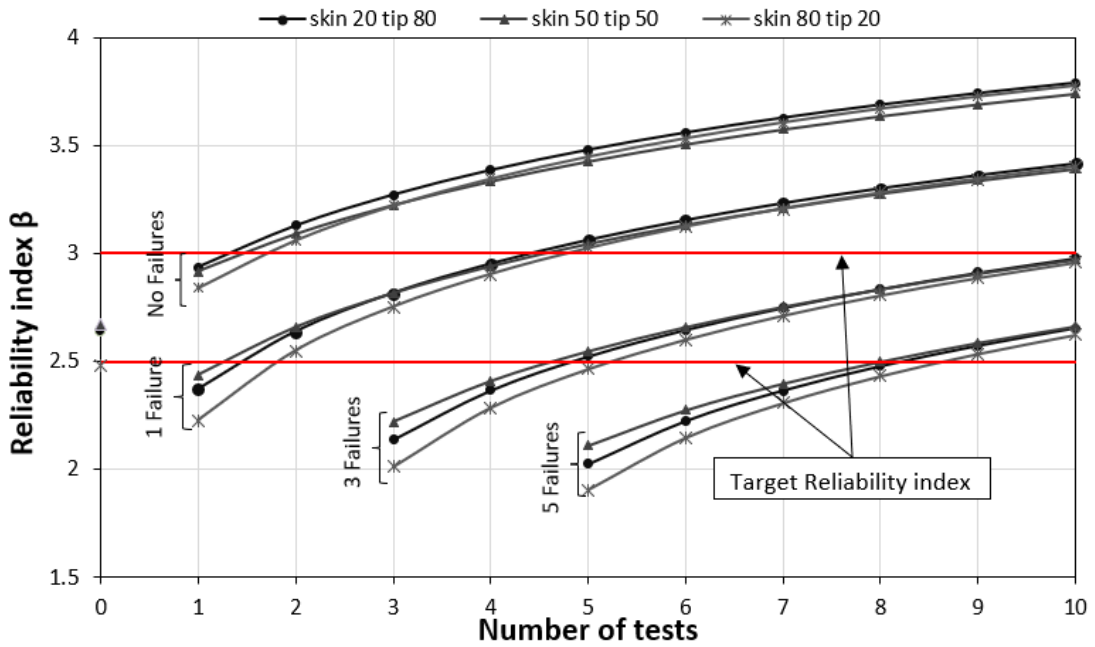


(a) API Method

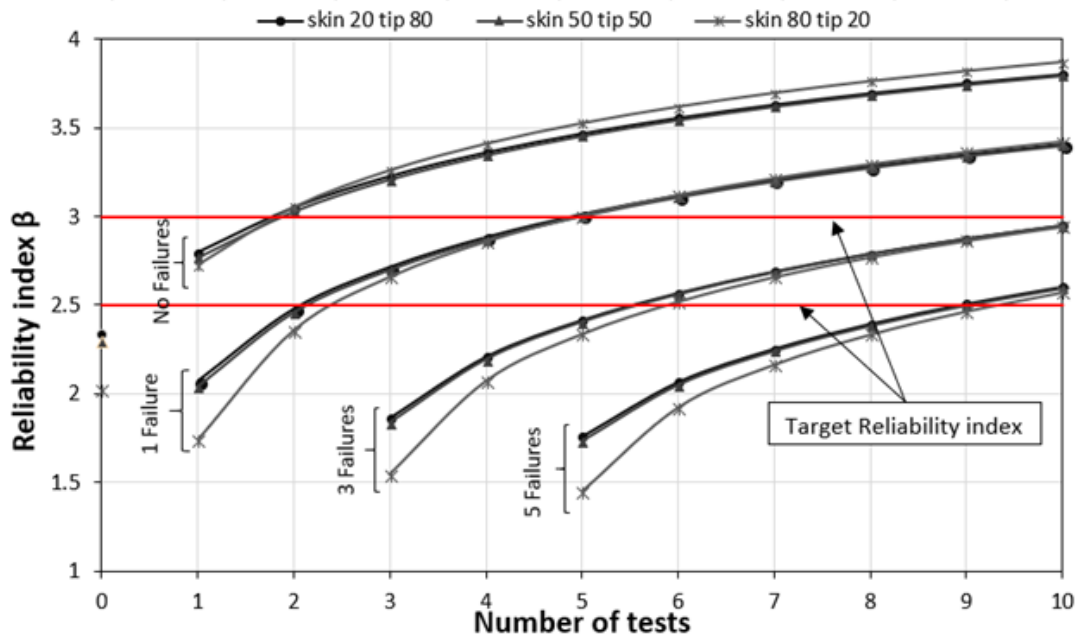


(b) FUGRO Method





(c) ICP Method



(d) UWA Method

Figure 11 The variation of the reliability index as a function of different proof load test outcome for (a) API method, (b) FUGRO method, (c) ICP method, and (d) UWA method (FS = 2. Rproof = 2xDL)

Similar to the ICP method, results for the UWA method (Fig. 11d) show that for the prior cases, a higher reliability index of about 2.35 is achieved when the pile resistance entails 20%-80% and 50%-50% combinations of skin friction to tip resistance. The prior reliability index is reduced to a low value of 2.0 for the case where the skin resistance governs (80%-20%). Upon implementing proof-load test programs, updated target reliability indices of 2.5 and 3.0 can be achieved with a minimum of 1 and 2 positive tests, respectively, irrespective of the skin friction to tip resistance proportions. For the cases involving possible failures, results indicate that test program with a minimum of 3 tests and at least 66% positive tests are required to achieve a target reliability index of 2.5. To achieve the higher reliability index of 3, at least 5 tests have to be conducted with a minimum of 80% of the tests being positive. These results are relatively similar to those observed in the ICP method.

To provide a one-to-one comparison between the prior and updated reliability indices for the different pile prediction methods, the results pertaining to the 50% skin – 50% tip resistance combination are presented for the API, ICP, and UWA methods on Figure 12. The curves on Fig. 12 clearly indicate that the pile prediction method plays a role in defining both the prior and updated reliability indices. The difference between methods is mostly portrayed for the cases involving proof load test programs with no failures. In these cases, the API method seems to result in the largest reliability indices compared to the other two methods. Interestingly, for cases involving failure, the results from the different methods start to converge, particularly for cases where the number of proof load tests and the number of failures increase. For cases with relatively high percentages of failed load tests (for example 3 and 4 proof tests with 3 failures and 5 and 6 tests with 5 failures), the results from the ICP

diverge slightly from the results of the other two methods with updated reliability indices that are relatively larger than the other two methods. These results confirm the need for incorporating the effect of the pile prediction method in any reliability-based decision making framework that aims at optimizing the value of proof-load test programs for driven piles.

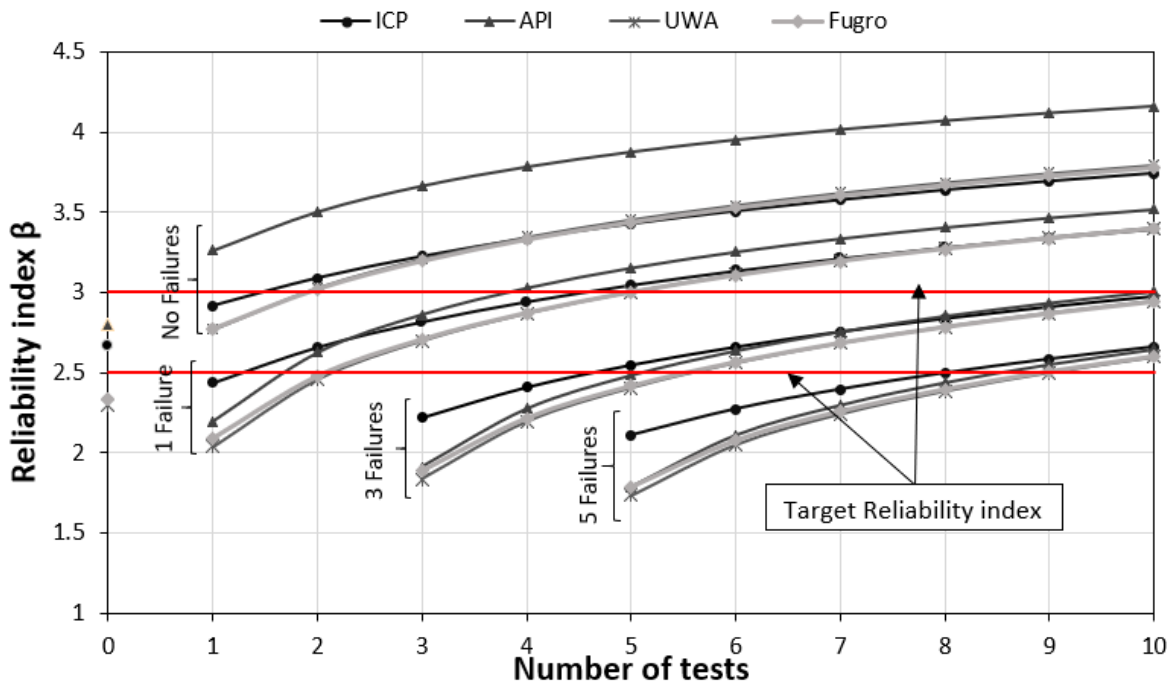


Figure 12 Comparison between the prior and updated reliability indices observed for (a) API method, (b) ICP method, and (c) UWA method ( $FS = 2$ ,  $r_{proof} = 2xDL$ )

In conclusion, the effect of different combinations of tip resistance and skin friction on the prior and updated reliability index of the pile varies from method to another, since this effect is directly linked to the statistics of the bias factor and the COV that varies from method to another.

#### 4.4.2 Sensitivity analysis for pile prediction methods for clay

Table 6 summarizes the statistics describing the model uncertainty for prediction methods involving driven piles in clays as presented in Lehane et al. (2017). For these methods, the mean bias factors range from 0.99 to 1.11 and the model uncertainty is represented by COVs ranging from 0.16 to 0.27. To investigate the sensitivity of the updating process to the pile prediction method, prior and updated reliability indices are calculated and plotted for cases involving proof load test programs that are conducted using proof load levels of 1.5xDL (Fig. 13a) and 2.5xDL (Fig. 13b). All cases pertain to piles that are designed using a reduced factor of safety of 2.0.

The prior results (no proof load tests are conducted) on Figure 13 show that the prior reliability indices vary between a minimum of 2 for the ICP method and a maximum of 2.5 for the NGI method, indicating that methods with the largest bias factors and the lowest COV yield the highest reliability indices. For the case involving the smaller proof load level of 1.5xDL, the updated reliability indices indicate that at least 2 positive tests are required to achieve a target reliability index of 2.5 and 9 positive tests are required to achieve the higher target reliability index of 3.0. These relatively large numbers are due to the relatively small proof load level of 1.5xDL. For the cases involving possible failures, results indicate that as little as one negative test result for a proof load level of 1.5xDL results in a significant reduction in the reliability index. If one failure occurs at this proof load level, the target reliability indices of 2.5 and 3 cannot be achieved even if 10 tests are conducted. This observation applies equally to all pile prediction methods.

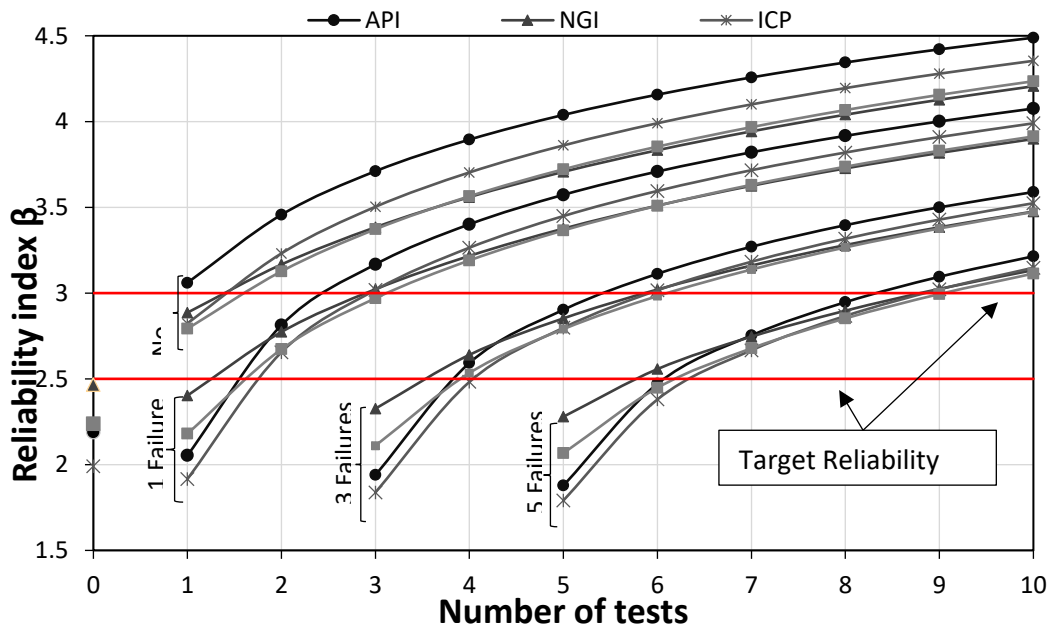
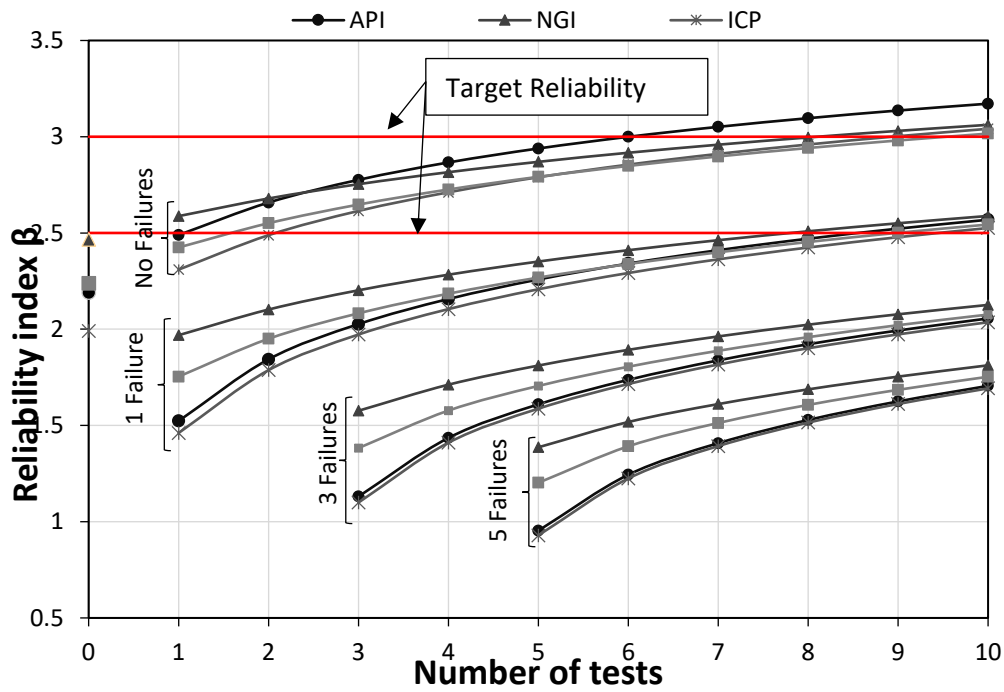


Figure 13 The variation of the reliability index as a function of different proof load test outcomes at  $r_{proof}$  equal to (a)  $1.5 \times DL$  and (2)  $2.5 \times DL$  for different pile prediction method in clay (FS = 2)

Figure 13b shows the reliability indices of different clay-based methods as a function of the number of static proof load tests conducted at 2.5xDL level. Results for this relatively high proof load level indicate that one positive proof load test is enough to increase the reliability index of the different methods above the target reliability index of 2.5. To achieve a higher target reliability index of 3.0, one positive test is enough for the API method while two positive tests are required for the other three methods. For cases involving possible failures, results on Fig. 13b indicate that at least 30% of the tested have to be positive so that a reliability index of 2.5 is achieved. This percentage of positive tests need to be increased to 50% for achieving a reliability index of 3.0. These conclusions are valid for all pile prediction methods.

Despite the uniformity in the recommendations regarding the number of tests needed to achieve a required reliability index in each pile prediction methods, the detailed results on Fig. 13a and 13b show significant differences between the updated reliability indices among methods. It is this expected that the pile prediction method will have a significant impact in the context of a decision making framework that aims that maximizing the value of proof load test programs for a given case study. The decision making framework will utilize the prior and updated reliability indices shown on Fig. 13 as input to the decision tree. As such, decision is expected to be significantly influences by the method used to predict the pile capacity even for piles in clay.

## CHAPTER 5

### DECISION MAKING FRAMEWORK

The main outcome in the study conducted by Najjar et al. (2017) is a rational decision making that would facilitate the choice of a load test program that has the maximum expected benefit to the project. The method relies on a pre-posterior approach (Ang and Tang 1984) which takes into consideration different possible outcomes of any decision alternative.

#### **5.1 Methodology of Decision Framework (Najjar et al. 2017)**

In the method presented in Najjar et al. (2017), the main decision alternatives were (1) the proof load level  $r_{\text{proof}}$  and (2) the number of proof load tests to be conducted,  $n$ . For each of the potential test outcomes that are associated with a given decision alternative, the updated reliability index could be evaluated using Bayesian techniques. The resulting updated reliability index will depend on the outcome, with relatively high indices expected for cases involving positive tests and relatively low indices for cases involving failures. These reliability indices could be lower or higher than a target reliability index that is set for the piles in the project. As a result, outcomes where the updated reliability index is below the target indicate that the allowable capacity per pile (design load per pile) will have to be reduced in light of the load test results. On the other hand, outcomes where the updated reliability index is above the target allow for an increase in the allowable capacity (design

load) per pile in comparison to the base case. The allowable pile capacity (design load) could be calculated by utilizing the updated capacity distribution for that particular outcome.

From a practical design standpoint, any increase or decrease in the allowable capacity per pile as a result of conducting the proof load tests can be translated to (1) reduction/increase in the total number of piles required to support the superstructure loads without changing the geometry of the piles, or (2) reduction/increase in the geometry of the piles (length and/or diameter) without changing the total number of piles required. For the work presented in Najjar et al. (2017), the consequences associated with the outcomes of any decision alternative are assumed to be reflected in the total number of required piles without resorting to any change in the pile length or diameter. Based on the above, the consequences of any potential test outcome will be reflected in the benefits/costs associated with reducing/increasing the required number of piles to support the superstructure load without changing the geometry of the piles under consideration.

The financial benefit is reflected in the cost savings associated with this reduction in the number of piles. On the other hand, there is a negative financial cost that is associated with the cost of conducting the load test program alternatives and the cost of replacing failed piles when relevant. The net benefit of any test outcome can be calculated by subtracting the benefits due to reducing (or cost due to increasing) the number of piles in the site from the costs associated with conducting the proof load tests including the cost of replacing failed piles. Once the net benefit of all the test alternatives and their associated potential outcomes are calculated, the “expected” benefit of each alternative load test program can be calculated.



The alternative pile testing program that has the highest expected benefit could then be selected as the test alternative that has the highest value.

To illustrate the practicality of the decision-making framework, Najjar et al. (2017) presented a practical design example that involves piles that are driven in a site consisting of medium dense sand is considered. The pile design consisted of closed-ended steel pipe piles with an outside diameter of 355 mm and a length of 25 m. The predicted nominal axial capacity of a single driven pile is 1.8 MN and the lower-bound is calculated to be equal to 0.9 MN accounting to about 0.5 of the nominal axial capacity. For the purpose of illustrating the decision-making methodology, hypothetical cases that involve different superstructure loads were adopted, and it was assumed that the superstructure load will be supported by a group of identical steel pipe piles that will share the superstructure load equally.

The example illustrating the use of the decision framework was limited to determining the optimum proof load level and the optimum number of tests to be conducted. The number of pile load tests that were considered as decision alternatives is 1, 2, 3, 5, 7, and 10 proof tests to be conducted at load levels of 1.5, 2, and 2.5 times the design load or 0.75, 1.0, and 1.25 times the predicted capacity. These decision alternatives are presented in the context of a simplified decision tree in Fig. 14 (Najjar et al. 2017) with detailed calculations pertaining to the case of the test alternative that includes a proof load level of 2.0 times the design load presented for illustration. The results indicate that the proof-load test program alternative that is based on conducting 5 proof load tests up to a proof load level of 1.5 times the design load yields the largest expected benefit (\$ 297,965) among all other test alternatives.

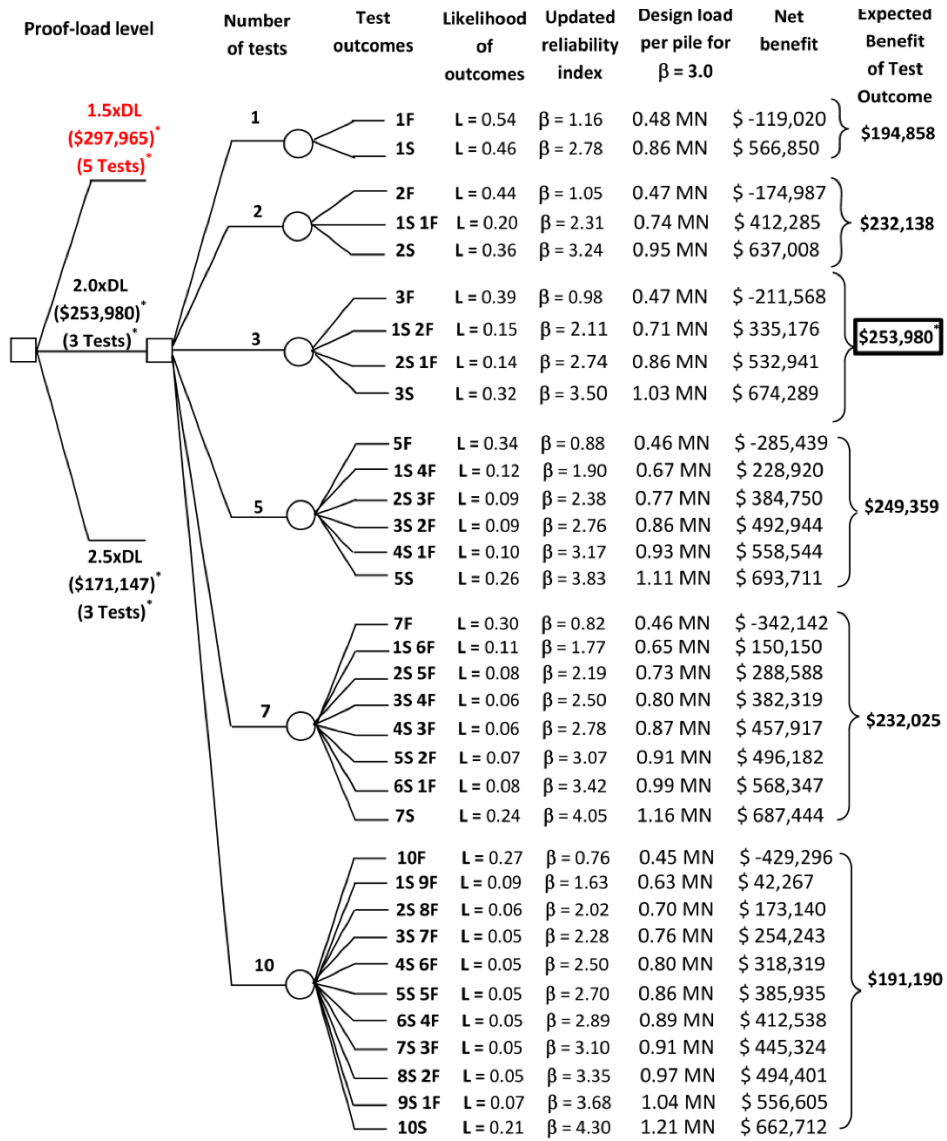


Figure 14 Sample Decision Making Example as Presented in Najjar et al. (2017)

## 5.2 Model and MATLAB code update

In this section, the mathematical framework of the pre-posterior decision analysis that pertains to the capacity model that was adopted in this study is presented. The decision

framework is based on that proposed by Najjar et al. (2017) and incorporates input related to the super structure load and pile capacity which depends on the type of soil, piles dimensions, and design method used to predict the capacity. To test the applicability of the decision framework, several sites were chosen to represent soils of different types, piles of different dimensions, and different design methods.

The main strength of the decision framework lies in its ability to incorporate different possible outcomes of any decision alternative. In the decision tree, each possible outcome is associated with a likelihood of occurrence. This likelihood is calculated for every outcome as a function of the parameters of the prior joint probability PMF or  $r_{mean}$  and  $r_{COV}$  such that:

$$p(\theta) = \sum_{i=1}^{n_1} \sum_{j=1}^{n_2} \frac{n!}{k!(n-k)!} \left[ \mathbf{1} - \Phi\left(\frac{\ln r_{proof} - \lambda_i}{\xi_j}\right) \right]^k \left[ \Phi\left(\frac{\ln r_{proof} - \lambda_i}{\xi_j}\right) \right]^{n-k} p_{R_{mean}, R_{COV}}(r_{mean,i}, r_{COV}), j \quad (20)$$

Where  $\frac{n!}{k!(n-k)!}$  is a factor that takes into consideration different combinations and permutations that characterize any possible outcome.

The first step in the pre-posterior analysis is to calculate the required number of piles if no tests are conducted according to equation 21.

$$N_{required} = S_{super} / DL_{no\ test} \quad (21)$$

Where  $N_{required}$  is the required number of piles in a certain site if no tests are conducted,  $S_{super}$  is the total load in the site, and  $DL_{no\ test}$  is the calculated dead load of each pile that ensures a reliability index of 3.

The required number of piles could be reduced after the implementation of a proof load testing program. For illustration, the number of pile load tests to be considered in the

decision alternative ranges from 1 to 10, and in some particular cases and sites, the number of tests can reach to 20 pile load tests. For each outcome of the alternative load tests, the likelihood is calculated according to equation 22, and the required DL to achieve a reliability index of 3 is calculated using the MATLAB code. The next step is to calculate the new required number of piles for each outcome according to equation:

$$N'_{required} = S_{super} / DL_{outcome} \quad (22)$$

Where  $N'_{required}$  is the updated required number of piles in a certain site due to the results of the proof load test,  $S_{super}$  is the total load in the site, and  $DL_{outcome}$  is the calculated dead load of each pile that ensures a reliability index of 3 after conducting the proof load test.

In order to choose the optimum proof load test program, the initial cost (no pile load tests are conducted) and the cost of each outcome need to be calculated. The net benefit of each outcome can be calculated by using the equation:

$$B(a_i, \theta_j) = N_{required} \cdot C_{pile} - N'_{required} \cdot C_{pile} - nC_{r,proof} - (n - k) \cdot C_{pile} \quad (23)$$

Where  $C_{pile}$  is the cost of manufacturing and installing the driven pile,  $C_{r,proof}$  is the cost of conducting a proof load test, and  $(n - k) \cdot C_{pile}$  is the cost of the replacing the piles that failed during the proof load test, if any.

Once the net benefit of all the test alternatives and their associated potential outcomes are calculated, the “expected” benefit  $E(B_{a_i})$  of each alternative load test program  $a_i$  can be calculated by multiplying the net benefit  $B(a_i, \theta_j)$  of each outcome by the likelihood of occurrence of that outcome  $P(\theta_j)$  and summing the contributions of all outcomes such that:

$$E(B_{a_i}) = \sum_{j=1}^n B(a_i, \theta_j) \cdot P(\theta_j) \quad (24)$$

The alternative pile testing program that has the highest expected benefit could then be selected as the test alternative that has the highest value.

The base case costs that were adopted in this study are specified as follows: (1) The cost of production and installing a single closed ended pile is 97\$/ft, and (2) the cost of running a static proof load test on such piles is in the order of 10\$/KN of test load.

## CHAPTER 6

### PRACTICAL APPLICATIONS FOR PROPOSED DECISION MAKING FRAMEWORK

One of the main objectives of this thesis is to apply the pre-posterior decision-making framework to a number of practical design scenarios that involve driven piles of different characteristics and soils of different nature. The ultimate goal is to formulate a general set of recommendations regarding the design of proof load test programs for driven piles that are designed using different empirical design procedures in soil profiles that range from cohesive to cohesionless soils. To achieve this ultimate goal, four published case histories with representative soil profiles and pile types were selected as indicated in Table 8. Two of the case histories involve sites that were predominantly sand and two involve clay sites. The Cimarron River site (Nevels and Snethen 1994) consists of loose to medium dense sands while the Pigeon Creek site (Paik et al. 2003) consists of dense sands. For the clays sites, the soil mainly consisted of slightly overconsolidated clays. The main difference between the two case histories is the in the length of used piles whereby the piles that were considered for the Port of Khorramshahr site (Hutchinson and Jensen 1968) were relatively short (13.9m) while the piles that were considered for the Louisiana site (Darragh and Bell 1969) were relatively long (30.5m). All of these case histories were included as part of the database analyzed in Lehane et al. (2017). The choice of these case histories was driven by the fact that the published papers included sufficient detailed information about the soil profile and properties to allow for a proper determination of the predicted pile capacity (SPT

and CPT-based) and lower-bound capacities (Gilbert et al. 2005 models) for all the prediction models that were analyzed in this thesis.

Table 8 Description of different sand and clay sites

Site Type	Site name	Reference	Dominant Type of soil at side	Type of soil at tip	Pile length (m)	Pile diameter (cm)
Loose to Medium <b>Sand</b>	Cimarron River	Nevels and Snethen 1994	Sand (M)	Sand (L)	19	66
Dense <b>Sand</b>	Pigeon Creek	Paik et al. 2003	Grav. Sand (D)	Grav. Sand (D)	6.9	35.6
<b>Clay</b> – Short Pile	Port of Khorramshahr, Iran	Hutchinson & Jensen (1968)	Slightly OC clay	-	13.9	35
<b>Clay</b> – Long Pile	Louisiana	Darragh & Bell (1969)	Slightly OC clay	-	30.5	32.4

### 6.1 Site No. 1: The Cimarron River Site (Driven Piles in Loose to Medium Sand)

The Cimarron River Site is located on the U.S. Highway 64 bridge over the Cimarron River in Northway, Oklahoma. Figure 15 shows the piles' dimension and the site conditions in addition to the SPT and CPT data collected from the site. The considered piles are closed ended precast concrete driven piles with a 66 cm diameter and a 19-m length. The soil in the site is a Quaternary terrace and alluvium deposit overlying the Flowerpot shale. This Flowerpot shale is about 122 m thick, whereas the Cimarron River deposits are approximately 20 m thick and involve a mixture of sand and gravel.

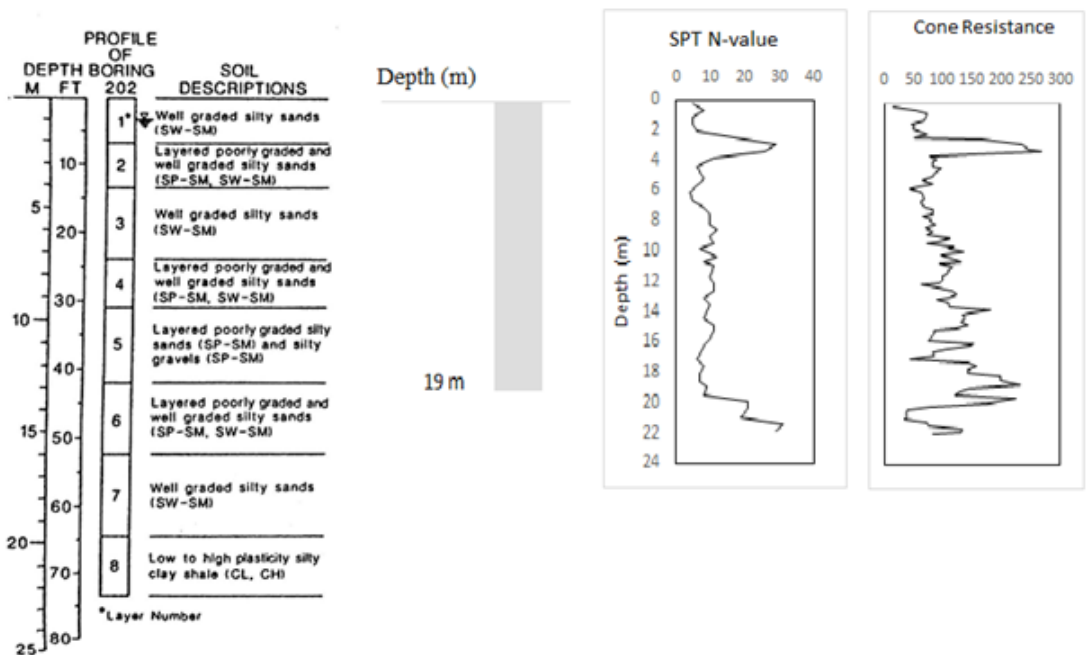


Figure 15 Characteristics of the Cimarron River Site

Table 9 summarizes the predicted capacities using the API (SPT-based), the ICP (CPT-based) and the predicted lower-bound capacities using the Gilbert et al. (2005) model. The current API method refers to API (2000) while the ICP-05 method refers to Jardine et al. (2005) and API (2007). A pre-posterior decision making analysis was conducted to investigate the optimal proof load test program for the piles in the Cimarron River Site. In the analysis, several cases of superstructure loads were assumed since the magnitude of the applied load is expected to directly correlate with the total number of piles in the site. In addition, the analysis was repeated for the SPT-based API method and for the CPT-based ICP method to study the impact of the pile prediction method on the resulting optimum test program.



Table 9 The pile's capacity according to different methods in the Cimarron River Site

Methods	Predicted Capacity	Bias Factor	Mean Pile Capacity
Current API	2206	1.66	3661
ICP-05	3609	1.04	3753
Lower-bound	1032	1.0	1032

To illustrate the procedure followed in choosing the optimal static proof load test, the case involving the ICP method for calculating the pile capacity in the Cimarron River Site is considered. The predicted pile capacity according to this method is 3609 KN as shown in Table 9. Using this predicted capacity and the statistics of the bias factor of the ICP method (Table 5), the probabilistic capacity model for the piles at the site can be developed. In the model, it is assumed that the within site variability ( $r_{cov}$ ) follows the truncated lognormal distribution with a mean of 0.2, a COV of 0.31, and a lower and upper bound of 0.1 and 0.3, respectively. This within site variability is assumed for all the case histories analyzed in this chapter.

For the above pile capacity distribution, the prior design load that a single pile could sustain while maintaining a target reliability index of 3.0 is calculated to be equal to 1214 KN (FS = 2.97). In the prior analysis which is needed to calculate the prior number of piles at the site, the load distribution is assumed to be lognormal with a mean that is equal to 1214 kN and a COV of 0.15 as is the convention. For illustration, if the total superstructure load is assumed to be carried by 300 piles in the site, the total prior design load will be equal to 365 MN.

For the case where alternative proof load-test programs are envisaged for the piles at the site, the piles will be initially designed with a reduced factor of safety of 2.0. For the

example case that is considered above, this will lead to a design load (DL) that is equal to the predicted capacity (3609 kN) divided by the factor of safety (2.0) with a value of 1804.5 kN. The pre-posterior analysis is conducted for alternative proof-load test programs consisting of static proof load tests at levels of 1.5xDL, 1.75xDL, 2xDL, 2.25xDL, and 2.5xDL. Based on the outcomes of the test program, the pile capacity distribution is updated and an updated pile design load is calculated to yield a desired target reliability index of 3.0. The updated design load is then used to calculate the updated number of piles needed to sustain the total load on the structure. If the updated number of piles is smaller than the prior number, cost savings will be incurred for the project cost resulting in a net cost benefit for that particular outcome.

Figure 16 shows the net expected benefit for all the decision alternatives as a function of the number of tests and the proof-load level. These results pertain to the illustrative case which involves 300 piles (prior analysis) in the Cimarron River Site with pile predictions made using the CPT-based ICP design method for driven piles in sand. The figure shows that the optimal test alternative is to conduct 3 static proof-load tests at 1.5xDL level with a maximum net expected benefit of 205,082 \$.

To test the sensitivity of the optimal load test program to the magnitude of the applied superstructure load (or total number of piles), the same analysis is repeated for number of piles varying from 50 (relatively small total foundation load) to 1000 piles (relatively large foundation load). The results of this exercise are presented in Figure 17 and include a depiction of the variation of the number and percentage of optimal proof load tests as a function of the total number of piles that is envisaged in the prior analysis.

The results on Fig. 17 show that for a small number of piles (50 piles) no tests are required. For example, a total load of 60 MN (50 piles in the site) requires no proof load tests and each pile can carry a dead load of 1214 kN (FS = 2.97) for a target reliability index of 3. When the number of piles increases in the site the optimal required number of proof load tests increases, but the required level of proof load test for the ICP method is always 1.5xDL. For 100 piles in the site, it is required to conduct 1 proof load test at 1.5xDL. However, the number of tests vary according to the number of piles. So, when the number of piles is between 200 and 300, 3 proof load tests are required, and when the number of piles in the site becomes between 700 and 1000, 6 proof load tests are required.

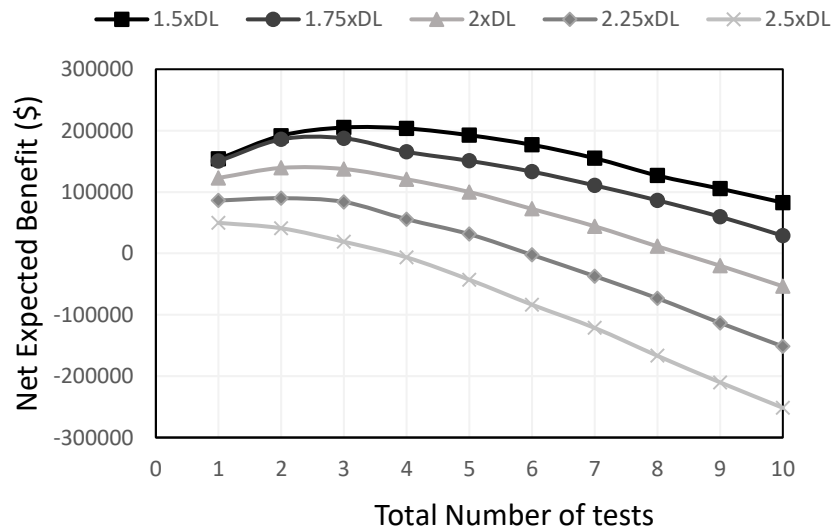


Figure 16 Expected benefit of alternative proof load test programs

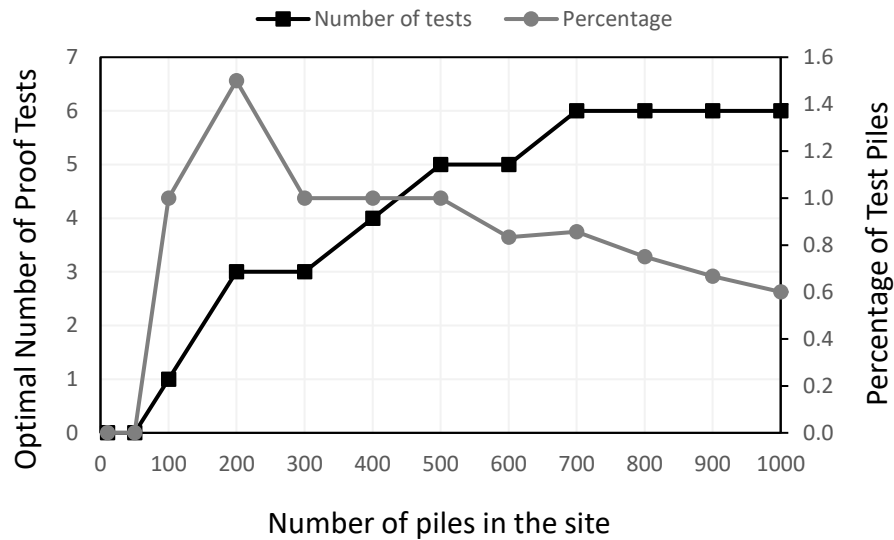


Figure 17 Optimal number of proof load tests and the percentage of tests (relative to the total number of piles) as a function of number of piles using the ICP method in the Cimarron River Site (optimal  $r_{proof} = 1.5DL$ )

Concerning the optimum percentage of proof load tests (relative to the total number of piles), results on Fig. 17 show that the optimum percentage of proof load tests test piles increases initially to a high value of 1.5% (for the case involving 200 piles), drops slightly to 1.0% and remains more-or-less constant up to a total number of piles of 500. For cases with higher number of piles, the percentage decreases more or less linearly with the total number of piles, reaching a low value of 0.6% for the case involving 1000 piles at the site.

When the same exercise is repeated using the API method (Fig. 18) as the main pile prediction method, results for the case involving 300 piles indicate that 5 tests (rather than 3 tests for ICP method) are required to maximize the value of the proof-load test program, with the optimum proof load level being 2.0 x DL rather than 1.5 x DL (ICP method). These results are important since they indicate the importance of the pile prediction method on the optimum proof load test program (level of proof load and number of proof load tests).

The results of Figure 18 demonstrate that for the API method no tests are required if the number of piles in the site is below 10. The optimal number of tests starts to increase when the number of piles is 50 and reaches 5 tests when the number of piles within the site reaches 300. The optimal number of static proof load tests remains at 5 when the number of piles in the site is above 300. As for the percentage of the tests, it is constant at 2% cases involving less than 200 piles and starts decreasing systematically when the number of piles within the site increases, reaching a minimum of about 0.5% for the cases involving 900 and 1000 piles. This decrease in the optimal percentage of test piles was also observed in the ICP method in the same site.

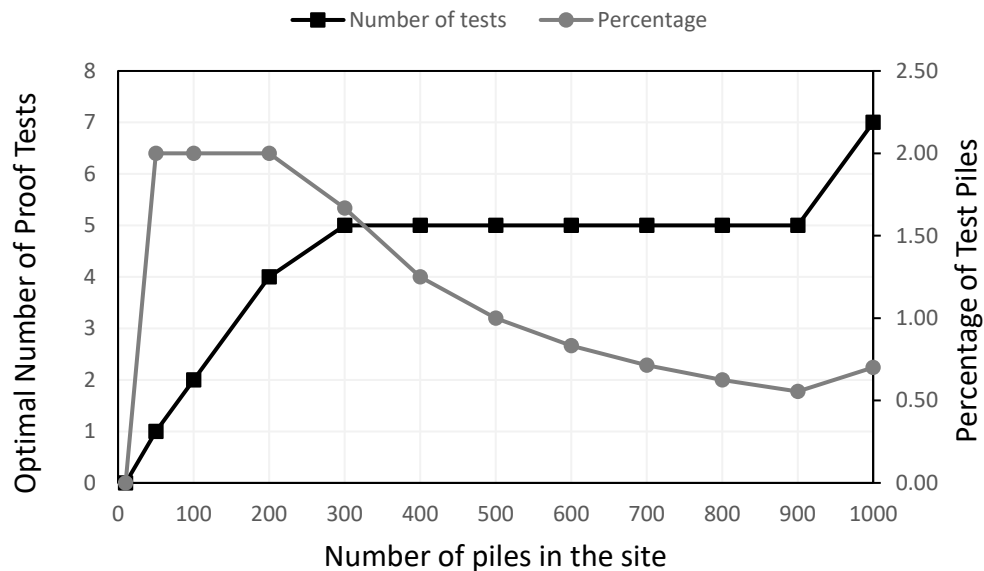


Figure 18 The optimal number of proof load test and the percentage of tests as a function of number of piles using the API method in the Cimarron River Site (optimal  $r_{proof} = 2 \times DL$ )

## 6.2 Site No. 2: The Pigeon Creek Site (Driven Piles in Dense Sand)

The Pigeon Creek site (Paik et al. 2003) is located at the south side of the Pigeon River in Indiana. The first 13 to 14 m in the site is predominantly gravelly sand in addition to 2 m of fill at the top that were removed before the pile installation. After 14 m, the soil is made up of stiff till, containing clays and silts. The dry unit weight of the gravelly sand ranges between 15.61 and 18.64 KN/m<sup>3</sup>. For the void ratios it also ranges between 0.41 and 0.68, whereas the specific gravity (Gs) is taken as 2.67. SPT and CPT test results in addition to the pile geometry are shown in Figure 19. The results of the SPT and CPT tests show that the sand is loose in the first 3 meters and then changes to dense and very dense state below that level. The piles used are closed-ended piles of 6.9m length and a diameter of 35.6 cm.

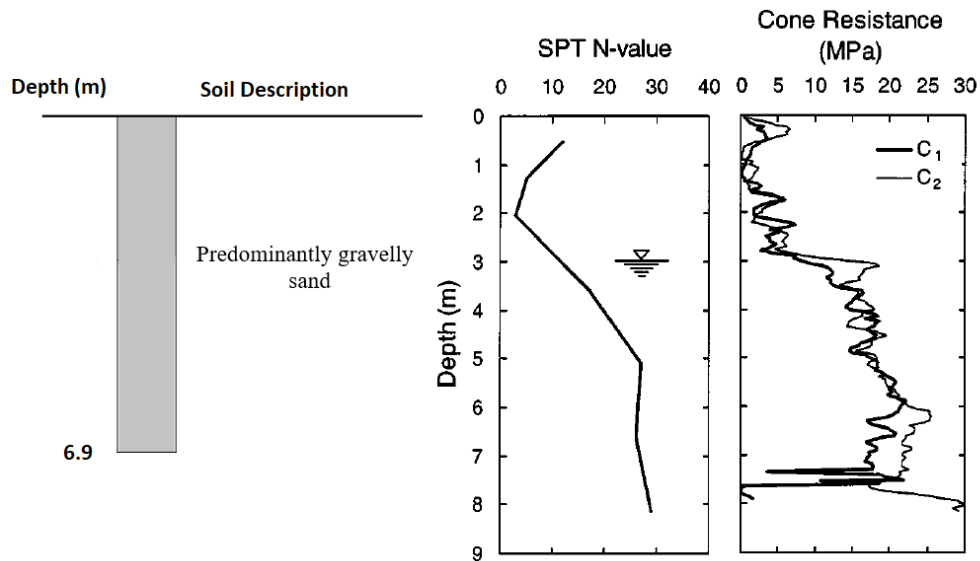


Figure 19 Characteristics of the Pigeon Creek Site

Table 10 summarizes the calculated capacities of the lower bound in addition to the calculated pile capacities using the API and ICP methods. The results of the decision making analysis for the piles in this site are presented in Figures 20 and 21 for the ICP and API methods, respectively. As is the case for the Cimarron River Site, results for the Pigeon Creek site indicate that the optimal proof load level for the ICP method is 1.5xDL level while that of the API method is 2.0 x DL. Moreover, the variation of the optimum number and percentage of proof load tests with the total number of piles in the site is relatively similar to that of the Cimarron River Site.

Table 10 pile's capacity according to different methods in the Pigeon Creek Site

Methods	Predicted Capacity	Bias Factor	Mean Pile Capacity
Current API	647	1.66	1074
ICP-05	1444	1.04	1502
Lower-bound	255	1.0	255

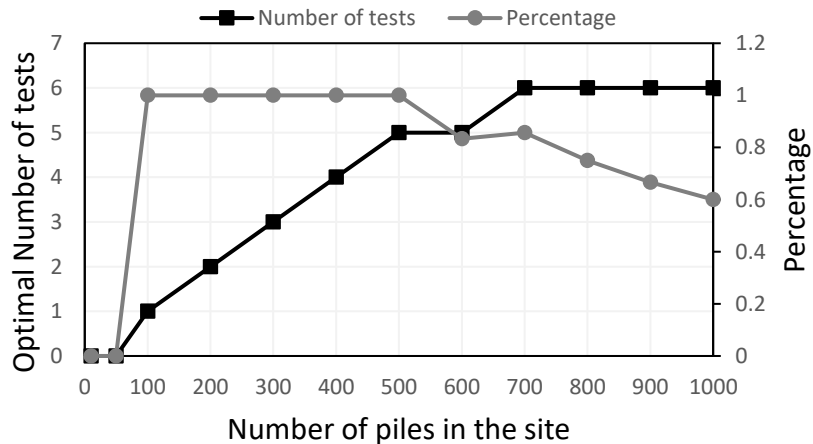


Figure 20 The optimal number of proof load test and the percentage of tests as a function of number of piles using the ICP in Pigeon Creek Site (optimal  $r_{proof} = 1.5DL$ )

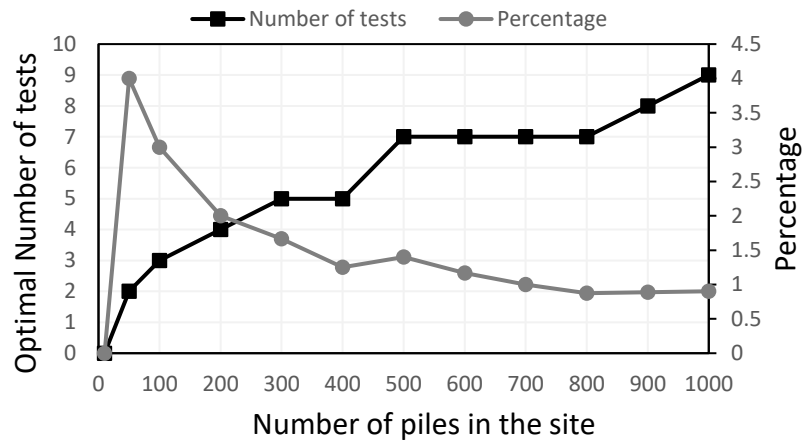


Figure 21 The optimal number of proof load test and the percentage of tests as a function of number of piles using the API in the Pigeon Creek Site (optimal  $r_{proof} = 2xDL$ )

For the ICP method, no static pile load tests are required as long as the number of piles is less than 50. After that, the number of proof-load tests increases gradually as the number of piles in the site increases, with an optimum percentage of tests being constant at 1% till we reach 500 piles. The optimal number of proof load tests for 500 piles is 5 tests. This optimal number of proof load tests increases to 6 and remains constant for a total number of piles ranging between 700 and 1000. In this range, the optimal percentage of proof load tests decreases from 1% to 0.6%.

For the API method, and similar to the Cimarron River Site, no tests are required in the site when the total number of piles is less than 10. When the number of piles within the site reaches 50, the optimal solution require conducting 2 tests conducted at  $2xDL$  level. As the number of piles in the site increases, the optimal number of tests increases too reaching 7 static proof load tests for the case involving 500 piles. After that (between 500 and 800 piles), the optimal number of tests stabilizes at 7 to increase again and reach value of 9 tests



for cases involving 1000 piles. The associated optimal percentage of test piles decreases exponentially from 4% (for cases involving 50 piles) to 1% (for cases involving 1000 piles).

### **6.3 Site No. 3: The Port of Khorramshahr, Iran (Short Driven Piles in Clay)**

The site in the third case study is situated in the port of Khorramshahr in Iran and the field data was collected from Hutchinson et al. (1968). The soil profile is predominantly clay with a top 2 to 3m of weathered crust (humus) that is underlain by a deep layer of normally consolidated to slightly over consolidated clay. Under this thick clay layer, a sequence of dense to very dense fine sand with occasional layers of stiff and over-consolidated clays exist. The liquid limit of the clay layer varies between 40 to 57%, its plastic limit varies between 18 to 27%, and its water content has an average of 33%. The bulk density of this silty clay is  $1.87 \text{ t/m}^3$  and its specific gravity is 2.74. The pile is a closed ended pile with a 35-cm and 13.9 m length. Figure 22 shows the piles dimensions, the soil description, in addition to the remolded and undisturbed shear strength profiles that will be used as basis for calculating the lower-bound capacity and the predicted pile capacity (see Table 11).

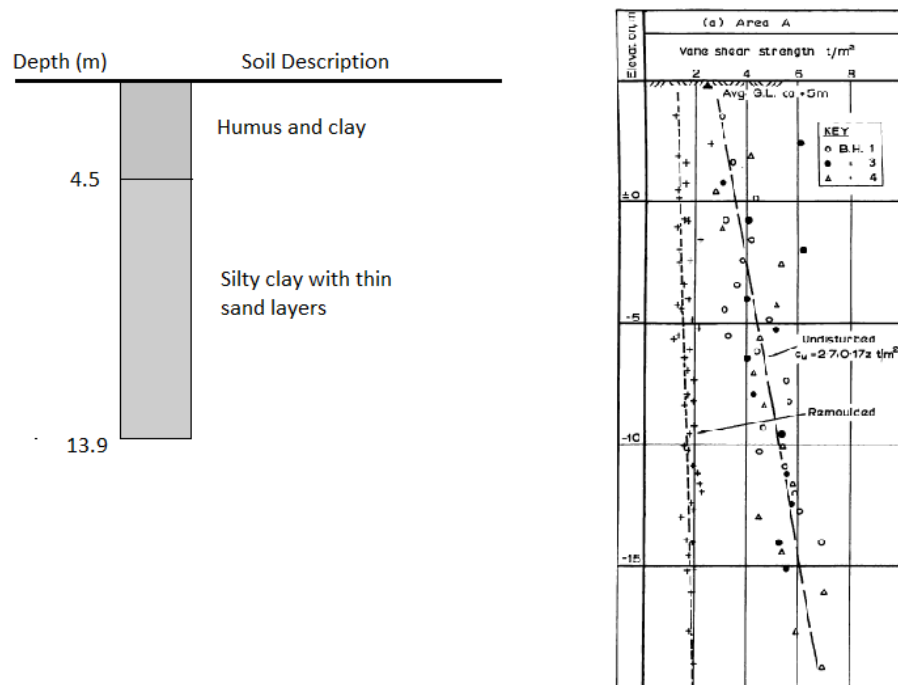


Figure 22 Characteristics of the port of Khorramshahr

Table 11 pile's capacity according to different methods in the port of Khorramshahr

Methods	Predicted Capacity	Bias Factor	Mean Pile Capacity
Current API	356	1.54	548
ICP-05	540	0.98	529
Lower-bound	226	1	226

Results in Table 11 indicate that the predicted pile capacity is 356 kN using the API method and 540 kN using the ICP method. The predicted lower-bound capacity using the remolded shear strength turned out to be equal to 226 kN.

The same decision-making framework was utilized to calculate the optimal proof-load test program for the piles in the port of Khorramshahr. The results of the ICP method are presented in Figure 23 while the results for the API method are presented in Fig. 24. For

the ICP method, results of the decision making exercise indicate that the optimum level for the proof load is 1.5xDL. On the other hand, results for the API method indicate that the optimum level of the proof load is 2.25xDL. These results are different than those witnessed for Sand sites using the API method where the optimal proof load level was found to be 2.0xDL. This observation points to the importance of conducting site specific decision analyses to optimize proof load test programs for driven piles.

Figure 23 and 24 show the results of the optimal number and percentage of static proof load tests as a function of the total number of piles in the Port of Khorramshahr clay site for the ICP and API pile prediction methods, respectively. For the ICP method, results indicate that there is no need for static proof load tests when the foundation system includes of less than 10 piles. As the number of piles increase beyond 10, the optimal number of proof load test increases to reach 7 tests when the piles in the site reach around 200 piles and remains constant at 7 tests up to a total number of piles of 400. The optimal number of proof load tests then starts to increase till we reach 17 tests at 600 piles. After that, the optimal number remains constant at 17 tests up to a total number of piles of 1000. The optimal number of piles when presented as a percentage of the piles at the site decreases from a high value of about 4% for cases involving only 50 piles to around 1.7% for the case where the foundation system involves 1000 piles.

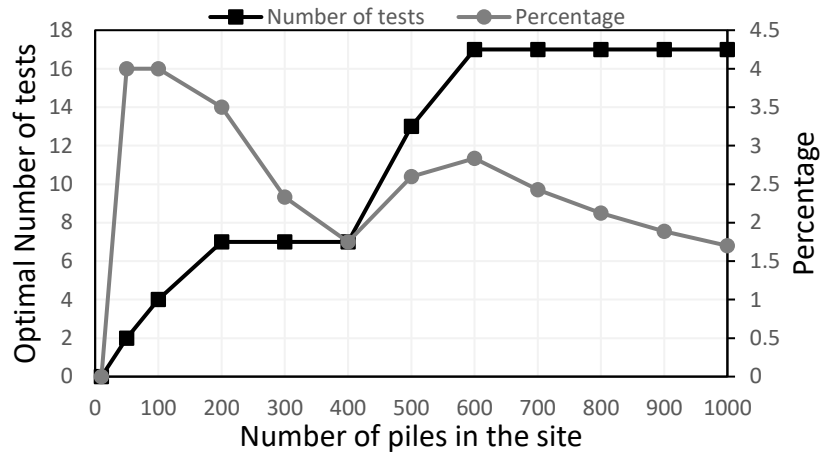


Figure 23 The optimal number and percentage of proof load tests as a function of number of piles using the ICP in the Port of Khorramshahr (optimal  $r_{proof} = 1.5 \times DL$ )

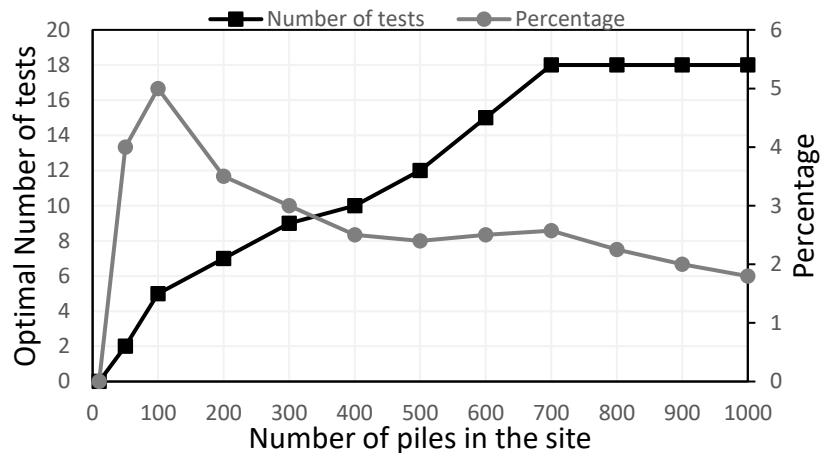


Figure 24 The optimal number and percentage of proof load test as a function of number of piles using the API in the Port of Khorramshahr (optimal  $r_{proof} = 2.25 \times DL$ )

For the API method (Fig. 24), the optimal number of proof load tests increases linearly from 2 tests (for the case involving 50 piles) to a maximum of 18 tests (for the case involving 700 piles). For a pile number ranging between 700 and 1000 piles, the optimal number of proof load test remains constant at 18 tests. When these numbers are expressed as a percentage, results indicate that 5% of the piles need to be tested if the number of piles is

small (100 piles). As the number of piles increases in the site, the optimal percentage of tested piles decrease, reaching minimum values of 1.8 % for 1000 piles.

#### **6.4 Site No. 4: Louisiana Site (Long Pile in Clay)**

The Louisiana site (Darragh et al. 1969) is located near the Mississippi River. The upper 30 feet in the site consist of natural levee clays. Underlying these clays are backswamp clays that extend up to 120 feet depth. Drying and wetting of these clay deposits had turned them into slightly overconsolidated clays. The water table in the site is shallow and ranges between 2ft (0.61m) and 4ft (1.22 m) below the ground surface. Table 12 summarizes the engineering properties of the two clay layers present in Louisiana site.

The piles used in the site are closed ended driven piles that are 30.5m long and 32.4 cm in diameter. Figure 25 shows the geometry of the pile used, in addition to the minimum and the design shear strength of the clay situated in the site at different depth, where these values are used to calculate the lower-bound and the pile's capacity, respectively. The calculated capacities of the lower bound and predicted capacities are presented in Table 13.

Table 12 Soil characteristics in the Louisiana site

Soil Type	Depth (ft)	Dry Density lb/ft <sup>3</sup>	Natural Moisture %	Liquid Limit	Plastic Limit	Percent Passing 200 sieve	Peak Shear Strength psf
Natural Level Deposit: layers and laminations of clays, silts, and fine sand	0 - 30	2 - 94	28 to 48	33 - 71	9 - 29	56 - 96	600 - 1000
Back swamp deposits layers and laminations of clays, silts, and fine sand	0 - 120	3 - 96	33 - 104	32 - 128	9 - 56	73 - 100	700 - 2900

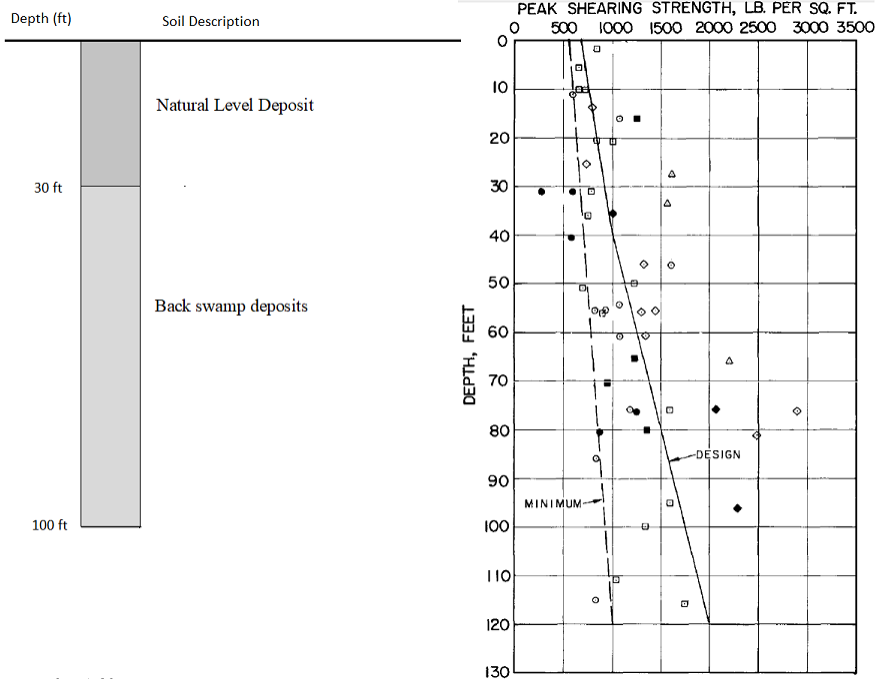


Figure 25 Characteristics of the Louisiana site

Table 13 pile's capacity according to different methods in the Louisiana site

Methods	Predicted Capacity	Bias Factor	Mean Pile Capacity
Current API	1167	1.54	1797
ICP-05	1762	0.98	1727
Lower-bound	1100	1.0	1100

The results of the ICP method for the Louisiana site are presented in Figure 26 while the results for the API method are presented in Fig. 27. As in the case of the first clay site, results of the decision making exercise indicate that the optimum level for the proof load is 1.5xDL for the ICP method and 2.25xDL for the API method.

Figure 26 and 27 show the results of the optimal number and percentage of static proof load tests as a function of the total number of piles in clay site for the ICP and API pile prediction methods, respectively. For the ICP method, results indicate that there that the first 10 piles in the site require no pile load testing. As the number of piles increase, the optimal proof load test increases gradually reaching 6 tests for the case involving 200 piles. Between 200 piles and 600 piles, the optimal number of piles increases very gradually reaching a value of 7 tests for the case involving 600 piles. For cases with number of piles exceeding 600, the optimal number of tests increases dramatically to reach a maximum number of 17 tests for the cases involving 900 and 1000 piles, respectively. The optimal number of piles when presented as a percentage of the piles at the site decreases from a high value of about 4% for cases involving only 50 piles to around 1.6% for the case where the foundation system involves 1000 piles.

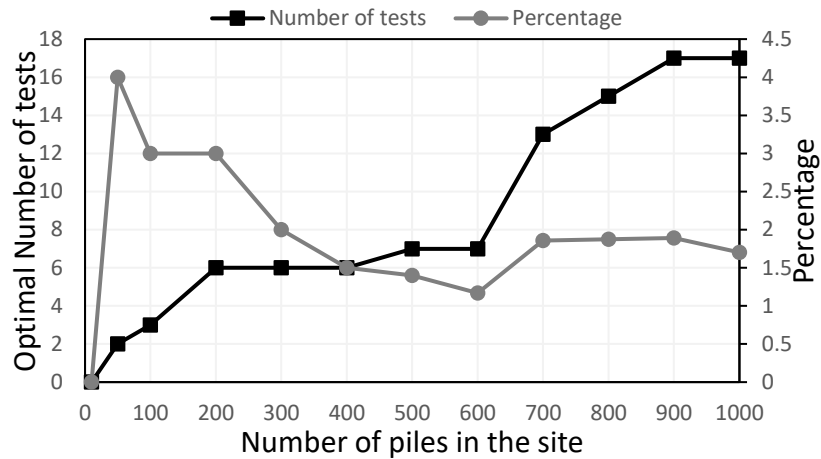


Figure 26 The optimal number of proof load test and the percentage of tests as a function of number of piles using the ICP in the Louisiana Site (optimal  $r_{proof} = 1.5 \times DL$ )

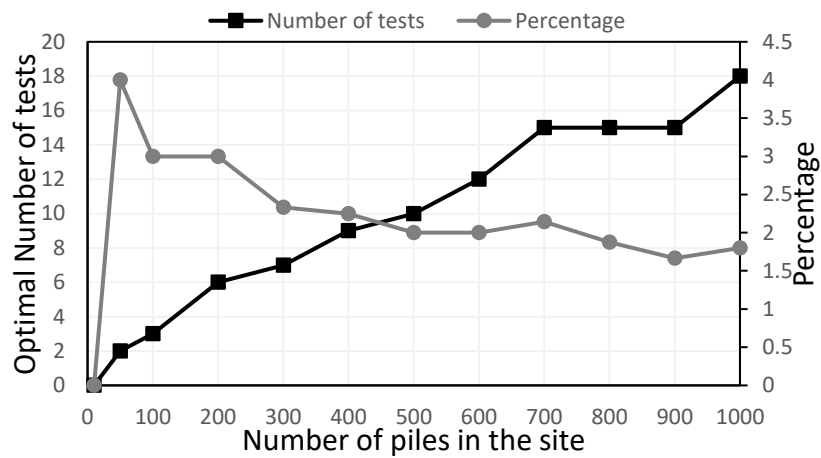


Figure 27 The optimal number of proof load test and the percentage of tests as a function of number of piles using the API in the Louisiana Site (optimal  $r_{proof} = 2.25 \times DL$ )

For the API method (Fig. 27), the optimal number of proof load tests increases linearly from 2 tests (for the case involving 50 piles) to a maximum of 15 tests (for the case involving 700 piles). For a pile number ranging between 700 and 900 piles, the optimal number of proof load test remains constant at 15 percent but jumps to 18 tests for the case involving 1000 piles. When these numbers are expressed as a percentage, results indicate that



4% of the piles need to be tested if the number of piles is small (50 piles). As the number of piles increases in the site, the optimal percentage of tested piles decrease, reaching minimum values of 1.8 % for 1000 piles.

## **6.5 Discussion of Case Histories**

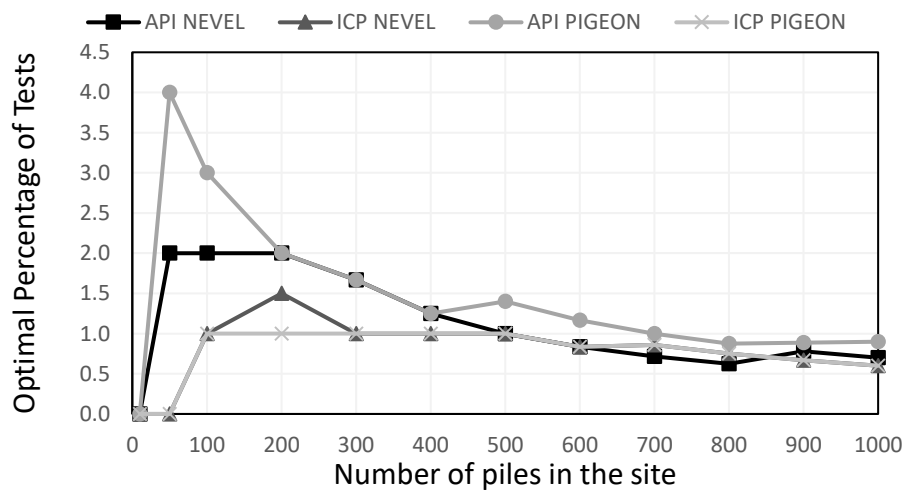
The results of the decision making exercises that were conducted in the four sites point to similarities in some aspects of the response and to differences in other aspects. For example, results for all ICP-based methods (in sand or clay) indicated that the optimum proof load level is 1.5xDL. On the other hand, the optimum proof load level was higher for the API-based methods which showed differences for sites in sand (2.0xDL) compared to sites in clay (2.25xDL). With regards to the optimal number and percentage of proof load tests, results indicated some similarities when it comes to the type of soil.

To shed more light on these similarities and to investigate the ability to generalize the response based on the type of soil, the results were grouped based on soil type and plotted on Figs. 28 (sand) and 29 (clay).

For any given prediction method (API or ICP), the results for the sand sites on Fig. 28 show a more or less similar variations in the optimal number and percentage of tests with the total number of piles at the site for the two different sand sites (loose sand versus dense sand). This similarity in the response is more pronounced in the ICP method whereby the two curves in the two sites almost overlapped. For the API method, some differences exist between the two sites in the required percentage of proof load test for cases involving a small

number of piles (less than 100 piles). The high percentage of tests for the low number of piles can be explained by the fact that the optimal number of static proof load tests when the site consists of 50 piles is 1 to 2 tests which reflects the percentage of 2 and 4% respectively due to the small number of piles.

For cases with greater number of piles (above 200 piles), the two curves from the two sites approach each other leading to more-or-less similar results from a practical point of view. In fact, one could argue that the curves representing the variation of the optimal percentage of tests with the number of piles almost converge to a value of 1.0% for cases with 400 to 500 piles. After that, all curves converge indicating that the optimal percentage of proof load test decreases from 1.0% to about 0.6% for the maximum number of piles considered (1000 piles in the site). Despite this fact, it is worth noting that the ICP method requires optimal static proof load tests to be conducted at 1.5xDL while the API method requires optimal tests to be conducted at 2.0xDL.



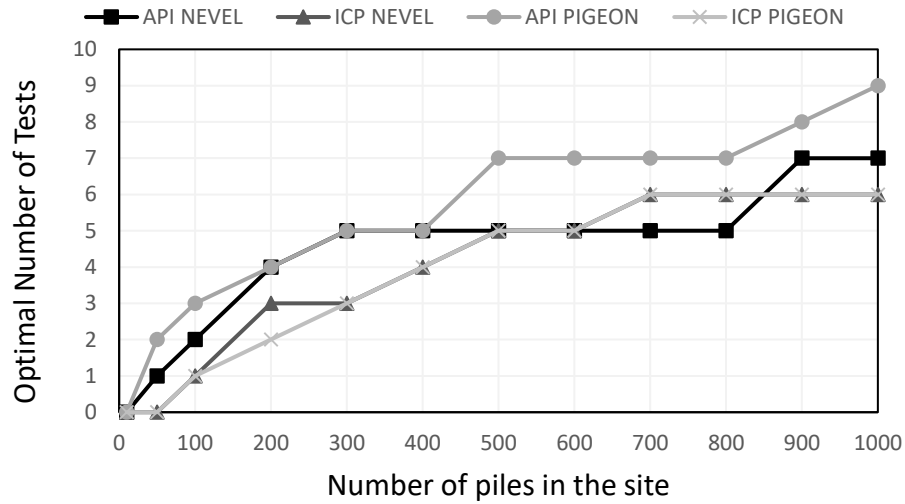


Figure 28 Comparison between (a) optimal percentage of proof load tests and (b) optimal number of tests for the 2 sand sites according to ICP (optimal  $r_{proof} = 1.5 \times DL$ ) and API method (optimal  $r_{proof} = 2.0 \times DL$ )

For the clay methods, the percentage and number of the optimal static proof load tests are presented for the two sites and the two prediction methods as a function of the total number of piles in Figure 29.

The results show that the ICP and the current-API method in clay converge more than in the sand profiles. The percentage of optimal static proof tests for both methods in the 2 sites is 4% if there is only 50 piles. For 100 piles, the percentage varies between 3 and 5% and then starts to decrease gradually to reach 2% of the total number of piles (in the four scenarios) for 1000 piles in the site. The higher percentages for the small number of tests is due to the relatively high number of tests (2 tests) compared to the relatively low number of total piles (50 piles).

The results also prove that the required optimal number of static load test for clay methods is higher than the number of optimal static proof load test in sands. This observation

is explained by the difference in pile's capacity in sand and clay. Piles having the same length have a greater capacity in sand than in clay. This low capacity in clay minimizes the effect of the positive load test of the pile (minimum change in the design load if the proof load test is positive).

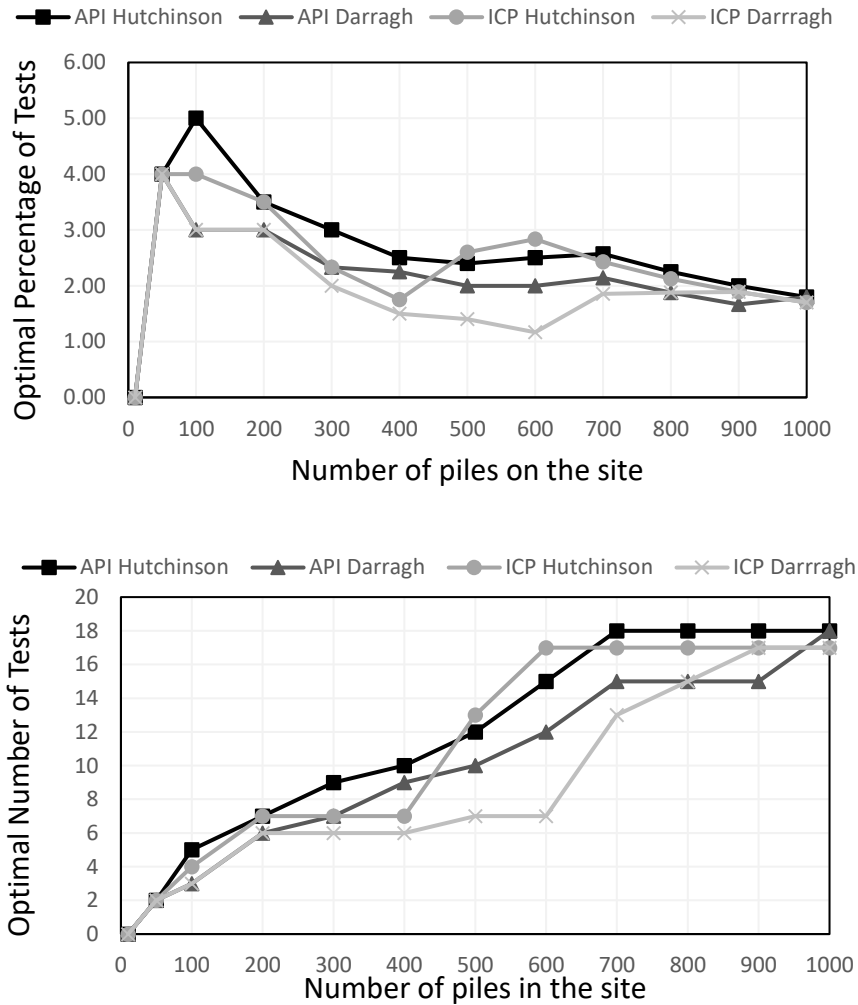


Figure 29 Comparison between (a) optimal percentage of proof load tests and (b) optimal number of tests for the 2 clay sites according to ICP (optimal  $r_{proof} = 1.5 \times DL$ ) and API method (optimal  $r_{proof} = 2.25 \times DL$ )

## CHAPTER 7

### SENSITIVITY ANALYSIS ON TEST AND PILE COSTS

To show the effect of the piles' production and installation costs and the proof load tests' cost on the calculated net benefit and therefore on the optimal number of proof load tests, a sensitivity analysis is conducted on the 4 cases analyzed in Chapter 6.

In the analysis conducted in Chapter 6, the cost of each pile was assumed to be equal to \$97 per linear foot of pile length. This cost includes pile material and pile installation costs which is considered relatively high in many areas of the world where the availability of pile driving contractors and local expertise in pile driving is generally limited. Moreover, a fixed cost of \$97 /ft was adopted for all case histories in Chapter 6 despite slight differences in the diameter of the piles adopted. In reality, the cost of piles including installation depends on the diameter of the pile and on local experience. As a result, the cost per linear foot could be smaller than 97\$/ft. For example, typical pile costs for the State of Michigan (2003) are presented in Table 14 for pre-cast concrete piles with diameters equal to those observed in the four case histories. These costs show that the pile costs could range from \$29/ft for piles with a relatively small diameter of 12 inches and could increase to about \$70/ft for piles with a diameter of 24 inches.

Similarly, the cost of pile testing could change from one site to the other. In Chapter 6, the cost of pile testing was priced at \$10 per kN of test load. In this chapter, the sensitivity of the results to the choice of the test cost will be investigated by increasing the cost to \$20 per kN as indicated in Table 14.

Table 14 The pile and test costs for different case histories

Case History	Pile Diameter	Assumed Pile Cost (chapter 6)	State of Michigan Cost (2003)	Test Cost (scenario 1)	Test Cost (scenario 2)
1	24"	97\$/ft	70\$/ft	10\$/KN	20\$/KN
2	14"	97\$/ft	35\$/ft	10\$/KN	20\$/KN
3	14"	97\$/ft	35\$/ft	10\$/KN	20\$/KN
4	12"	97\$/ft	29\$/ft	10\$/KN	20\$/KN

### 7.1. Case of Sand Sites

Figure 30(a) shows the base case result for the 2 sand sites and the 2 capacity prediction methods calculated in chapter 6 using a pile cost of 97\$/ft and a test cost of \$10/kN. On the other hand, Figure 30(b) shows the number of optimal proof load tests when the pile's cost is obtained from the State of Michigan and the test cost is kept at 10\$/KN. Finally, Figure 30(c) shows the optimal proof load test number while keeping the pile's prices of the State of Michigan (2003) and increasing the test cost to 20\$/KN. The associated optimal percentages of proof load tests for the 3 different cost combinations are shown in Figure 31.

The results of Figure 30(b) show that a drop in the pile's cost (compared to 97\$/ft) translates into a decrease in the optimal number of tests required in the site. For example, if we have 500 piles in the site, the optimal number of piles in the 2 sand sites decreases from 5 to 7 proof load tests (1 and 1.4%) if the pile's cost is 97\$/ft to a smaller number of 2 to 5 tests (0.4 to 1%) if the pile's cost in the State of Michigan (2003) is adopted. Since the piles

in the two sites have two different diameters (24'' in site 1 compared to 14'' in site 2), there is a difference in the pile's cost per linear feet based on the State of Michigan costs. This variation in the cost is reflected in the number of optimal proof load tests where Figures 30b and 31b show that the optimal number of tests (for the case of 500 piles as an example) in the Pigeon Creek site (14'' diameter) drops from 5 to 7 optimal proof load tests to 2 to 4 optimal proof load tests. This drop is greater than that witnessed for the Cimarron River site (24'' diameter) where the optimal proof load tests drop from 5 to 7 tests to 3 to 5 tests.

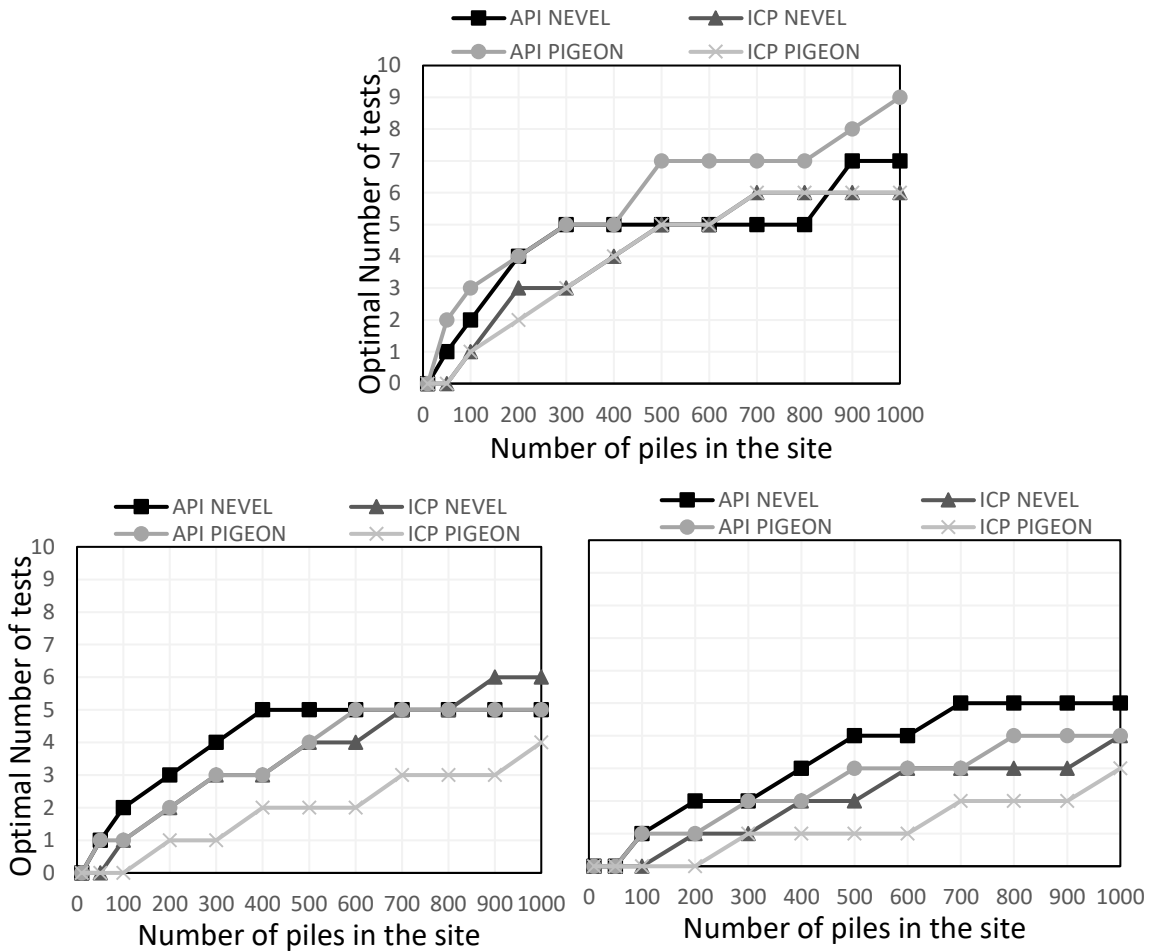


Figure 30 The optimal number of piles in sand sites (a) test cost 10\$/KN and price 97\$/ft (b) test cost 10\$/KN and the piles' cost of state of Michigan (2003), and (c) test cost 20\$/KN and the piles' cost of state of Michigan (2003).

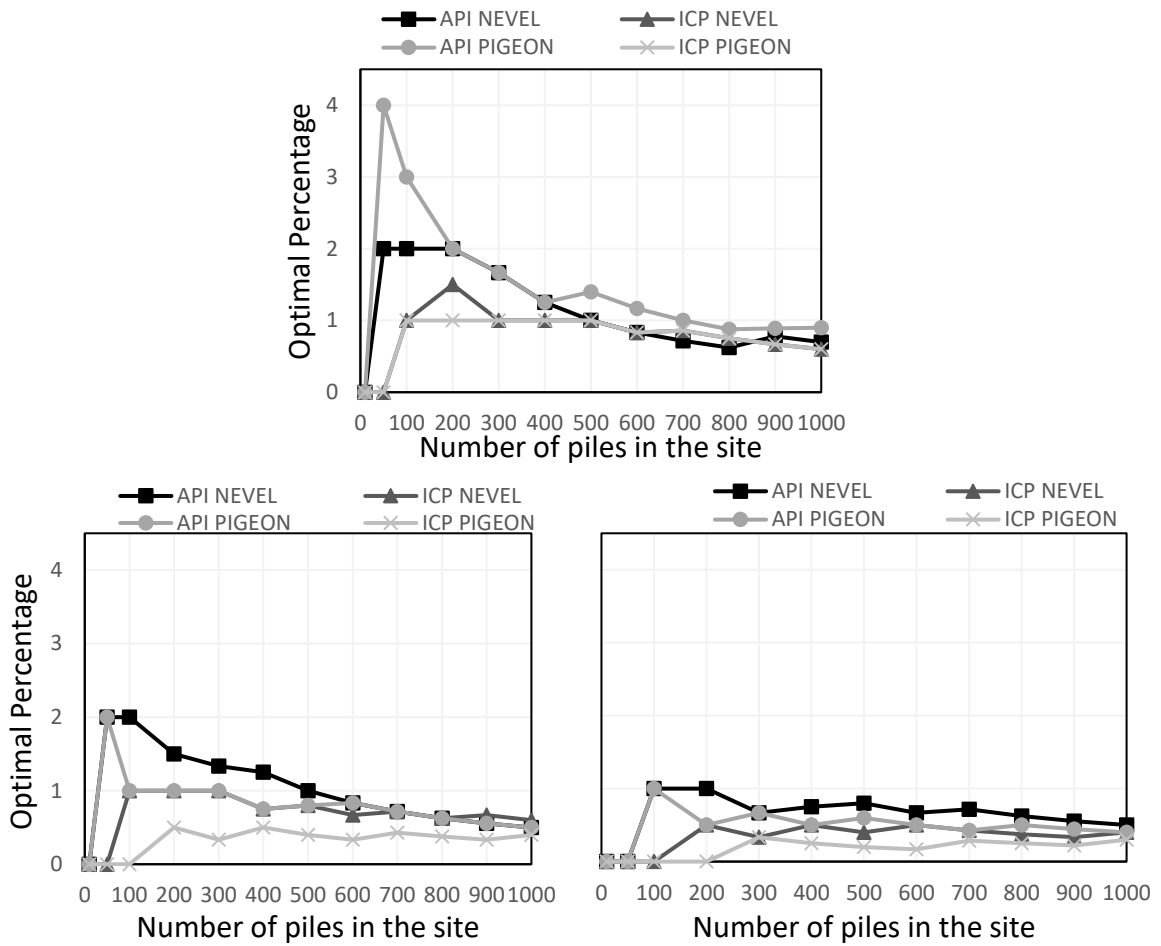


Figure 31 The percentage of piles in sand sites (a) test cost 10\$/KN and price 97\$/ft (b) test cost 10\$/KN and the piles' cost of state of Michigan (2003), and (c) test cost 20\$/KN and the piles' cost of state of Michigan (2003).

The sensitivity analysis regarding the test cost is shown in Figures 30c and 31c for the sand sites. In this analysis, the pile's cost is based on the State of Michigan prices, but the test cost is increased to 20\$/KN. The results of the optimal proof load tests show an additional decrease in the number of proof load tests as the test cost increases. Taking the



same example of 500 piles in the site, the range of optimal number of tests is in the range of 1 to 4 (0.2 to 0.8%) pile load tests compared to 2 to 5 tests (0.4% to 1.0%).

## **7.2. Case of Clay Sites**

The same cost sensitivity analysis is conducted in the clay sites. Figure 32(a) shows the base case result for the 2 clay sites and the 2 capacity prediction methods calculated in chapter 6 using a pile cost of 97\$/ft and a test cost of \$10/kN. On the other hand, Figure 32(b) shows the number of optimal proof load tests when the pile's cost is obtained from the State of Michigan and the test cost is kept at 10\$/KN. Finally, Figure 32(c) shows the optimal proof load test number while keeping the pile's prices of the State of Michigan (2003) and increasing the test cost to 20\$/KN. The associated optimal percentages of proof load tests for the 3 different cost combinations are shown in Figure 33.

The clay sites show the same behavior as the sand sites, where the number of optimal proof load test drops when the cost of the pile decreases from 97\$/ft to the assigned prices by the State of Michigan (2003). For the same example where the prior number of piles in the site is 500, the optimal number of proof load tests drops from 7-13 tests (1.4-2.6%) till 5-7 tests range (1-1.4%). It is important to note that the results of the 2 sites drop in the same manner since the pile's diameter in these 2 case histories is approximately the same (14 inches versus 12 inches). The second sensitivity analysis is defined by an increase in the test cost from 10\$/KN to 20\$/KN keeping the pile's cost given by the State of Michigan (2003). This increase in the test cost reveals an additional decrease in the optimal proof load test, as in the sand sites, where the range of optimal proof load test decreases from 5 to 7 tests (for

the case of \$10/kN) to a lower range of 2-5 tests range (for the case of \$20/kN) if the prior number of piles in the site is 500 piles.

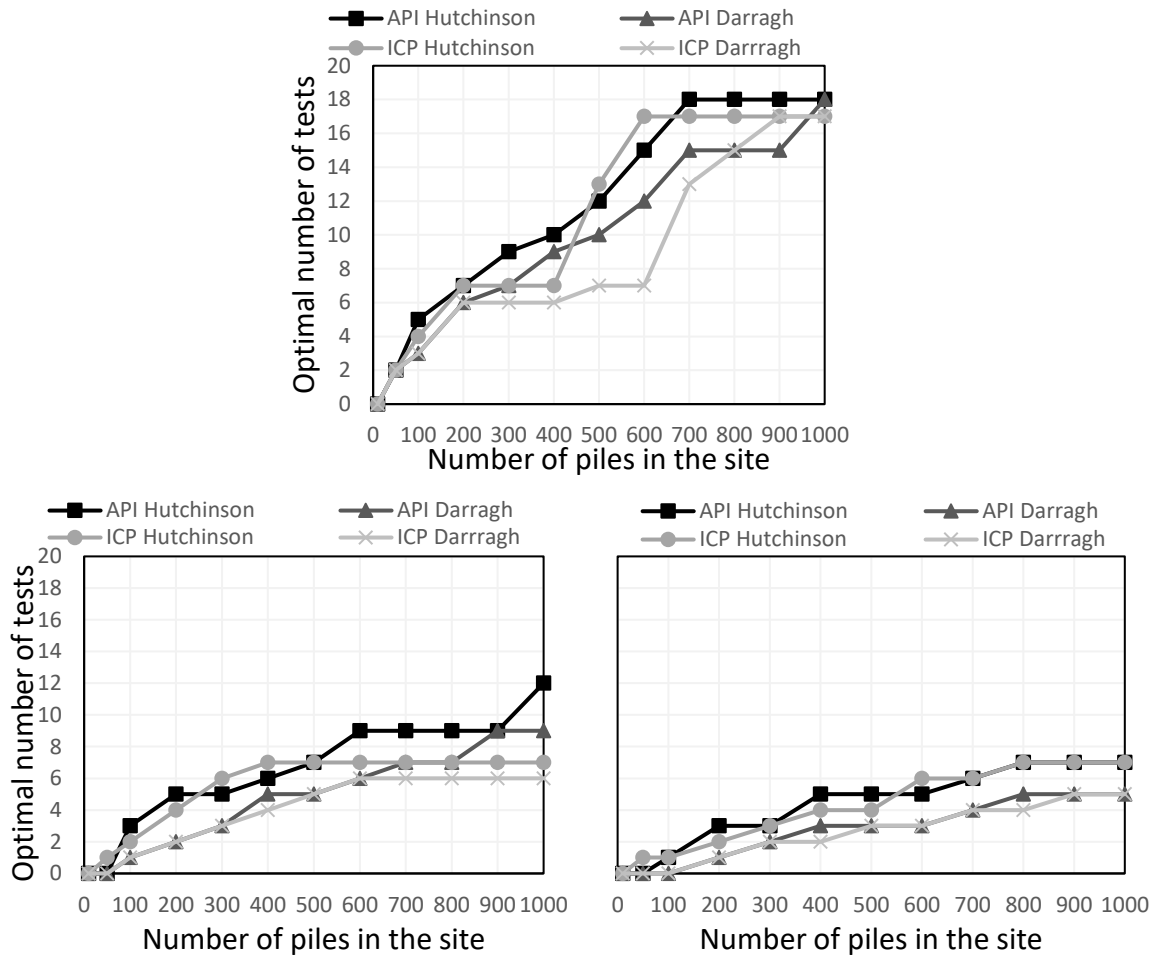


Figure 32 The optimal number of piles in clay sites (a) test cost 10\$/kN and price 97\$/ft (b) test cost 10\$/kN and the piles' cost of state of Michigan (2003), and (c) test cost 20\$/kN and the piles' cost of state of Michigan (2003).

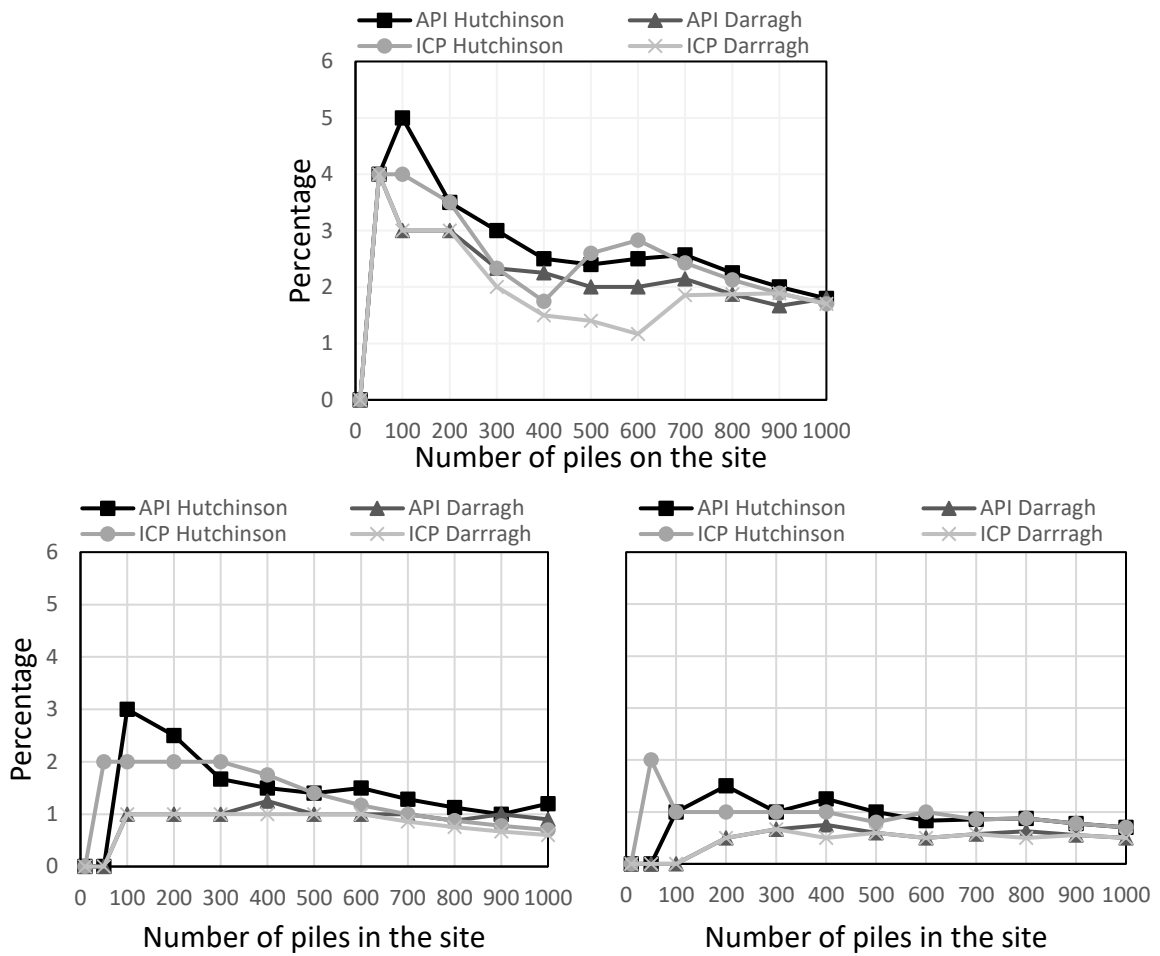


Figure 33 The percentage of piles in clay sites (a) test cost 10\$/KN and price 97\$/ft (b) test cost 10\$/KN and the piles' cost of state of Michigan (2003), and (c) test cost 20\$/KN and the piles' cost of state of Michigan (2003).

## CHAPTER 8

### CONCLUSIONS

In this thesis, the statistical model that was proposed by Najjar et al. (2017) to be a basis for a decision making framework that would optimize proof load test programs was updated to take into consideration an uncertain COV for the within-site variability in pile capacity. This uncertain  $r_{COV}$  was incorporated in the pile capacity model and updated after implementing a proof-load test program in the site. A sensitivity analysis was then conducted to investigate the effect of incorporating an uncertain  $r_{COV}$  (which represent the site variability), and the lower-bound capacity, and the mean capacity (which represent the method variability) on the updated reliability index. It was shown that the lower-bound has a significant effect on the prior values of the reliability index in addition to the negative proof-load test. This effect of the lower-bound starts to decrease and vanish when 1 or more positive test results are applied in the site. For the sensitivity analysis mean capacity a huge analysis is applied where the methods are differentiated between methods in sand and other in clays. Moreover, the sand methods are divided into skin and tip resistances in order to verify the effect of each of these parameters. It was shown that the bias factor of the method plays a significant role on affecting the prior reliability index, where high bias factors reveal for a high prior reliability index. Whereas for the COV, it was shown that small COVs increase the prior reliability index but decrease the effect of updated results of the proof load test, and

the high COV decrease the prior reliability index but have a positive effect on the updated reliability index when the static proof load testing is positive.

In order to generalize an optimal static proof load test, 4 sites were chosen (2 sand sites and another 2 clays sites). The piles capacities were calculated according to 2 methods the current-API method and the ICP method. Several pre-posterior analyses were conducted on these two sites and it was shown that clay sites require higher number of static proof load tests than the sand sites for the same prior number of piles in the site. In addition, the results show that there is a high percentage of static proof load tests for small prior number of piles and this percentage starts to decrease and converge for different methods and sites when the prior total number of piles in the site increase. For the proof load test level, it was shown that the level for the ICP method is 1.5xDL for both clay and sand sites. Whereas, the static proof load test level for the current API method is 2xDL and 2.25xDL for the sand and clay sites respectively. This indicates that the methods having bias factor close to one requires a 1.5xDL level test, and methods having higher bias factor requires higher levels of tests.

In addition, a sensitivity analysis was conducted on the cost of the proof load test and that of installing and fabricating the pile in order to see the effect of the cost on the optimal proof load test. The results show that the number of proof load tests decrease when the cost of the pile decrease, since this decrease in the pile cost increase the effect of the test cost and the efficiency on each test which reveals a decrease in the proof load test number. In addition, the increase in the cost of the test from 10\$/KN to 20\$/KN also decrease the number of static proof load tests since the price of the test increase so the greater the tests are the more the expected benefit decreases.

## REFERENCES

- Abdallah, Y., Najjar, S.S., and Saad, G. (2015). "Impact of proof load test programs on the reliability of foundations." *Proceedings of International Foundations Exposition and Equipment Exposition*, San Antonio, Texas, March 17-21.
- Abdallah, Y., Najjar, S.S., and Saad, G. (2015). "Reliability-based design of proof load test programs for foundations." *Geotechnical Engineering*, 46, (2), 63-80. ASTM D1153. (1994). "Standard test method for piles under static axial Compression load." *Annual book of ASTM standards*, 4.08, ASTM International.
- Ang, A. H-S. and Tang, W. H. (1984). "*Probability Concepts in Engineering Planning and Design.*" Vol. II. *Decisions, Risk and Reliability*, John Wiley & Sons, New York City.
- API. (2000). API RP 2A-WSD: "Recommended Practice for Planning, Designing and Constructing Fixed Offshore Platform-Working Stress Design," 21st Edition. Washington, DC: API Publishing Services.
- ASTM D1153. (1994). "Standard test method for piles under static axial Compression load." *Annual book of ASTM standards*, 4.08, ASTM International.
- Darragh, R.D., and Bell, R.A., (1969) "Load Tests on Long Bearing Piles." Performance of Deep Foundations, ASTM STP 444, American Society for Testing and Materials, 1969, pp. 41-67
- Gilbert, R.B., Najjar, S.S., and Choi, Y.J. (2005). "Incorporating lower-bound capacities into LRFD codes for pile foundations." Proc. Geo-Frontiers 2005, Site Characterization and Modeling, GSP No. 138, ASCE, Reston, VA.
- Huang, J., Kelly, R., Li, D., Zhou, C. and Sloan, S., (2016) "Updating Reliability of Single Piles and Pile 712 Groups by Load Tests." *Computers and Geotechnics*, 2016, 713 <http://dx.doi.org/10.1016/j.compgeo.2015.12.003>.

- Hutchinson, J.N., and Jensen, E.V., (1968) “Loading Tests on Piles Driven Into Estuarine Clays at Port of Khorramshahr, Iran, and Observations on the Effect of Bitumen Coating on Shaft Bearing Capacity.”
- Jardine, R.J., Chow, F.C., Overy, R. and Standing, J.R. (2005). “*ICP design methods for driven piles in sands and clays.*” Thomas Telford.
- Lacasse, S., Nadim, F., Anderson, K.H., Knudsen, S., Eidvig, U.K., Yetginer, G., Guttormsen, T.R., and Eide, A., (2013). "Reliability of API, NGL, ICP, and Fugro Axial Pile Capacity calculation Methods." Paper OTC-24063-MS. Houston, Texas, May 2013.
- Lacasse, S., Nadim, F., Langford, T., Knudsen, S., Yetginer, G., Guttormsen, T.R., and Eide, A., (2013). "Model Uncertainty in Axial Pile Capacity Design Method." Paper OTC-24066-MS. Houston, Texas, May 2013.
- Lehane, B.M., Lim, J.K., Carotenuto, P., Nadim, F., Lacasse, S., Jardine, R.J. and van Dijk, B.F.J. (2017). “Characteristics of Unified Databases for Driven Piles.” Offshore Site Investigation and Geotechnics. *Smarter Solutions for Future Offshore Developments*. Vol. 1.
- Matsumoto, T., Matsuzawa, K., and Kitiyodom, P., (2008). “A role of pile load test – Pile load test as element test for design of foundation system.” Proc 8<sup>th</sup> Int. Conf. on The Application of Stress-Wave Theory to Piles: Science, Technology and Practice, Jaime Alberto dos Santos.
- Najjar, S.S., and Gilbert, R.B. (2009a). “Importance of proof-load tests in foundation reliability.” *Geotechnical Special Publication No. 186, Proceedings of IFCEE 2009*,

*Contemporary Topics in In-Situ Testing, Analysis, and Reliability of Foundations*, ASCE, Orlando, Florida, 340-347.

Najjar, S.S., and Gilbert, R.B. (2009b). "Importance of lower-bound capacities in the design of deep foundations", *J. of Geotech. and Geoenvironmental Engineering*, ASCE, 135 (7): 890-900.

Najjar, S.S., Saad, G., and Abdallah, Y. (2017). "Rational Decision Framework for Designing Pile Load Test Programs." *Geotechnical Testing Journal*.

Nevels, Jr., James, B., Snethen, and Donald, R. (1994). "Comparison of settlement predictions for single pile in sand based on penetration test results." *Geotechnical Special Publication*, vol. 2

Paik, K., Salgado, R., Lee, J., and Kim, B. (2003). "*Behavior of Open- and Closed-Ended Piles Driven into Sands.*" *Journal of Geotechnical and Geoenvironmental Engineering* 10.1061/(ASCE)1090-0241(2003)129:4(296)

Park, J.H., Kim, D., and Chung, C.K. (2011). "Reliability Index Update for Driven Piles Based on Bayesian Theory Using Pile Load Test Result." *International Journal of Offshore and Polar Engineering*. 330-336.

Park, J.H., Kim, D., and Chung, C.K. (2012). "Implementation of Bayesian theory on LRFD of axially loaded driven Piles." *Computers and Geotechnics*, 42, 73–80.

Su, Y. (2006). "Bayesian updating for improving the accuracy and precision of pile capacity predictions." *The Geological Society of London*, IAEG, Paper number 374.



Zhang, J., Zhang, L. M., and Tang, W.H., (2011). "Reliability-Based Optimization of Geotechnical Systems." American Society of Civil Engineers. DOI: 10.1061/(ASCE)GT.1943-5606.0000551.

Zhang, L. (2004). "Reliability verifications using proof pile load tests." J. Geotechnical and Geoenvironmental Engrg. 130 (11): 1203-1213.

Zhang, L., and Tang, W. (2002). "Use of load tests for reducing pile length." Proceedings of the International Deep Foundations Congress, February 14-16.

## Appendix 1: Sensitivity Analysis of the Lower-bound

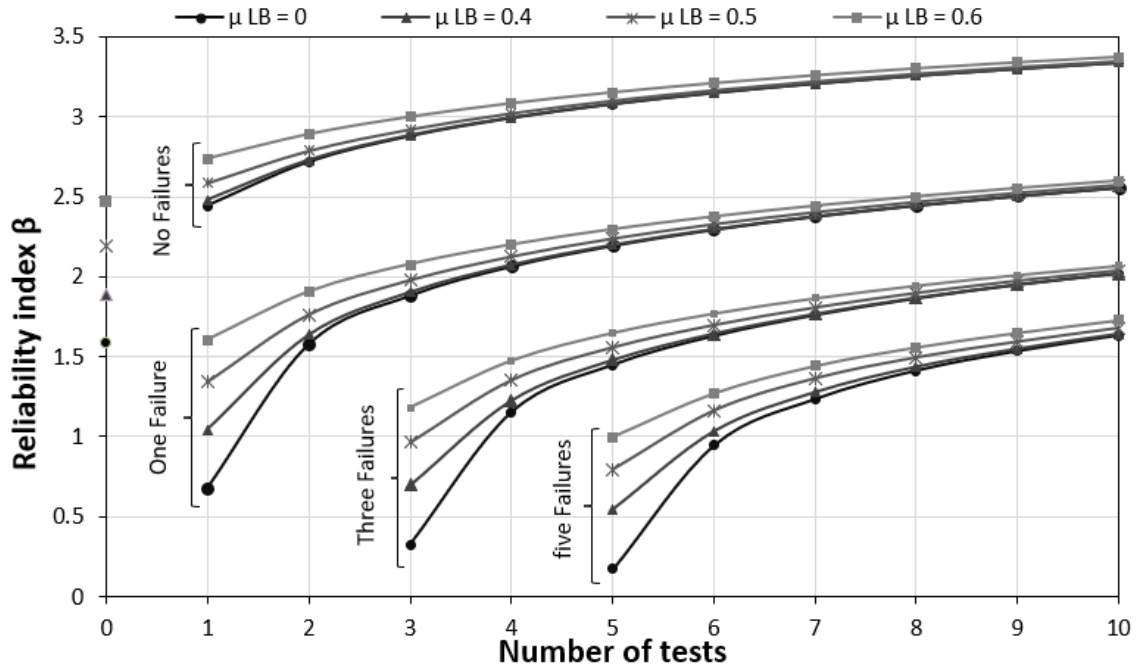


Figure 34 The variation of the reliability index as a function of positive proof load tests of 1.5xDL level for different lower-bound to mean ratio applied at a 0.5 COV mean distribution (FS = 2)

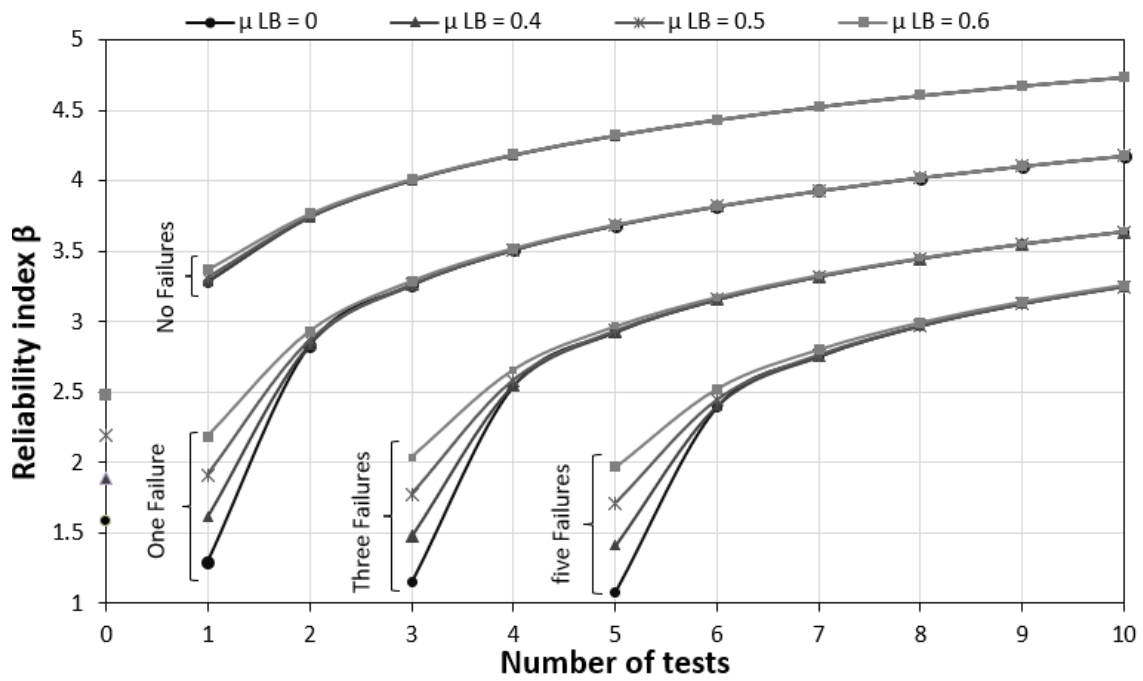


Figure 35 The variation of the reliability index as a function of positive proof load tests of 2.5xDL level for different lower-bound to mean ratio applied at a 0.5 COV mean distribution (FS = 2)

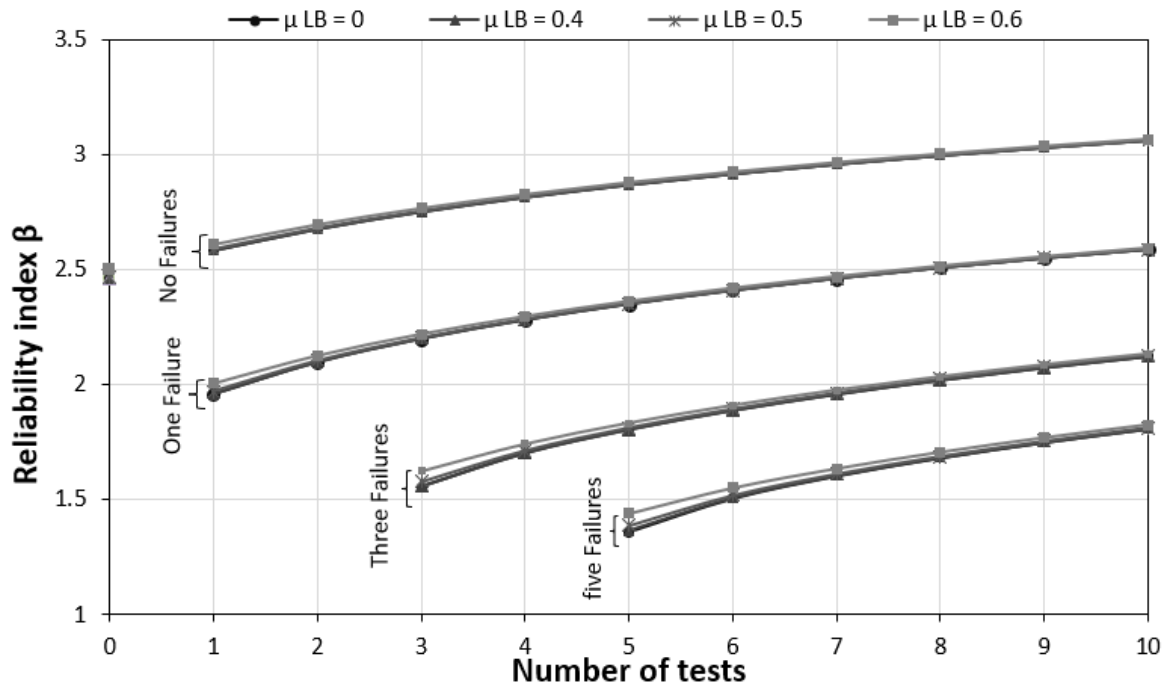


Figure 36 The variation of the reliability index as a function of positive proof load tests of 1.5xDL level for different lower-bound to mean ratio applied at a 0.15 COV mean distribution (FS = 2)

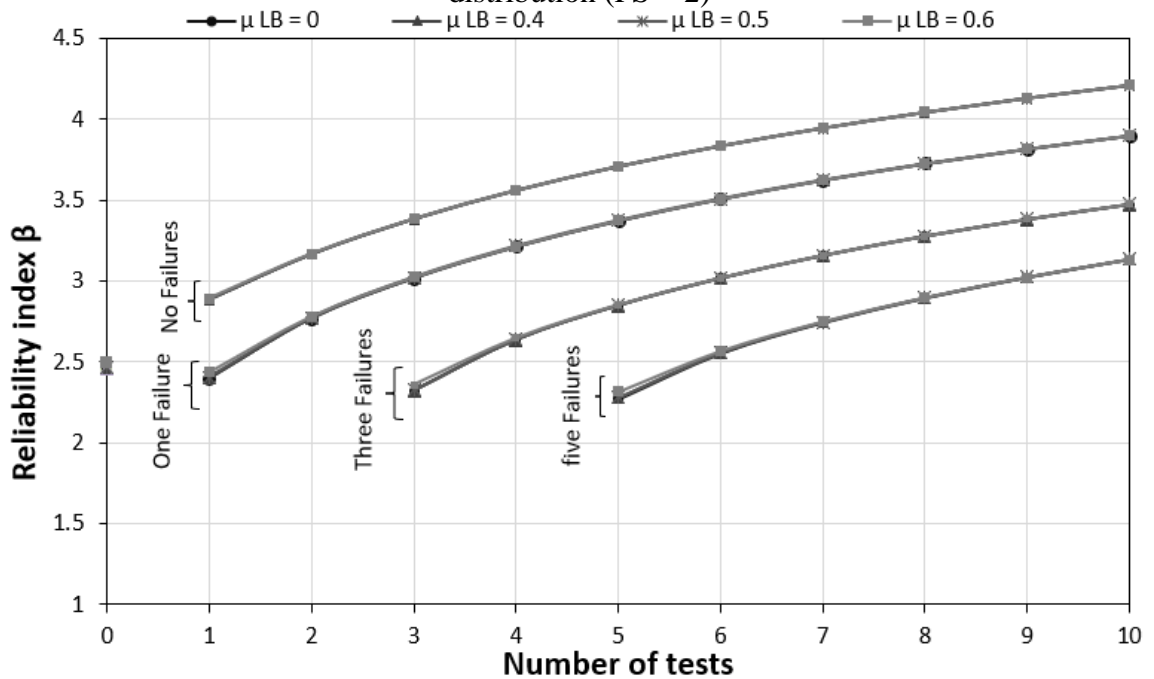


Figure 5 The variation of the reliability index as a function of positive proof load tests of 2.5xDL level for different lower-bound to mean ratio applied at a 0.15 COV mean distribution (FS = 2)

## Appendix 2: Mean Sensitivity

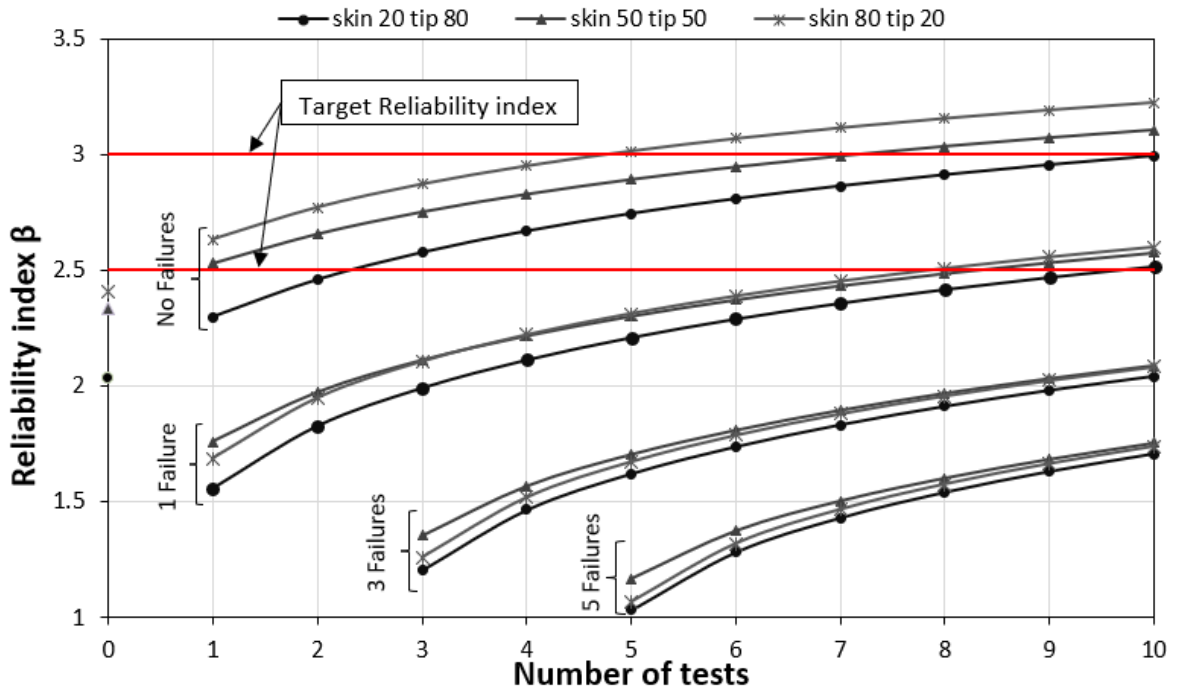


Figure 38 The variation of the reliability index as a function of different proof load tests outcome conducted at 1.5xDL level for different skin-tip combinations for Fugro method (FS = 2)

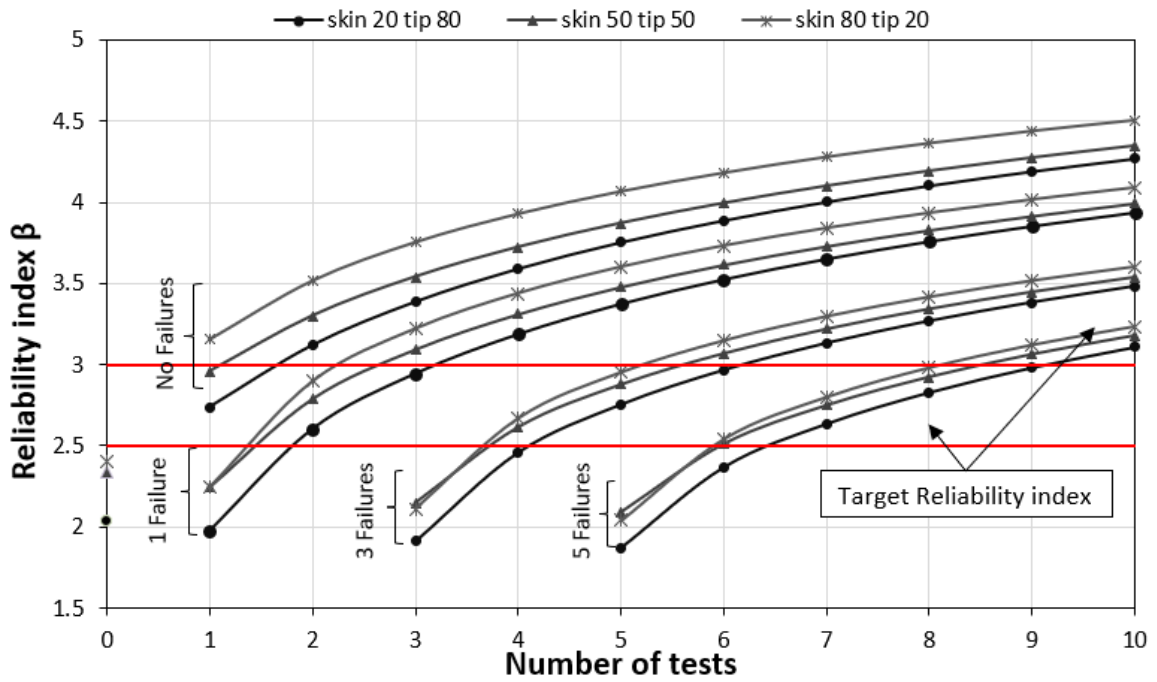


Figure 39 The variation of the reliability index as a function of different proof load tests outcome conducted at 2.5xDL level for different skin-tip combinations for Fugro method (FS = 2)

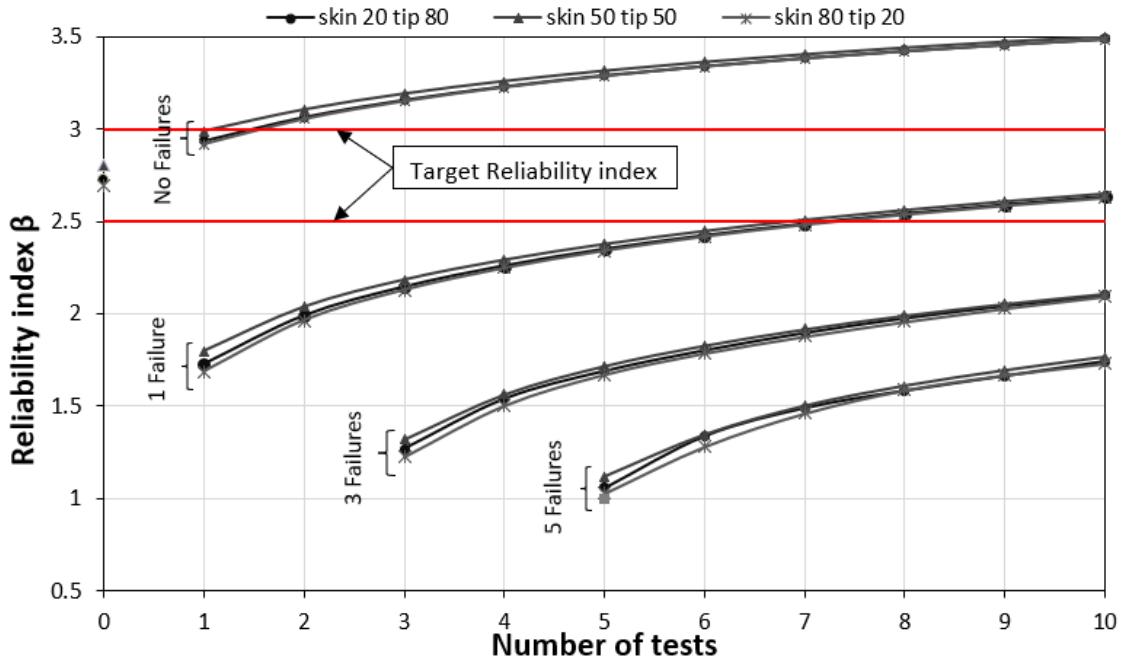


Figure 40 The variation of the reliability index as a function of different proof load tests outcome conducted at 1.5xDL level for different skin-tip combinations for API-05 method (FS = 2)

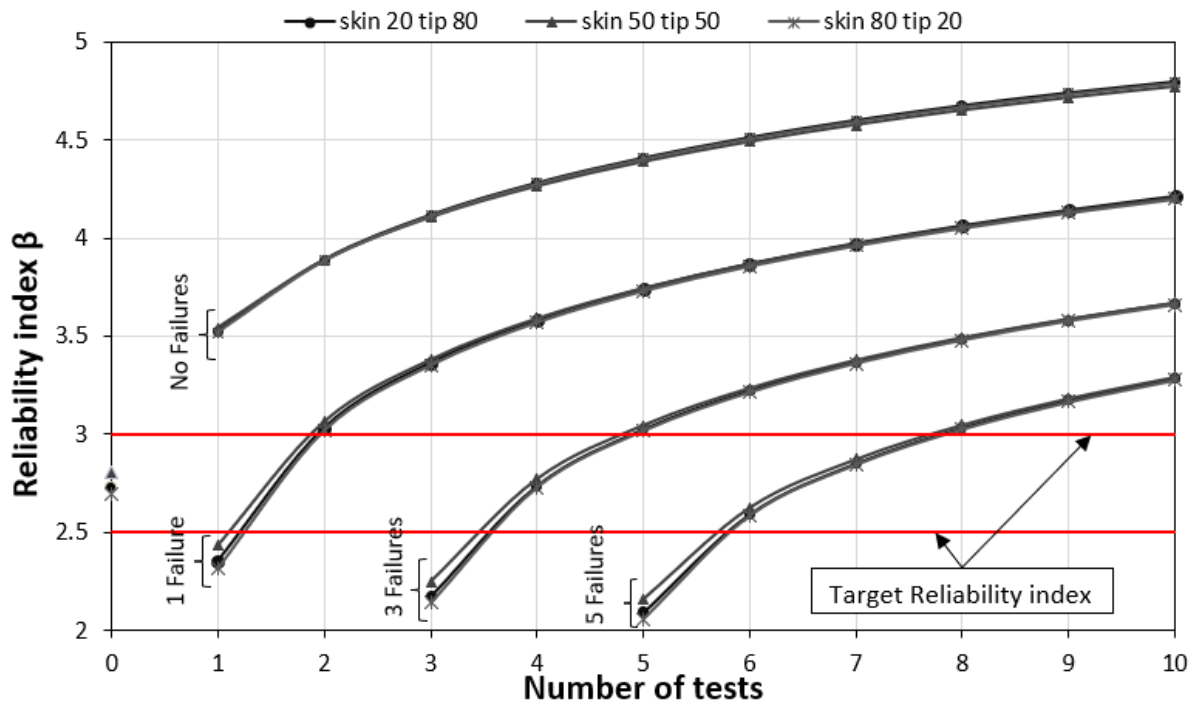


Figure 41 The variation of the reliability index as a function of different proof load tests outcome conducted at 2.5xDL level for different skin-tip combinations for API method (FS = 2)

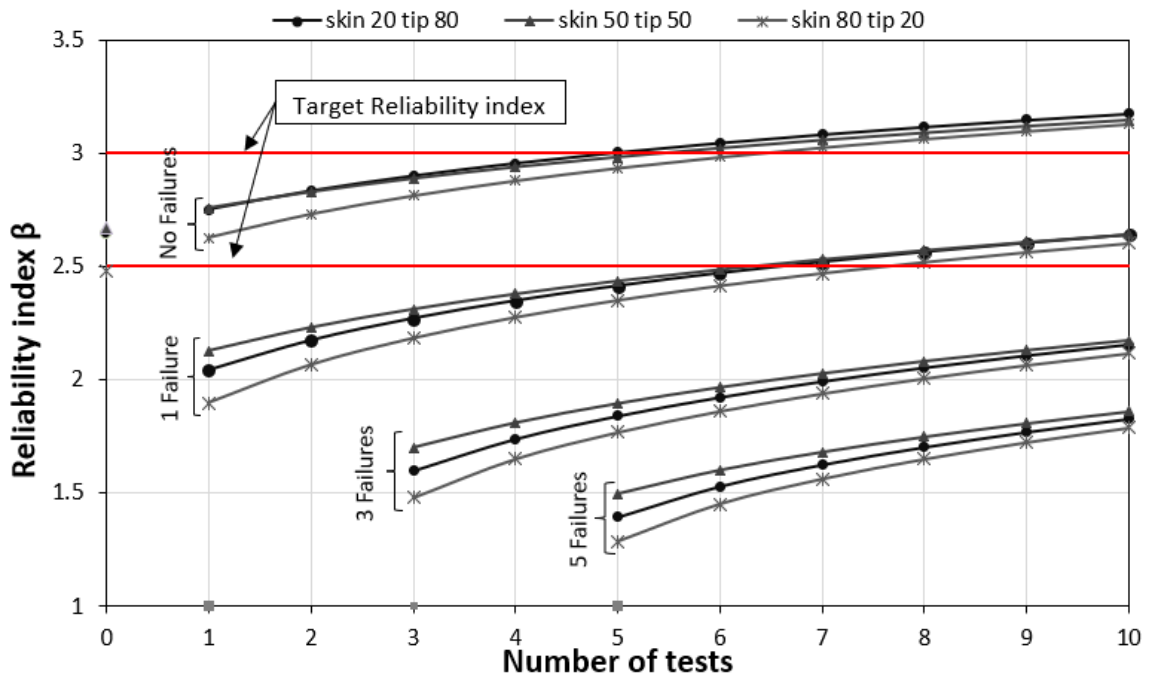


Figure 42 The variation of the reliability index as a function of different proof load tests outcome conducted at 1.5xDL level for different skin-tip combinations for ICP-05 method (FS = 2)

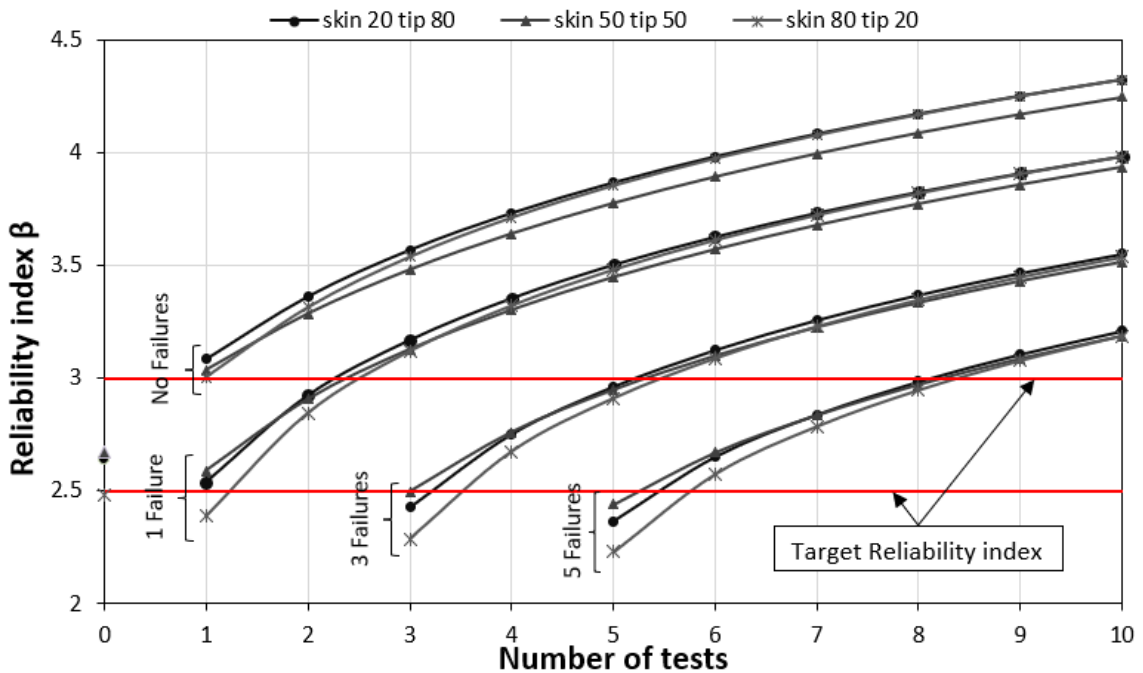


Figure 43 The variation of the reliability index as a function of different proof load tests outcome conducted at 2.5xDL level for different skin-tip combinations for ICP-05 method (FS = 2)



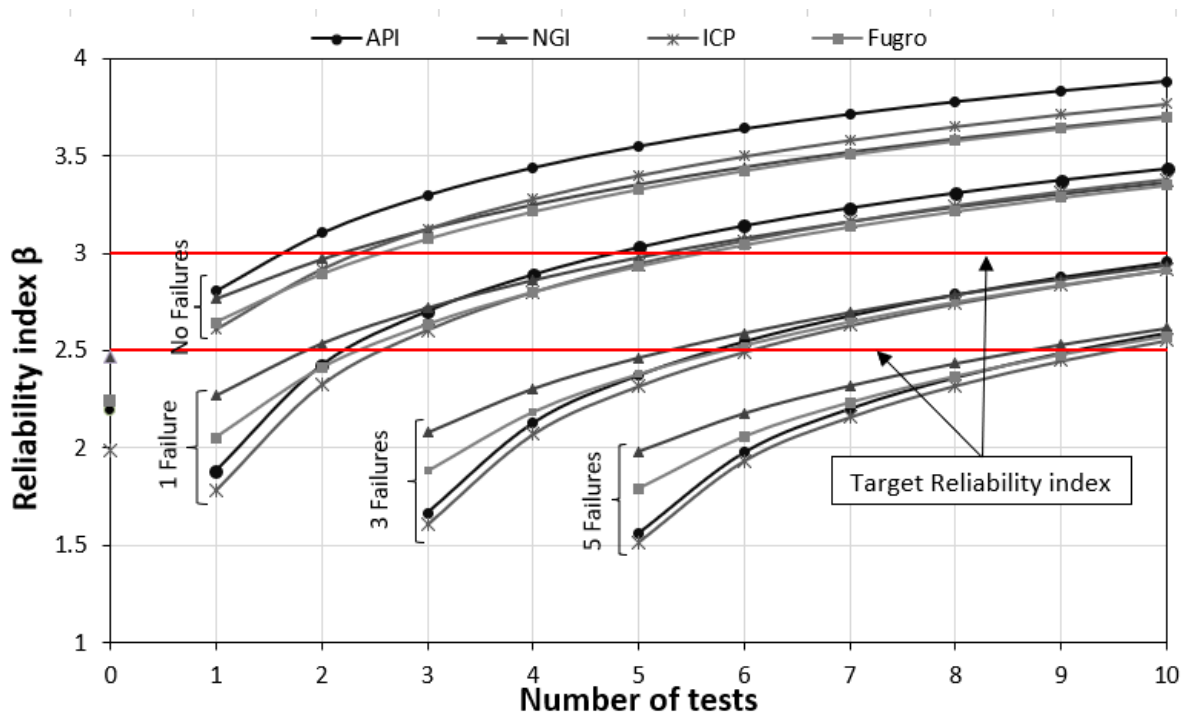


Figure 44 The variation of the reliability index as a function of different proof load tests outcome conducted at 2xDL level for different clay methods (FS = 2)